NOTICES

This report was prepared as an account of work sponsored by an agency of the United States Government. Neither the United States Government nor any agency thereof, nor any employees, nor any of their contractors, subcontractors, or their employees make any warranty, expressed or implied, or assume any legal liability or responsibility for the accuracy, completeness, or usefulness or any privately owned rights. Reference herein to any specific commercial process, or service by trade name, trademark, manufacturer, or otherwise does not necessarily constitute or imply its endorsement, recommendation, or favoring by the United States Government or any agency, contractor, or subcontractor thereof. The views and opinions of the authors expressed herein do not necessarily state or reflect those of the United States Government or any agency, contractor, or subcontractor thereof.

When Government drawings, specifications, or other data are used for any purpose other than in connection with a definitely Government-related procurement, the United States Government incurs no responsibility or any obligations, whatsoever. The fact that the Government may have formulated or in any way supplied the said drawings, specifications, or other data, is not to be regarded by or otherwise in any manner construed, as licensing the holder or any other person or corporation; or as conveying any rights or permission to manufacture, use or sell any patented invention that may in any way be related thereto.

This technical report has been reviewed by the Public Affairs Office (PA) and is releasable to the National Technical Information Service, where it will be available to the general public, including foreign nationals.

This report has been reviewed and is approved for publication,

Thomas B. Stauffer

THOMAS B. STAUFFER, PhD
Project Manager

Michael G. Katona

MICHAEL G. KATONA, PhD
Chief Scientist, Environics Directorate

JIMMY C. CORNETTE, PhD
Chief, Environmental Research Division

Neil J. Lamb.

NEIL J. LAMB, Colonel, USAF, BSC
Director, Environics Directorate

REPORT DOCUMENTATION PAGE

Form Approved
OMB No. 0704-0188

1. AGENCY USE ONLY (Leave blank)	2. REPORT DATE	3. REPORT TYPE AND DATES COVERED
	April 1994	Final October 1989 - September 1992

4. TITLE AND SUBTITLE

Degradation of Aromatic Hydrocarbons in an Aquifer During a Field Experiment Demonstrating the Feasibility of Remediation by Natural Attenuation

5. FUNDING NUMBERS

JON 1900-7064
PE 62206F

6. AUTHOR(S)

Thomas B. Stauffer, Christopher P. Antworth, Riki G. Young, William G. MacIntyre, J. Mark Boggs, Lisa M. Beard

7. PERFORMING ORGANIZATION NAME(S) AND ADDRESS(ES)

Tennessee Valley Authority
Engineering Laboratory
Norris, Tennessee 37828

8. PERFORMING ORGANIZATION REPORT NUMBER

9. SPONSORING/MONITORING AGENCY NAME(S) AND ADDRESS(ES)

AL/EQC-OL
139 Barnes Drive, Suite 2
Tyndall Air Force Base, Florida 32403-5323

10. SPONSORING/MONITORING AGENCY REPORT NUMBER

AL/EQ TR 1993-0007

11. SUPPLEMENTARY NOTES

Additional publications include EPRI Report No. TR-101998, March 1993, and Water Resources Research, Vol. 29, No. 12, Dec. 1993, pp. 4045-52.
For further information contact: Dr. Thomas B. Stauffer, (904)-283-6059

12a. DISTRIBUTION/AVAILABILITY STATEMENT

This technical report has been reviewed by the Public Affairs Office (PA) and is releasable to the National Technical Information Service, where it will be available to the general public, including foreign nationals.

12b. DISTRIBUTION CODE

13. ABSTRACT *(Maximum 200 words)*

The purpose of this experiment was to perform a controlled field experiment, involving the injection of several aromatic hydrocarbons and a nonreactive tracer into an uncontaminated aquifer. By monitoring the plume development of these solutes, and by measuring a number of physical and chemical characteristics of the aquifer, this study was designed to provide data on those properties which significantly control the propagation of dissolved contaminants in groundwater systems. A secondary objective was to measure the *in situ* degradation rates of the selected organic compounds. The disappearance and transformation of the organic solutes during this experiment demonstrated that natural degradation processes were able to effectively reduce these levels of dissolved organic contaminants in a reasonable time frame. This represents the most important result of this field study, since active remediation would not be needed in situations where natural degradation rates were sufficient to reduce contaminant concentrations to safe levels. The monetary and environmental cost savings of allowing natural biological restoration of the residual contaminants are potentially enormous. It appears that this study is the first field experiment to prove conclusively that hydrocarbon solute losses were due to chemical degradation rather than physical losses.

14. SUBJECT TERMS

Natural attenuation; Groundwater contamination; *In situ* biodegradation; Jet fuel components; Natural gradient experiment

15. NUMBER OF PAGES

121

16. PRICE CODE

17. SECURITY CLASSIFICATION OF REPORT	18. SECURITY CLASSIFICATION OF THIS PAGE	19. SECURITY CLASSIFICATION OF ABSTRACT	20. LIMITATION OF ABSTRACT
UNCLASSIFIED	UNCLASSIFIED	UNCLASSIFIED	UL

(The reverse of this page is blank.)

PREFACE

This report was prepared by the Armstrong Laboratory Environics Directorate (AL/EQC), 139 Barnes Drive, Suite 2, Tyndall Air Force Base, Florida 32403-5323, and the Tennessee Valley Authority (TVA) Engineering Laboratory, Norris, Tennessee 37828, in conjunction with the Electrical Power Research Institute (EPRI). The reported work was cofunded by the Air Force and EPRI through an interdepartmental procurement action with TVA.

This final report describes the second MacroDispersion Experiment (MADE-2) conducted at Columbus AFB, MI; the experimental methodologies that were used to analyze site characteristics, inject chemical tracers and solutes into the aquifer, and monitor the resulting plume; the data analysis techniques that were used; and an explanation of the significance of these experimental observations. EPRI TR-101998 provides a more general description of the experiment.

The work was performed between October 1989 and September 1992. The AL/EQC project manager was Dr. Thomas B. Stauffer.

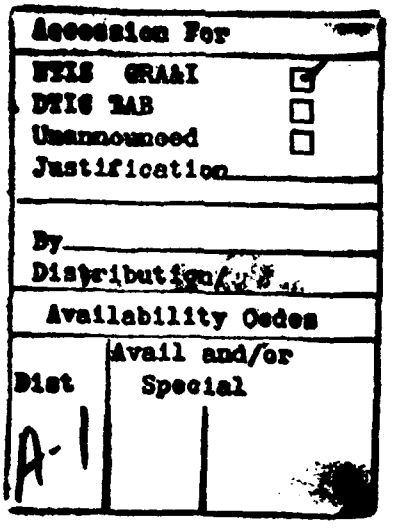

(The reverse of this page is blank)

EXECUTIVE SUMMARY

A. OBJECTIVE

The purpose of this experiment was to perform a controlled field experiment, involving the injection of several aromatic hydrocarbons and a nonreactive tracer into an uncontaminated aquifer. By monitoring the plume development of these solutes, and by measuring a number of physical and chemical characteristics of the aquifer, this study was designed to provide data on those properties which significantly control the propagation of dissolved contaminants in groundwater systems. Data of this type are quite rare, and are extremely useful for validating numerical fate and transport models which include complex processes, such as solute advection-dispersion, geochemical attenuation, and microbial degradation. A secondary objective was to measure the *in situ* degradation rates of the selected organic compounds, in order to investigate the possibility of utilizing natural attenuation processes as an alternative to active remediation techniques.

B. BACKGROUND

Groundwater contamination is an important environmental concern for both military and civilian industrial operations. The organic constituents of fuels such as JP-4, gasoline, and diesel (e.g., benzene, toluene, naphthalene, xylene, etc.) and cleaning solvents (e.g., trichloroethylene) have resulted in serious contamination problems at many DOD facilities. Many of these chemical components of fuels and solvents are regulated by EPA as hazardous substances, and have stringent concentration limits in drinking water (Geraghty and Miller, Inc., 1991). Their presence in groundwater at concentrations exceeding the EPA's maximum contaminant levels generally requires the use of costly water purification methods. The lack of an adequate quantitative understanding of the processes that govern the environmental fate of these contaminants has constrained the development of cost-effective groundwater remediation techniques.

A great number of research efforts have studied various physical, chemical and biological mechanisms that influence the transport of pollutants in the environment. Most have been performed within laboratories, but some relatively recent experiments have been conducted at field sites to determine the effects of natural conditions and heterogeneities on these processes (Boggs *et al.*, 1992; Harvey *et al.*, 1993; Sudicky, 1986). Additionally, the accidental discharge of contaminants into groundwater systems has allowed some limited studies of the *in situ* transport of pollutants. However, the lack of specific information about the initial conditions of contaminant mass and location hinders the ability to draw meaningful conclusions from such research.

Previously, a few field experiments have reported the attenuation of test solutes, and claimed that the results were possibly due to microbial degradation processes (e.g., Sutton and Barker, 1985). While laboratory studies have proven that soil organisms are capable of utilizing a great variety of chemical compounds, similar work showing natural degradation in the field has not previously been possible, for a number of reasons. Although it is generally accepted that the *in situ* biodegradation of chemical contaminants does occur, conclusive experimental evidence is lacking in the current literature.

C. SCOPE

This report describes the research conducted at a field site at Columbus Air Force Base, Mississippi. Section I provides an introduction to the objectives of this study and pertinent background information. Section II describes the physical and geochemical characteristics of the test site. Section III outlines the methods that were used to conduct the field experiment. Section IV discusses the results of the data analysis and some general observations. Section V presents a more detailed mathematical overview of the spatial moments analysis of the solute plumes. Section VI shows how the degradation rates were calculated for the aromatic hydrocarbons. Section VII reviews the dispersivity computations, and section VIII presents the researchers conclusions and recommendations.

D. METHODOLOGY

To effectively monitor the development of the plume of hydrocarbons and the tritium tracer, a well field consisting of 328 multilevel and 56 BarCad® samplers was available to the researchers. Because of time and cost constraints, only five complete, three-dimensional sample sets were taken at about 100-day intervals during the study. Additional, smaller sampling events were used to observe plume activity on a shorter time scale. Since it is neither physically nor economically possible to sample an entire aquifer, a three-dimensional network of wells must be used to determine the location and concentration of groundwater contaminants. To obtain a complete "picture" of this plume, geostatistical techniques (e.g., kriging) were employed to mathematically fill in the spatial gaps between sampling wells. This technique is the most sophisticated and accurate method available for use in generating stochastic models and computer graphics of subsurface contaminant transport.

Although the measurement of degradation rates was a principal objective of this study, no attempts were made to classify or quantify the microbial populations. While a detailed analysis of enzymatic activity before, during and after the movement of the plume through a given area would greatly support observations of biodegradation, such work was beyond the scope of this study and is left for future research efforts. In order to distinguish solute degradation from losses due to sorption, dilution or evaporation, and to permit the detection of degradation products, ^{14}C-labeled p-xylene was included in the injection solution.

Previous work at this site characterized many of the important physical properties of this aquifer (Boggs *et al.*, 1992). In this study, soil samples were taken at various locations and depths, then analyzed for particle sizes, organic carbon content, surface area, and partition coefficient (K_d). Groundwater samples were also tested for a number of elemental components and chemical characteristics. Finally, a set of piezometers was used to measure temporal fluctuations in the hydraulic gradient of the aquifer, which were due to a combination of both daily rain events and evapotranspiration, and seasonal factors.

E. TEST DESCRIPTION

The natural gradient field experiment was conducted to investigate the transport and degradation of four dissolved aromatic organic compounds (benzene, naphthalene, p-xylene, and o-dichlorobenzene) and one nonretained tracer in an aquifer. The study was done at Columbus AFB, Mississippi, in a shallow, unconfined alluvial aquifer having considerable

heterogeneity in physical and chemical properties. A two-day pulse of 9.7 cubic meters of tritiated water and the hydrocarbons in a dilute aqueous solution was injected into the aquifer. The initial concentrations of the organic test compounds in solution ranged from about 7 to 70 mg/L, which was prepared and stored on-site using ambient groundwater from an upgradient local well. The injection was made into five wells, spaced 1 meter apart and aligned transverse to the direction of groundwater flow. Each injection well was screened over a 0.6 meter interval, which was placed within the saturated zone of the aquifer.

The solute concentration distributions were monitored at one to three month intervals over a 15-month period, using a three-dimensional network consisting of over 6000 sampling points. Selected points within the network were sampled more frequently to produce time-series sets of solute concentrations. Spatial moments calculated from the three-dimensional network concentration data and from the time-series concentration data, were used to determine the fate and transport behavior of each solute.

Stable organic compounds in groundwater samples were analyzed by gas chromatography (GC). Deuterated toluene and 4-bromofluorobenzene internal standards were added to 20 mL water samples, which were then extracted with 2 mL of n-pentane. These extracts were then analyzed for benzene, p-xylene, naphthalene and o-dichlorobenzene, also by GC. Sensitivity of the method was 50 μg/L for benzene and 4 μg/L for the other compounds. All samples were extracted and analyzed within 21 days of collection. Quality control for the organic analyses was ensured by using several techniques, including the use of sample duplicates, certified standard control solutions, internal standards for all analyses, and independent verification of our analytical results by another laboratory.

Tritium and ^{14}C in samples from the wells were analyzed by liquid scintillation counting in dual isotope mode, by the Water Resources Research Center at Mississippi State University. Samples were counted for 20 minutes or to a 1 percent error at the 95 percent probability level, whichever was attained first. Background levels of tritium and ^{14}C in ambient groundwater at the test site dictated the analytical sensitivity for these measurements, and were approximately 2 and 3 pCi/mL, respectively. The statistical errors associated with 20-minute measurements at these levels are about $\pm$20 percent at the 95 percent probability level. A set of tritium and ^{14}C standards was counted every 108 samples to check analytical accuracy and verify instrument performance. Every 25th sample was counted twice to estimate measurement precision and repeatability. As an overall check on the radiological measurements, duplicate field samples amounting to roughly 5 percent of the total field samples were analyzed independently by the TVA Western Area Radiological Laboratory.

Dissolved oxygen (DO) measurements were performed at 2- to 3-month intervals at selected locations during the experiment. DO data were intended to demonstrate whether aerobic conditions for possible degradation of the organic compounds were maintained, and were collected from 16 multilevel samplers (MLS) located along the longitudinal axis of the tracer plume, and 6 piezometers. Samples were collected in 60 mL BOD bottles after purging approximately 100 mL from the MLS tubes, and measurements were made with a calibrated DO probe immediately after sample collection. The DO measurements at the 6 piezometers were made in conjunction with pH, conductivity, and oxidation-reduction potential measurements.

F. RESULTS

The tritium plume was characterized by extreme skewness in the longitudinal direction. The evolution of the plume was consistent with the measured hydraulic head and conductivity fields, and was primarily due to the increasing mean hydraulic conductivity with distance from the injection site. Measurements of hydraulic conductivity produced a mean Darcy's Law groundwater velocity of 5 m/yr near the injection wells, whereas local velocities in the far field were found to exceed 400 m/yr. The dispersivity of the alluvial aquifer was estimated by fitting the tritium data to general spatial moments equations for two-dimensional advective-dispersive transport in a nonuniform flow field. A longitudinal dispersivity of approximately 10 meters provided the best representation of the first and second longitudinal moments of the tritium plume.

The aromatic hydrocarbons degraded significantly during the experiment. Analysis for the degradation products of ^{14}C p-xylene revealed that about 80 to 90 percent of the ^{14}C present was associated with dissolved $^{14}CO_2$ and intermediate products, indicating aerobic degradation of the p-xylene. Dissolved oxygen in the pulse plume maintained aerobic conditions throughout the experiment, and was always greater than 2.6 mg/L. Degradation kinetics calculated from the whole-field data set were approximately first-order with the following rate constants: benzene, 0.0070 d^{-1}; p-xylene, 0.0107 d^{-1}; naphthalene, 0.0064 d^{-1}; o-dichlorobenzene, 0.0046 d^{-1}. Similar reaction rates were also obtained from a near-field subset of the data, using a model based on the hydrologic characteristics of the aquifer. The shapes of the degradation rate curves were consistent with microbial degradation processes. Maximum degradation rates obtained are presumed to be characteristic of the microbial population's metabolism. A least-squares inversion method of fitting time-series data to an analytical one-dimensional transport model, containing first-order decay and linear equilibrium sorption terms, yielded the following mean first-order rate constants: benzene, 0.010 d^{-1}; naphthalene, 0.013 d^{-1}; p-xylene, 0.016 d^{-1} and o-dichlorobenzene, 0.005 d^{-1}.

Sorption had some affect on the transport of the organic compounds, but it was a relatively minor process compared with the degradation. Because of the dominant influence of the degradative processes, field-average retardation factors could not be estimated from a comparison of the mean displacement rates of the aromatic compound and tritium plumes. However, analysis of time-series data at each of 17 sample points located within a distance of approximately 20 meters of the injection point produced mean retardation factors for benzene, naphthalene, p-xylene, and o-dichlorobenzene of 1.20, 1.45, 1.16, and 1.33, respectively. Agreement between these results and retardation factors calculated from sorption coefficients obtained in laboratory batch and column experiments, suggests that laboratory retardation measurements may be reliable indicators of sorption behavior in the field.

G. CONCLUSIONS

The disappearance and transformation of the organic solutes during this experiment demonstrated that natural degradation processes were able to effectively reduce these levels of dissolved organic contaminants in a reasonable time frame. This result suggests that, for similar organic compounds, it might be best to restrict aquifer remediation activities to the contaminant source region. By reducing this source, the resulting plume of organic solutes

could possibly maintain a steady-state limit, given the correct physical, chemical and biological conditions. In such an aquifer, the spatial boundary of this plume would be determined primarily by the hydrology and geochemistry of the site, solute sorption, biodegradation by indigenous microbes, redox capacity, and oxygen and nutrient supply.

This observation represents the most important result of this field study, and could have important implications for the restoration of aquifers contaminated by organic chemicals. Active remediation would not be needed in situations where natural degradation rates were sufficient to reduce contaminant concentrations to safe levels before they were transported to regions where they might be dangerous to human health or the environment. Remediation by natural degradation processes is likely to be applicable to residual organic contaminants (i.e., NAPL organics immobilized by capillary forces that cannot be effectively removed from the aquifer by pumping). The monetary and environmental cost savings of allowing natural biological restoration of the residual contaminants are potentially enormous. After a review of the current scientific literature, it appears that this study is the first field experiment to prove conclusively that hydrocarbon solute losses were due to chemical degradation rather than physical losses, such as sorption and vaporization.

H. RECOMMENDATIONS

Further research is needed to build upon results of this study, to further support the observation of natural attenuation and to attempt to quantify the environmental requirements for this process. The degradation rates determined for the four aromatic compounds in the Columbus aquifer are now being used in the design and modeling stages of a new field test which will use an emplaced NAPL source. This test at the Columbus site will be a demonstration of the practicality of natural degradation (natural attenuation) as a remediation action for a steadily leaching source in an aquifer. This experiment more closely emulates the effects of a fuel spill. Assuming that a steady-state contaminant concentration situation is attained in this test, natural degradation will be a verified groundwater contaminant treatment option.

It is proposed that experiments similar to this one should be done at several other test sites to prove the general applicability of this method, and to measure both aerobic and anaerobic degradation rates for use in the development of more accurate fate and transport models. The technique of using ^{14}C-labeled compounds is suggested for future field experiments, because it distinguishes solute degradation from solute losses by sorption and evaporation, and permits the demonstration of more accurate mass balances throughout the course of the investigation. If multiple test sites become available, they could then be used to conduct NAPL studies which might further support the natural attenuation treatment option, and might even suggest this technique as the action of first choice in certain groundwater contamination situations.

(The reverse of this page is blank)

TABLE OF CONTENTS

LIST OF ILLUSTRATIONS

(Reverse of this page is blank)

LIST OF TABLES

SECTION I
INTRODUCTION

OBJECTIVE

The purpose of this experiment was to perform a controlled field experiment, involving the injection of several aromatic hydrocarbons and a nonreactive tracer into an uncontaminated aquifer. By monitoring the plume development of these solutes, and by measuring a number of physical and chemical characteristics of the aquifer, this study was designed to provide data on those properties which significantly control the propagation of dissolved contaminants in groundwater systems. Data of this type are quite rare, and are extremely useful for validating numerical fate and transport models which include complex processes, such as solute advection-dispersion, geochemical attenuation, and microbial degradation. A secondary objective was to measure the *in situ* degradation rates of the selected organic compounds, in order to investigate the possibility of utilizing natural attenuation processes as an alternative to active remediation techniques.

BACKGROUND

Groundwater contamination is an important environmental concern for both military and civilian industrial operations. The organic constituents of fuels such as JP-4, gasoline, and diesel (e.g., benzene, toluene, naphthalene, xylene, etc.) and cleaning solvents (e.g., trichloroethylene) have resulted in serious contamination problems at many DOD facilities. Many of these chemical components of fuels and solvents are regulated by EPA as hazardous substances, and have stringent concentration limits in drinking water (Geraghty and Miller, Inc., 1991). Their presence in groundwater at concentrations exceeding the EPA's maximum contaminant levels generally requires the use of costly water purification methods. The lack of an adequate quantitative understanding of the processes that govern the environmental fate of these contaminants has constrained the development of cost-effective groundwater remediation techniques.

Degradation rate constants, for use in fate and transport models of reactive organic compounds, must be determined by experimentation. Field experiments to determine degradation rates are desirable because laboratory values may not be valid for the actual conditions in an aquifer. Madsen (1991) notes that the "determination of microbial activity in disturbed, displaced environmental samples incubated in the laboratory is likely to be quantitatively, even qualitatively different from the same determination *in situ*." Determination of a degradation rate in an aquifer should meet criteria that are applied to rate measurements in laboratory batch reactor systems.

Therefore, a known mass of a pure compound must be introduced into the aquifer at a specific location and time, followed by observation of the changes in concentration over space and time. Because aquifers are open systems, water samples should be analyzed for both the reactive compound and its degradation products, and a mass balance should be maintained for all of these components. Since a rate constant calculated from the disappearance of the contaminant may represent physical losses rather than chemical degradation, the demonstration of degradation in an aquifer requires the identification and quantification of reaction products. Field measurements of organic compound degradation

rates that meet these criteria were not found in the literature. The natural attenuation experiment conducted by Barker *et al.* (1987) measured mass loss rates of aromatic compounds from a pulse plume, but did not establish that observed losses were due to degradation.

An earlier natural gradient experiment, referred to as MADE-1, involving bromide and three fluorobenzoate tracers, was conducted between October 1986 and June 1988 at the same site. Boggs *et al.* (1992) described the test site, experimental design and procedures, and present qualitative observations regarding the migration behavior of the bromide tracer plume. A comprehensive description of the hydrogeology of this site is given by Boggs *et al.* (1990).

Adams and Gelhar (1992) provided a spatial moments analysis of the bromide data for the MADE-1 field experiment. Their analysis indicates that the bromide mass recovery decreased to approximately 50 percent by the end of the study due to the combined effects of plume truncation, sampling bias, and sorption. However, they showed that the relationship of longitudinal variance and mean plume displacement was relatively insensitive to the bromide mass loss during the experiment. Application of a nonuniform advection-dispersion model to the bromide plume moments lead to an estimate of longitudinal dispersivity of 5 to 10 meters for the alluvial aquifer (Adams and Gelhar, 1992).

During MADE-1, the borehole flowmeter was demonstrated to be a practical device for obtaining the three-dimensional distribution of horizontal hydraulic conductivity. Rehfeldt *et al.* (1989a) evaluated the accuracy and reliability of the technique through a series of field and laboratory tests, and provided theoretical and practical guidelines for its implementation. Application of the flowmeter and other methods for estimating hydraulic conductivity variability and aquifer dispersivity at the test site is discussed by Rehfeldt *et al.* (1989b, 1992).

SCOPE

The location of this field study at the Columbus AFB, Columbus, MS, macrodispersion experiment (MADE) site, is shown in Figure 1. In this natural gradient experiment, referred to as MADE-2, the researchers made a pulse injection of a dilute aqueous solution of tritiated water, benzene, p-xylene, naphthalene and o-dichlorobenzene (o-DCB). The injection was made into the saturated zone of the unconfined aquifer. The degradation rates of these compounds in the Columbus aquifer were calculated, and these rates were related to the aquifer's structure and hydrologic properties.

The MADE-2 experiment was initiated with a 2-day pulse injection, beginning on June 26, 1990. Tritiated water tracer and organic solute concentration distributions were subsequently monitored in three dimensions at 1- to 3-month intervals over 15 months, using an extensive network of saturated zone multilevel samplers. Selected samplers were monitored more frequently during the experiment to develop complete concentration time-series at several points located in the path of the solute plume.

Migration behavior of the solutes during the experiment was primarily determined by spatial moments analysis of the concentration measurements. This method permitted comparison of the major features (e.g., relative mass, mean displacement, spatial covariance, skewness, and kurtosis) of the various solute plumes. Estimates of the relative mass (zeroth moment) of the conservative tracer during the study demonstrated the overall effectiveness

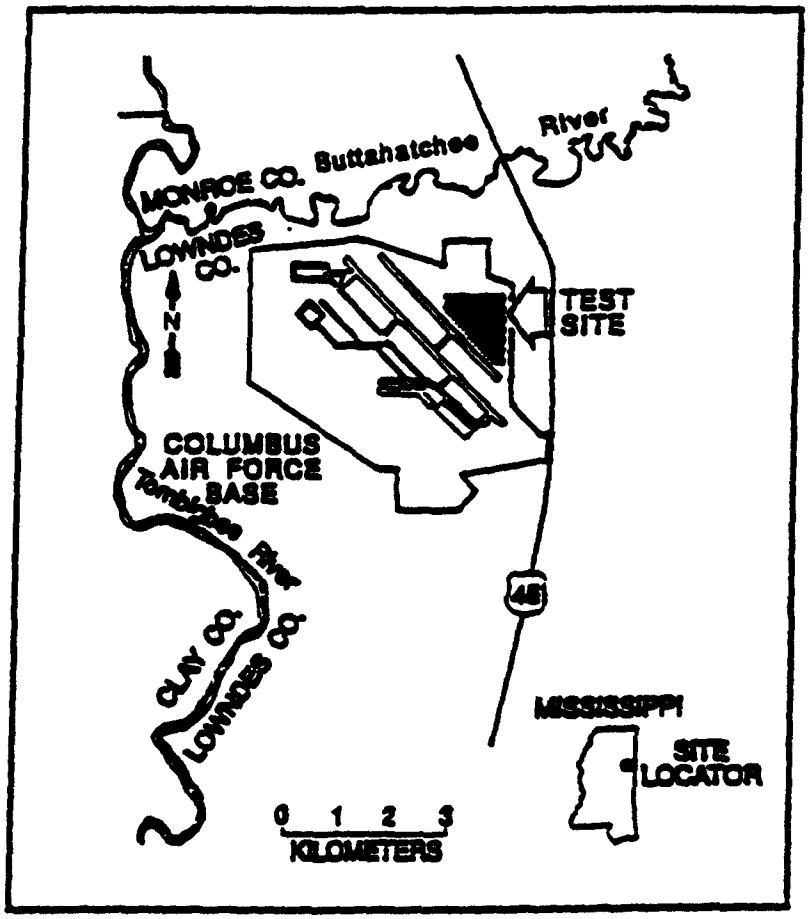

Figure 1. Test Site Location Map.

of the sampling program. Application of a nonuniform advection-dispersion model to the first three moments of the conservative tracer data was used to estimate the apparent aquifer dispersivity for the site. Comparisons between the relative mass estimated for the conservative tracer and the organic solutes provided a means of quantifying organic mass losses due to the combined effects of sorption and degradation.

A separate analysis of time-series data at selected points was done to estimate retardation factors and degradation rates for the organic solutes. Field estimates of sorption coefficients for these organic compounds, derived from this time-series analysis, were compared with estimates obtained from laboratory batch and column experiments. Results of these comparisons help establish the effectiveness of laboratory sorption measurements for predicting field-scale sorption behavior.

SECTION II
SITE DESCRIPTION

Hydrogeologic and geostatistical descriptions of the aquifer at the test site have been presented in several earlier publications (e.g., Boggs *et al.*, 1990 and 1992; Rehfeldt *et al.*, 1992). Relevant results from these works are summarized below, and provide the reader background information for use in interpreting the descriptions of solute behavior given in this report.

AQUIFER CHARACTERISTICS

The shallow unconfined aquifer which immediately underlies the site consists of alluvial terrace deposits averaging approximately 11 meters in thickness. The aquifer is composed of poorly- to well-sorted sandy gravel and gravelly sand with variable silt and clay content. Sediments are generally unconsolidated, and occur as irregular horizontal or nearly horizontal lenses and layers. Marine sediments belonging to the Eutaw Formation and consisting of clays, silts, and fine-grained sands, form an aquitard beneath this alluvial aquifer. Hydrogeologic properties of the Columbus aquifer and a description of the MADE site were given by Boggs *et al.* (1992).

Aquifer porosity, bulk density, and particle density were determined by gravimetric and volumetric analyses of 84 minimally disturbed soil cores by Boggs *et al.*, (1990). The sample mean bulk density of the 84 samples was 1.77 g/cm^3, and the standard deviation of the measurements was 0.18 g/cm^3. The mean and standard deviation of the particle density measurements were 2.57 and 0.07 g/cm^3, respectively. The mean and standard deviation of the porosity measurements were 0.31 and 0.08, respectively. A porosity of 0.35 is assumed for the spatial moments analysis presented later in the report, based on an estimation of core compaction used in analysis of the MADE-1 data (Adams and Gelhar, 1992). Boggs *et al.* (1990) also presented data showing the wide range of aquifer material particle sizes and the spatial heterogeneity of the particle size distributions within the Columbus aquifer.

Geostatistical analysis of 2187 measurements of the horizontal radial component of the hydraulic conductivity, K_h, by the borehole flowmeter method (Rehfeldt *et al.*, 1989a) indicates that the variance of the natural logarithm of K_h is 4.5 for the aquifer (Boggs *et al.*, 1990; Rehfeldt *et al.*, 1992). Hereafter in this report, K_h is referred to as the hydraulic conductivity, but this usage refers to the results of the bore-hole flow meter measurements, and does not represent a complete hydraulic conductivity tensor. Horizontal and vertical correlation scales of 12.8 and 1.6 meters, respectively, were also estimated from these data.

The K_h profile and the vertically-averaged K_h map presented on Figure 2 illustrates the extreme heterogeneity of this aquifer. Hydraulic conductivities measured at discrete vertical intervals in fully screened test wells typically range over two to four orders of magnitude at each test well. The spatial distribution of hydraulic conductivity varied from approximately 10^{-4} to 10^{0} cm/s. The magnitude of this K_h variability is apparent from comparison with the much less variable (10^{-4} to 10^{-3} cm/s) K_h field at the Borden Canadian Forces Base, Ontario, described by Robin *et al.* (1991). The mean hydraulic conductivity along the tracer travel path increases from approximately 10^{-3} cm/s near the injection point, or near field, to 10^{-2} cm/s and larger in the far-field. At the northern extreme of the test

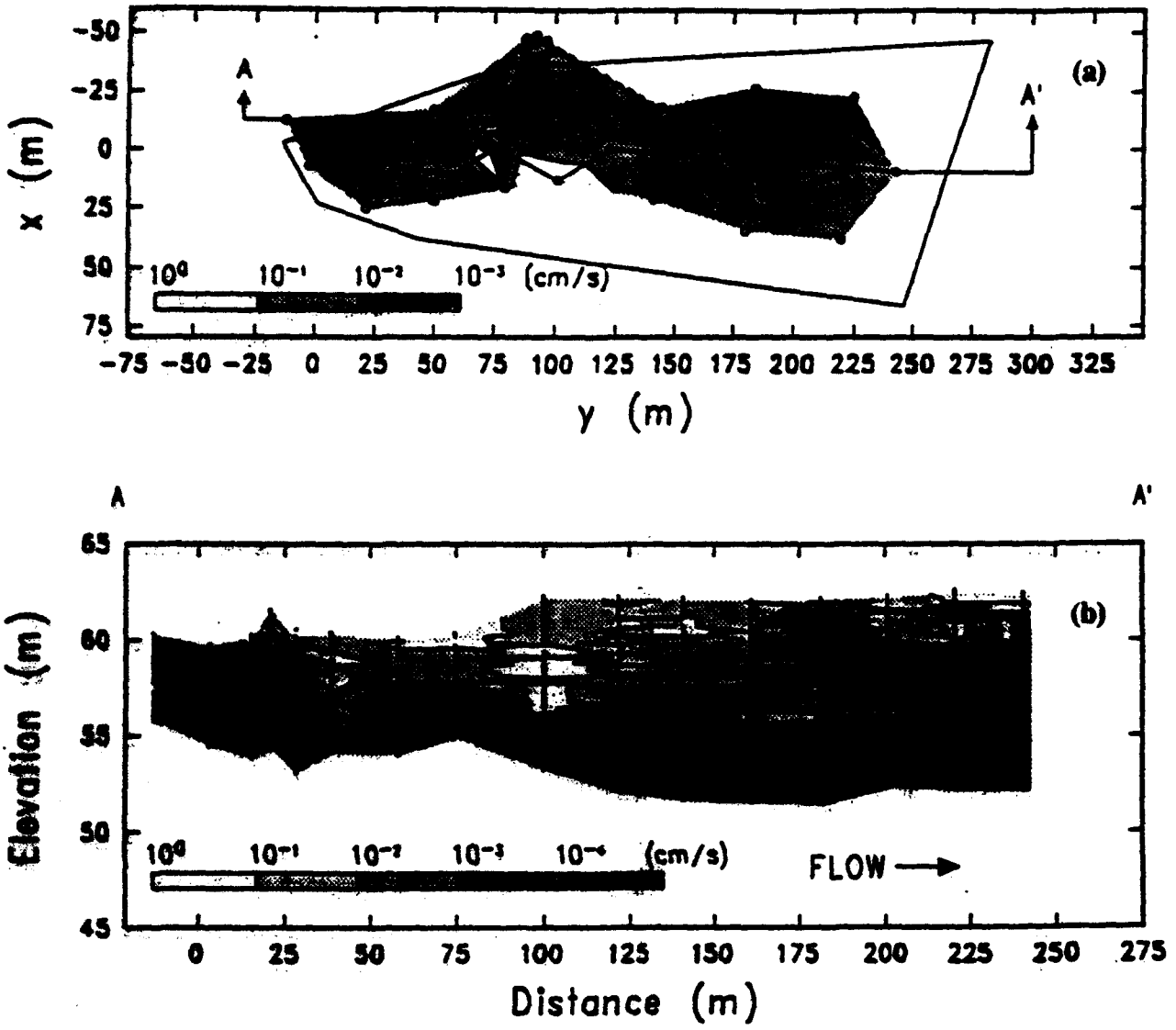

Figure 2. (a) Plan View Map of Vertically Averaged Hydraulic Conductivity, and (b) Hydraulic Conductivity Distribution Along Section A-A'.

site, the mean K_h again decreases to about 10^{-3} cm/s. The central region of relatively high mean K_h roughly corresponds to a former river meander. This meander trends southwest to northeast, and is at about a 45-degree angle to the general direction of groundwater flow (Figure 3). However, tracer tests indicate that groundwater flow does not follow the axis of the meander channel as might be expected if the channel represented a regionally continuous zone of relatively high mean K_h (Rehfeldt *et al.*, 1992). Note that all elevations presented in this report are referenced to mean sea level (MSL).

The large-scale spatial variations in mean K_h at the test site are related to the region of horizontally converging groundwater flow shown on Figure 3. The zone of convergent flow is associated with relatively high hydraulic conductivity sediments present downgradient of the injection point. Based on the observed migration of the bromide plume during MADE-1, groundwater velocity increases downgradient from this zone of convergence. The mean groundwater velocity probably decreases near the northern end of the sampling network due to a decrease in mean K_h.

SOIL MINERALOGY

Sand and gravel particles in the aquifer are composed of quartz, feldspar, and mica. Fine-grained materials (i.e., those passing the 0.074 mm sieve) consist of quartz, potassium feldspar, muscovite, and clay minerals. Clay minerals present are predominantly kaolinites and illites with minor amounts of montmorillonites and vermiculites. Soil particles are commonly coated with iron oxides. Measurements of free iron oxides range from 2.0 to 3.9 percent by weight for particles less than 2 mm in diameter, and from 0.5 to 0.8 percent for particles larger than 2 mm (Boggs *et al.*, 1990). MacIntyre *et al.* (1991) report low organic carbon contents for 50 samples of alluvium with measurements ranging from 0.02 to 0.06 percent by weight.

GROUNDWATER CHEMISTRY

Some chemical characteristics of the groundwater from wells in the alluvial aquifer at the site prior to this test are summarized in Table 1. The groundwater had a low total dissolved solids content averaging 43 mg/L. The ionic composition of the groundwater was dominated by sodium, silica and chloride. Total acidity averaged 71 mg/L (as $CaCO_3$). Alkalinity averages 10 mg/L, mainly in the form of bicarbonate. Dissolved carbon dioxide was quite high at the groundwater pH, which averages 4.8. The free CO_2 content averaged 57 mg/L, representing about 3 percent of the total dissolved gas concentration. The mean Eh of 543 mV indicates an oxidizing groundwater environment (Boggs *et al.*, 1990). These observations of groundwater chemistry are preliminary and only intended to describe the general chemical conditions the solutes might encounter. The number of wells sampled was not sufficient to allow estimation of the statistical significance of the measurements, and the set of chemical parameters sampled did not allow estimation of closeness to redox equilibrium in the groundwater. A more complete geochemical survey of the site is now being carried out to support micobiological experiments planned for a new test at the site.

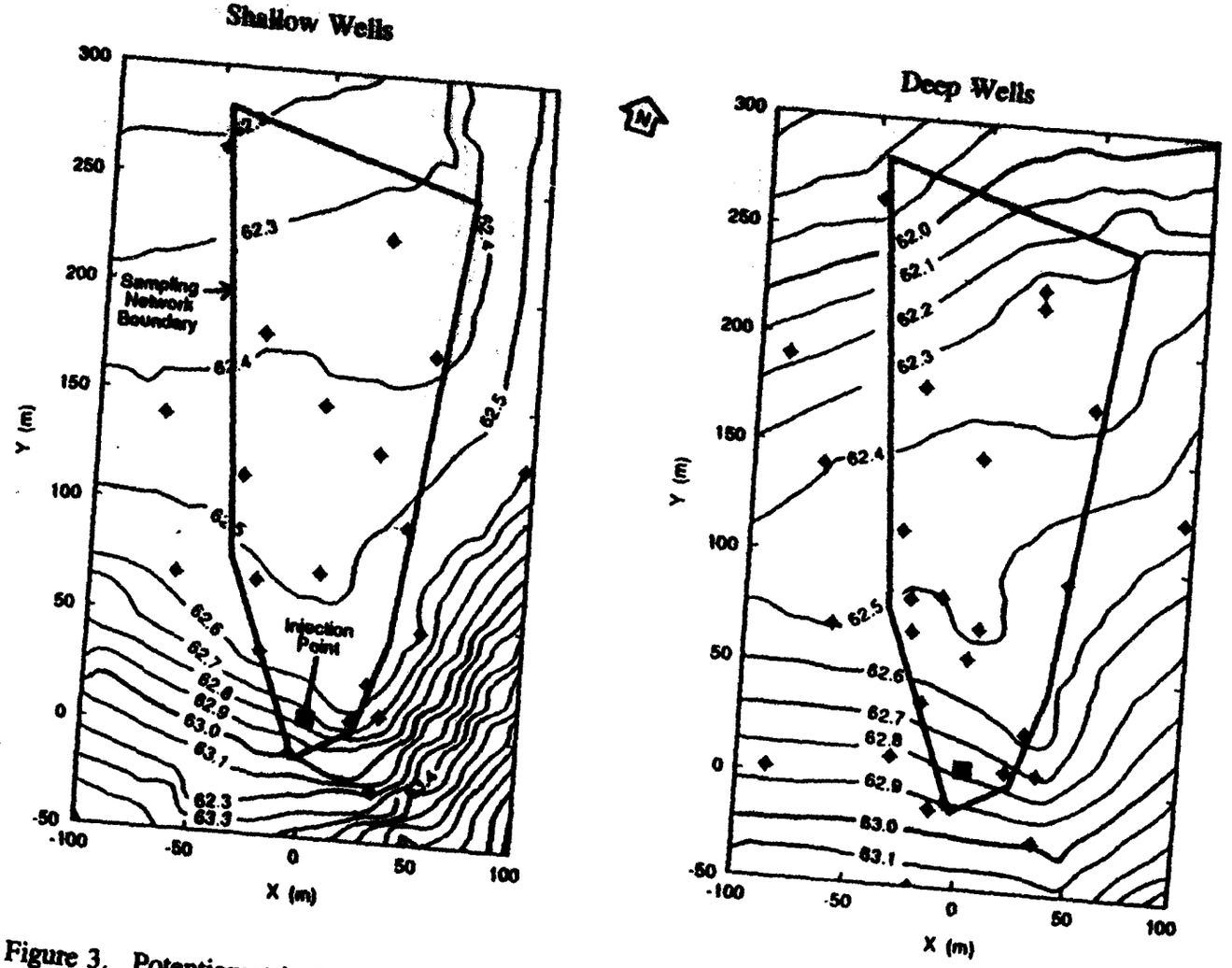

Figure 3. Potentiometric Surface Maps Derived from June 1990 Head Measurements in Shallow and Deep Observation Wells, Showing Regions of Converging Groundwater Flow.

TABLE 1. SUMMARY OF GROUNDWATER CHEMICAL CHARACTERISTICS

	mean	min	max	N
pH	4.8	4.3	5.2	21
Eh (mV)	543	410	672	16
conductivity (mmhos/cm)	45	25	74	16
temperature (°C)	17.9	9.8	20.9	18
total dissolved solids (mg/L)	43	30	70	6
acidity (mg/L $CaCO_3$)	71	36	93	11
alkalinity (mg/L $CaCO_3$)	10	2	35	15
Ca-Mg hardness (mg/L $CaCO_3$)	7.8	7.7	8.0	2
total organic carbon (mg/L)	2.3	--	--	1
sodium (mg/L)	5.3	--	--	1
silica (mg/L)	5.0	--	--	1
calcium (mg/L)	1.8	1.7	1.8	2
magnesium (mg/L)	0.84	0.77	0.92	2
potassium (mg/L)	0.6	--	--	1
iron (μg/L)	15	--	--	1
copper (mg/L)	7.5	5	10	2
zinc (mg/L)	2.6	--	--	1
manganese (mg/L)	1.5	--	--	1
chloride (mg/L)	8.0	6.0	10.0	2
sulfate (mg/L)	2.0	1.0	3.0	2
nitrate-nitrite (mg/L)	1.5	1.1	1.8	2
bromide (mg/L)	0.05	0.04	0.06	7
sulfide (mg/L)	8	7	8	2
total dissolved gas (%)	110	105	114	6
dissolved oxygen (mg/L)	4.2	1.6	6.7	14
free CO_2 (mg/L)	56	56	57	2
CO_2 (mg/L)	73	58	88	2

SECTION III
METHODS

TRACERS AND REACTIVE SOLUTES

Solutes selected for the experiment are listed in Table 2, along with the initial concentration and total injected mass (activity) for each solute. Tritiated water served as the conservative reference tracer. The four organic compounds chosen, benzene, naphthalene, p-xylene, and o-dichlorobenzene (o-DCB), are common constituents of various fuels and solvents. These compounds vary considerably in their mobility in aquifer materials and in their susceptibility to biotransformation in laboratory systems. Tabak *et al.* (1981) reported significant degradation with rapid adaptation for laboratory studies involving benzene and naphthalene, whereas o-dichlorobenzene showed slower rates of degradation with gradual adaptation followed by a de-adaptive process. A small fraction of the injected p-xylene was ring-labeled with ^{14}C to permit measurement of the degradation of p-xylene to its reaction products.

TABLE 2. INITIAL SOLUTE CONCENTRATIONS AND MASSES (ACTIVITIES)

Tracer	Mean Concentration	Mass/Activity Injected
tritium	55,610 pCi/mL	0.5387 Ci
^{14}C (p-xylene)	2770 pCi/mL	0.0268 Ci
benzene	68.1 mg/L	659.7 g
p-xylene	51.5 mg/L	402.0 g
naphthalene	7.23 mg/L	70.0 g
o-dichlorobenzene	32.8 mg/L	317.7 g

SOLUTE INJECTION

The method of solution injection was similar to that used in the earlier MADE-1 bromide experiment (Boggs *et al.*, 1992). The solution was injected through five wells spaced 1-meter apart in a linear array (Figure 4). Each injection well was screened over a 0.6-meter interval between the elevations of 57.5 and 58.1 meters. The entire injection was completed over a period of 48.5 hours beginning June 26, 1990, at a uniform rate of 3.3 L/min. The total volume of solution injected was approximately 9.7 cubic meters. The maximum increase in hydraulic head near the injection wells was 0.45 meters.

The injection solution was prepared and stored on-site. Ambient groundwater from a well located approximately 75 meters upgradient from the injection point was used to prepare the solution. The tritium and pure-phase organic compounds were mixed and stored in two thermally insulated 2.7 m^3 volume tanks, each equipped with a floating lid and an impeller mixer. Samples of the injection solution were collected at 1- to 2-hour intervals from the

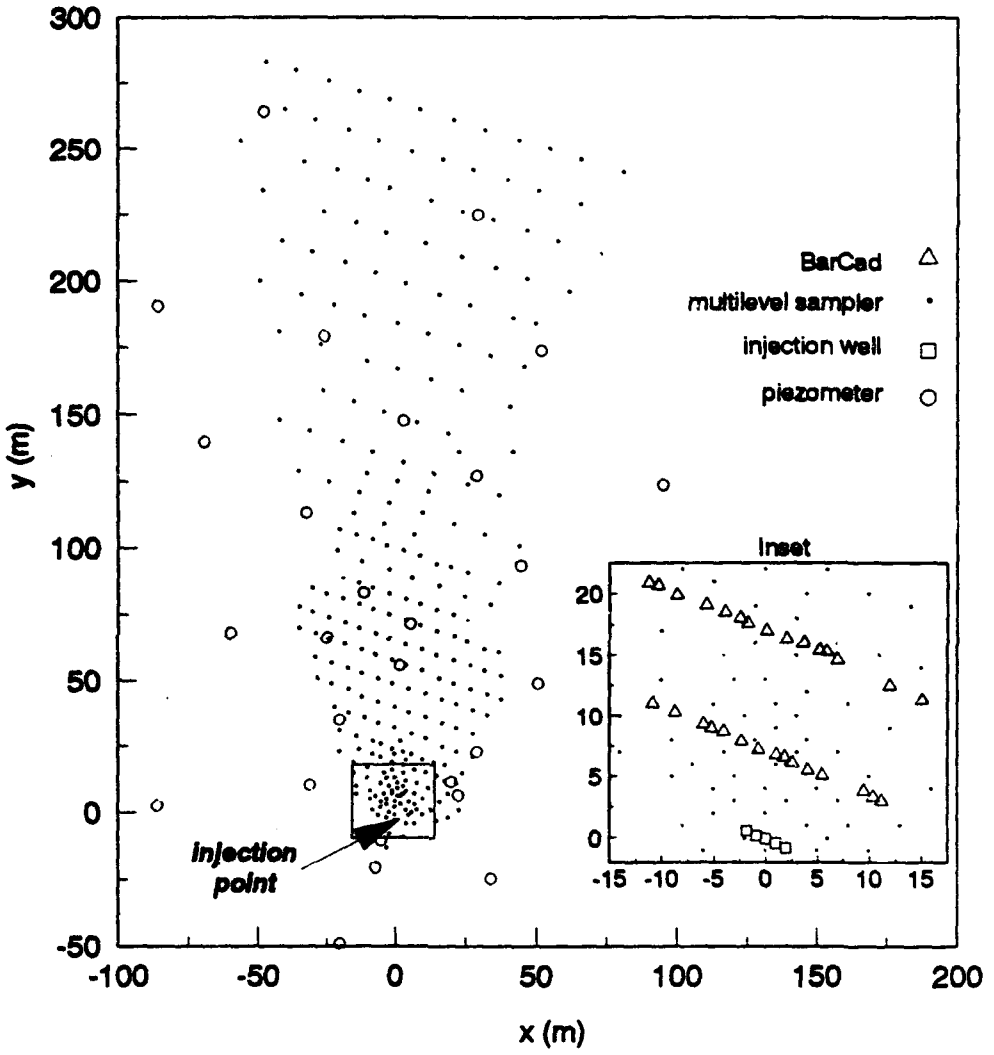

Figure 4. Map of Well Network Showing Injection Wells, MLS, and BarCad® Samplers.

tubes leading to the injection wells. The injected mass (activity) for each solute was calculated from the concentration measurements for the samples taken during injection.

SOLUTE MONITORING

Figure 4 also shows the locations of the 328 multilevel samplers (MLS) used to monitor the solute plumes in three dimensions during the experiment. Locations of sampling points are defined in a three-dimensional Cartesian coordinate system, with the origin at the center of the injection. The x axis is approximately normal to the plume trajectory, the y axis is approximately parallel to the plume trajectory, and the z axis represents the elevation of sampling points above MSL. Specifically, the positive y axis points in a direction 12 degrees West of true North.

Details regarding the design and construction of the multilevel samplers are given by Boggs *et al.*, 1988. Each MLS was equipped with 20 to 30 sampling points spaced 0.38 meters apart in the vertical dimension. Groundwater samples from each MLS were simultaneously collected using a mobile sampling cart equipped with three, 10-channel peristaltic pumps. Sampling protocols required the purging of 120 mL (approximately four sample tube volumes) of groundwater prior to the collection of a 25 mL sample in a glass vial with a Teflon®-lined septum cap. Before sealing, 0.1 mL of a 10 percent sodium azide solution (a bacteriostat) was added to each water sample. Finally, they were refrigerated at approximately 4°C and stored in an inverted position (i.e., capped end down) until analyzed. Five, three-dimensional sampling events (snapshots) of the solute plumes were performed at approximately 100-day intervals during the study. General information related to these sampling events is given in Table 3. Note that the fifth snapshot, conducted at 440 days, only defined the organic solute plumes, which occurred in the region near the injection wells and did not cross the well field boundaries. At 440 days, the tritium and ^{14}C plumes had crossed the downgradient boundary of the well field, and thus were not completely sampled during the fifth snapshot.

TABLE 3. GROUNDWATER SAMPLING SUMMARY

Sampling Event*	Date	Elapsed Time (days)	No. Wells Sampled	Samples Analyzed
F01	Jul 9-11, 1990	13	26	264
S21	Jul 23-27, 1990	27	99	1226
F02	Aug 13-17, 1990	48	31	287
F03	Sep 17-19, 1990	83	53	185
F04	Oct 5-17, 1990	111	39	72
S22	Nov 5-8, 1990	132	111	871
F05	Dec 3-4, 1990	160	29	195
F06	Jan 8-9, 1991	195	25	196
S23	Feb 5-7, 1991	224	190	1976
F07	Apr 3-5, 1991	281	42	387
S24	May 21-23, 1991	328	205	2345
S25	Sep 9-11, 1991	440	79	460

* F = fenceline event; S = snapshot

Fifty-six positive displacement BarCad® water samplers, manufactured by Goldberg, Zoino and Associates, Newton MA, were installed in wells that formed two parallel rows or "fencelines" oriented normal to the general flow direction. Their locations are also shown in Figure 4. The BarCad® samplers were permanently installed at fixed depths in uncased, back filled boreholes. Several samplers were installed in each borehole to allow sampling at multiple depths.

The BarCad® sampler contains a check valve and porous filter through which water passes before exiting to the surface in a small riser tube, which is inside of a larger gas drive tube (0.5 and 1.3 cm diameter, respectively). The device uses a closed-system pressure drive principle (positive inert gas displacement) to collect the sample and maintain sample integrity. Ceramic filters were selected for this application based on the results of laboratory tests of sampler efficiency, using standard hydrocarbon solutions.

The two fence rows were located at distances of approximately 6 and 16 meters from the injection point. The vertical distribution of the sampling points across each row is shown in Figure 5. BarCad® sampling devices were installed in 15 cm diameter auger holes with no more than two samplers per hole. Bentonite seals approximately 0.6 meters thick were placed in the annular space above and below each sampling point to hydraulically isolate sampling points installed in the same auger hole.

Samples from the fence rows of BarCad® points were taken at frequent intervals to provide time-series data for analysis of organic solute sorption, retardation and degradation. The sampling frequency varied from 2 week intervals initially to 3 month intervals later in the study, as shown in Table 3. Time-series samples were also collected at a few MLS points concurrently with the BarCad® fence row samplings. Results from both of the samplers were used to determine the similarity of hydrocarbon sorption and degradation

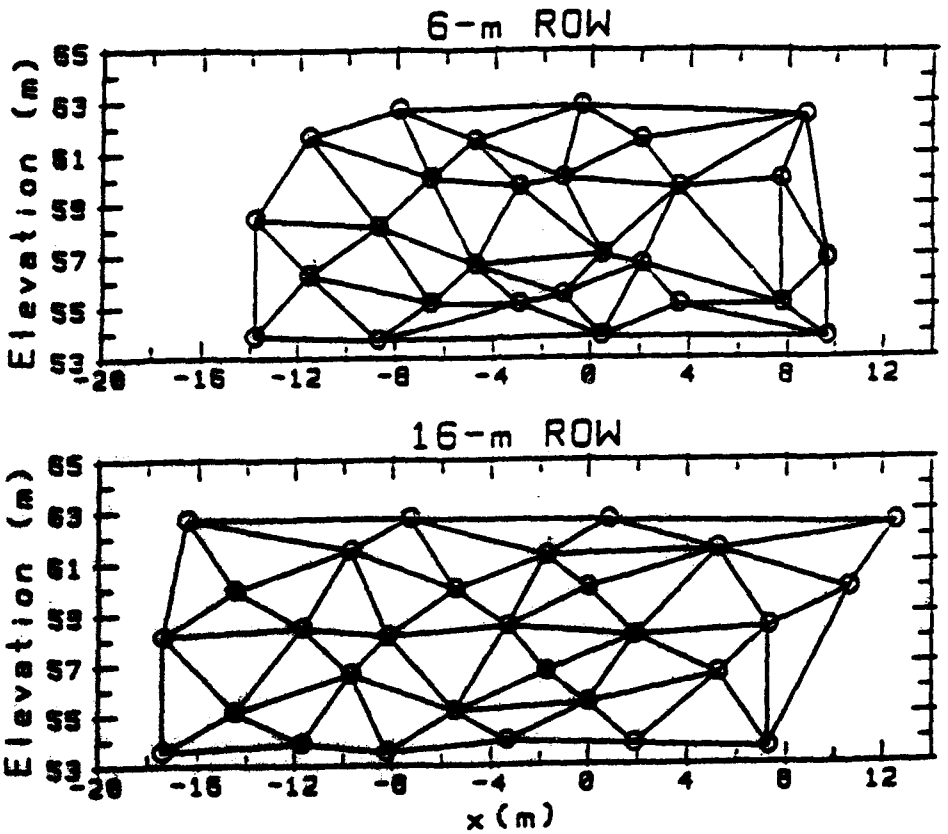

Figure 5. Vertical Profile of BarCad® Sampling Points (Open Circles); Lines Between Points Represent the Triangular Interpolation Grid.

parameters calculated from time-series MLS data and from time-series BarCad® data. This test of sampler similarity is described in more detail in Section 6.

As shown in Figure 4, the spatial density of MLS wells near the injection wells is high, and BarCad® sample points in the fence row wells are close to MLS sample points in the nearby MLS wells. This proximity enables comparisons to be made between concentrations of solutes obtained simultaneously by the MLS and BarCad® samplers during the field experiment. The BarCad® samplers thus provided an indirect test of the probability of solute loss during sampling due to sorption and vaporization. Since the principles of operation and materials of construction differed between the two sampler types, the observed agreement of concentration results for samples from proximal BarCad® and MLS sample points indicates that losses associated with a particular sampler were probably small. If such losses did occur, it is unlikely that they would be equal for the different sample devices. The use of BarCad® samplers rather than MLS samplers in the fence rows served three purposes: (1) to demonstrate the utility of BarCad® samplers, (2) to obtain time-series concentration data, and (3) to demonstrate that solute losses during sampling did not pose a problem. The third purpose is obviously critical to attainment of the first two, and fortunately, the BarCad® data compared well with MLS data from adjacent wells. This agreement could be confirmed by a nearest neighbor comparison of solute concentrations between BarCad® and MLS well points , but this task would be extremely tedious. An alternative comparison is made here, based on the presence (see Figure 4) of rows of MLS wells immediately upgradient and down gradient of the BarCad® fence rows.

At each sampling time, an average concentration for each solute was computed separately for all of the BarCad® sampling points in each fence row, and for the sampling points in the associated upgradient and downgradient MLS rows. Results for the fence row at 6 meters from the injection wells are given in Table 4. Comparison of the average concentrations of solutes in the two sampler types shows that the results are reasonable, with a general trend of decreasing values from the upgradient MLS row to the BarCad® fence row, and finally to the downgradient MLS row. These findings appear to support the utility of BarCad® samplers for such a purpose. Unfortunately, this comparison must be mainly subjective due to the heterogeneity of the aquifer and the unavoidable spatial separation of MLS and BarCad® sampling points.

ANALYTICAL METHODS

Stable organic compounds in water samples were analyzed by gas chromatography (GC). Deuterated toluene and 4-bromofluorobenzene internal standards were added to 20 mL water samples, which were then extracted with 2 mL of n-pentane. The extracts were analyzed for benzene, p-xylene, naphthalene and o-dichlorobenzene by GC, using a 30-meter long, 0.32 mm i.d. fused silica column with 1 μm thick DB-5 bonded phase coating and flame ionization detection. Helium carrier gas flow was set at 3-5 mL/min and the split ratio was 10:1. The initial column temperature was held at 50°C for 1 minute and was then increased at 10°C/min to 150°C, which was held for 5.5 minutes. Sensitivity of the method was 50 μg/L for benzene and 4 μg/L for the other compounds. All samples were extracted and analyzed within 21 days of collection.

Quality control for the organic analyses was ensured by using several techniques. First, analytical precision was checked through duplicate analysis of sample extract splits for

TABLE 4. AVERAGE SOLUTE CONCENTRATIONS IN 6 METER FENCE ROW BARCAD® SAMPLERS AND IN ADJACENT ROWS OF MLS SAMPLERS (μg/L for Hydrocarbons and pCi/mL for Radioisotopes)

Upgradient MLS row

T(days)	[Ben]	[Nap]	[p-Xyl]	[o-DCB]	[^{3}H]	[^{14}C]
83	416.0	26.2	226.2	176.8	611.4	6.1
132	573.6	57.4	458.9	406.3	915.2	34.0
160	525.4	73.6	453.4	468.7	957.4	35.5
224	387.5	55.7	271.5	353.4	701.1	25.5
279	372.9	41.2	59.0	268.5	526.8	20.5
328	140.3	16.3	35.7	99.1	344.5	13.2
440	148.2	14.8	9.4	93.3	243.5	9.1

BarCad® fence row

T(days)	[Ben]	[Nap]	[p-Xyl]	[o-DCB]	[^{3}H]	[^{14}C]
83	388.4	24.1	246.3	218.0	529.3	16.9
132	167.2	16.1	127.4	153.8	457.9	12.3
160	122.2	14.0	81.9	133.7	349.2	9.9
224	191.9	18.1	123.6	154.7	400.1	11.5
279	121.2	12.3	60.2	113.1	295.6	9.3
328	61.7	4.6	7.5	57.4	486.0	15.5
440	86.5	11.6	18.3	90.2	254.0	7.3

Downgradient MLS row

T(days)	[Ben]	[Nap]	[p-Xyl]	[o-DCB]	[^{3}H]	[^{14}C]
132	235.4	25.9	163.3	197.2	383.4	14.7
224	127.3	14.5	62.3	97.0	230.1	9.8
328	81.3	8.1	11.9	46.0	158.0	6.9
440	104.8	10.7	13.4	77.4	193.4	8.2

5 percent of the field samples. Second, certified standard solutions obtained from an independent source were used to make 100 μg/L control standards for each organic solute. These control standards were analyzed at a frequency equivalent to approximately 5 percent of the field samples to verify analytical accuracy. Third, 4-bromoflourobenzene was added as an internal standard for all analyses, and deuterium-labeled toluene was used as a surrogate. Finally, duplicate field samples representing approximately 5 percent of the total field samples collected for each sampling event were analyzed by the Mississippi State Chemical Laboratory located at Mississippi State University (MSU), as an independent verification of the analytical results.

Tritium and ^{14}C in samples from the wells were analyzed by liquid scintillation counting in dual-isotope mode, by the Water Resources Research Center at MSU. A 5.0 mL aliquot of each sample was emulsified in 15 mL of Pico-Flour 40 (Packard Instrument Co.) cocktail, and held in darkness for at least 1 hour prior to counting. Samples were counted on

a Packard Model 2250A for 20 minutes or to a 1 percent error at the 95 percent probability level, whichever was attained first. Background levels of tritium and ^{14}C in ambient groundwater at the test site dictated the analytical sensitivity for these experimental measurements, and were approximately 2 and 3 pCi/mL, respectively. The statistical errors associated with 20-minute measurements at these levels are about ± 20 percent at the 95 percent probability level.

A set of tritium and ^{14}C standards, including one National Bureau of Standards traceable standard, was counted every 108 samples to check analytical accuracy and verify instrument performance. Every twenty-fifth sample was counted twice to estimate measurement precision and repeatability. As an overall check on the radiological measurements, duplicate field samples amounting to roughly 5 percent of the total field samples were analyzed independently by the TVA Western Area Radiological Laboratory. The quality control data for the radiological and stable compound analyses can be obtained from the Tennessee Valley Authority Engineering Laboratory, Norris TN.

DISSOLVED OXYGEN MONITORING

Dissolved oxygen (DO) measurements were performed at 2- to 3-month intervals at selected locations during the experiment. DO data were intended to demonstrate whether aerobic conditions for possible degradation of the organic compounds were maintained. As shown in Figure 6, DO monitoring wells included 16 MLS located along the longitudinal axis of the tracer plume, and 6 piezometers. Three DO samples were collected from each MLS using a peristaltic pump. The mean elevations of these sample points were approximately 54.0, 57.4, and 61.2 meters above MSL, corresponding to the lower, middle and upper sections of the aquifer. Samples were collected in 60 mL BOD bottles after purging approximately 100 mL from the MLS tubes. Measurements were made with a calibrated DO probe immediately after sample collection. The DO measurements at the 6 piezometers were made in conjunction with pH, conductivity, and oxidation-reduction potential measurements. Samples were collected from the piezometers using a bladder pump, and DO was measured with a calibrated in-line probe. Field DO data and coordinate locations of the DO sampling points are given in Appendix A.

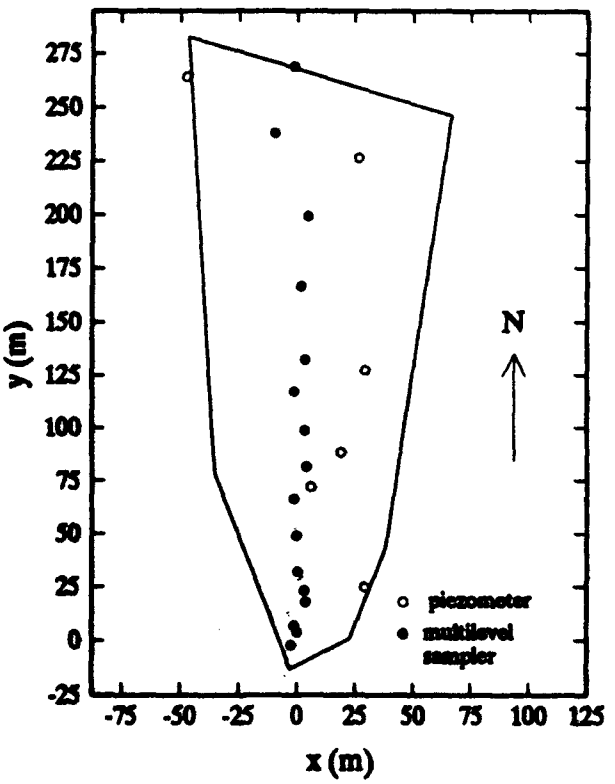

Figure 6. Locations of Dissolved Oxygen Monitoring Points.

SECTION IV
EXPERIMENTAL OBSERVATIONS

The observed transport and fate of tritium and organic solutes during the experiment are qualitatively represented and described in this section. Evolution of the various solute plumes in space and time are shown in a series of graphs of the spatial concentration distributions of each solute for each snapshot. To facilitate direct comparison of the transport behavior of the various solutes, all concentration data are presented in terms of relative concentrations, i.e., concentrations have been normalized to their respective initial injection concentrations.

Relative (normalized) concentrations are generally used in this report. The raw concentrations and other field data can be obtained by request from the Tennessee Valley Authority Engineering Laboratory, Norris, TN.

TRITIUM PLUME

Vertical profiles (sections) of tritium activity along the longitudinal axis of the plume for the first four snapshots are presented in Figure 7. Note for reference that ground surface level is at approximately 65 meters above MSL in these profiles. A similar set of plots showing horizontal sections through the tritium plume at elevation 59.5 meters is given in Figure 8. The dominant feature indicated by both figures is the extreme asymmetry of the tritium activity distribution in the longitudinal dimension. In this respect, the tritium plume was quite similar to the MADE-1 bromide plume described by Adams and Gelhar (1992). After 328 days, the most concentrated region of the plume remained within roughly 20 meters of the injection point, while the leading edge of the plume extended downgradient a distance in excess of 260 meters.

This tritium migration behavior is consistent with the hydraulic conductivity distribution along the plume travel path, shown in Figure 9. The slow rate of displacement of the main body of the plume in the near-field corresponds to the relatively low mean hydraulic conductivity (approximately 10^{-3} cm/s) in this region. At about 20-30 meters downgradient of the injection point, the mean conductivity of the aquifer increases by one to two orders of magnitude. Based on the 260 meter minimum displacement of the tritium front within 224 days of injection, groundwater velocities within the more permeable sediments in the far-field in excess of 400 m/yr are indicated. The most likely conclusion is that the extreme skewness of the tritium plume was produced by accelerating groundwater flow, which was itself caused by large-scale spatial variations in mean hydraulic conductivity.

ORGANIC SOLUTE PLUMES

Longitudinal profiles through the benzene, naphthalene, o-dichlorobenzene, p-xylene, and ^{14}C plumes for each snapshot are presented in Figures 10-14. Corresponding tritium plume profiles for each date are given at the top left of each figure for comparison of solute transport. Benzene and naphthalene showed similar transport behavior during the study. Both had limited horizontal displacement compared with tritium, and the maximum downgradient extent of both plumes was only about 25 meters. The gradual disappearance of

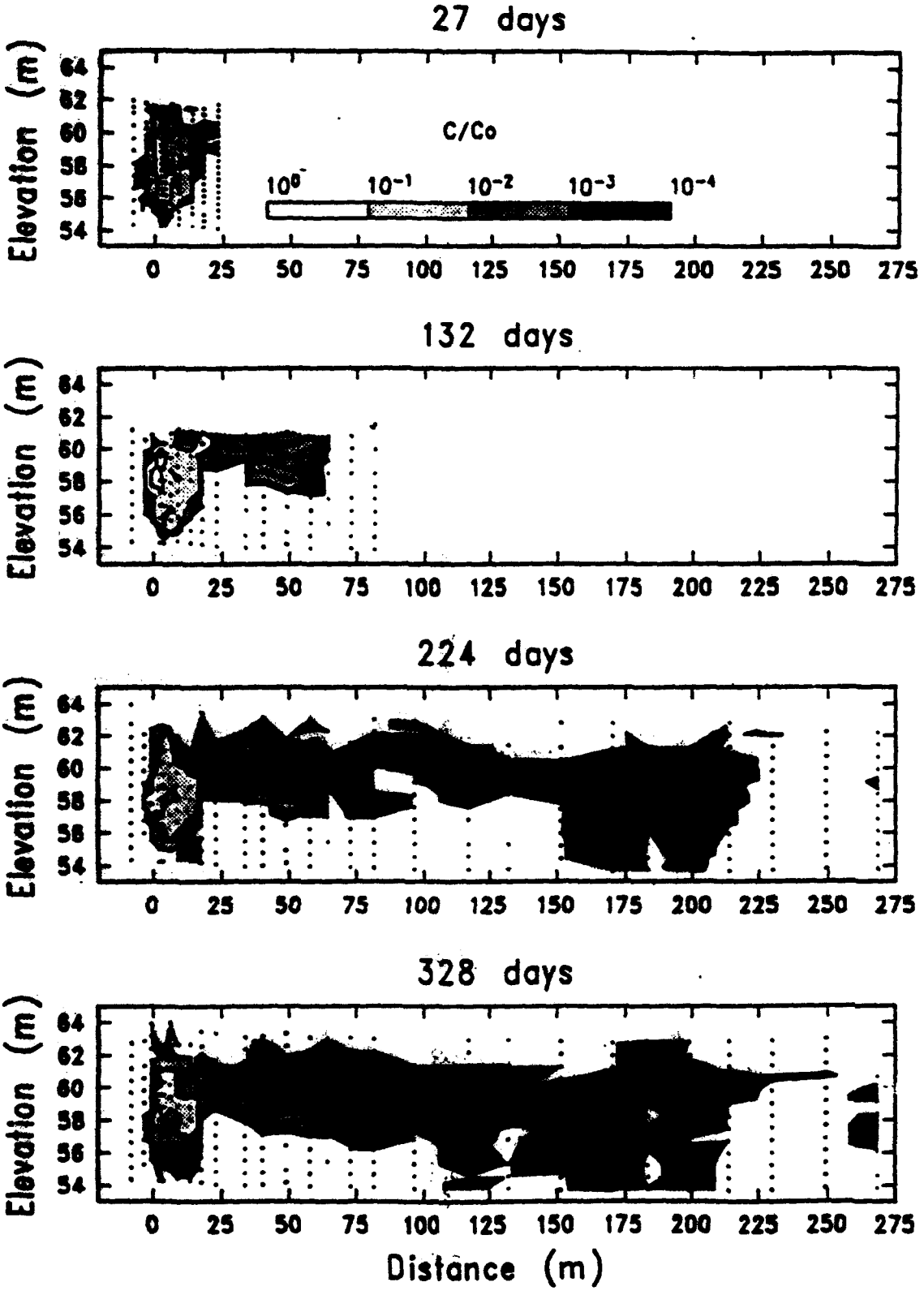

Figure 7. Tritium Relative Activity Profiles in the Longitudinal Direction.

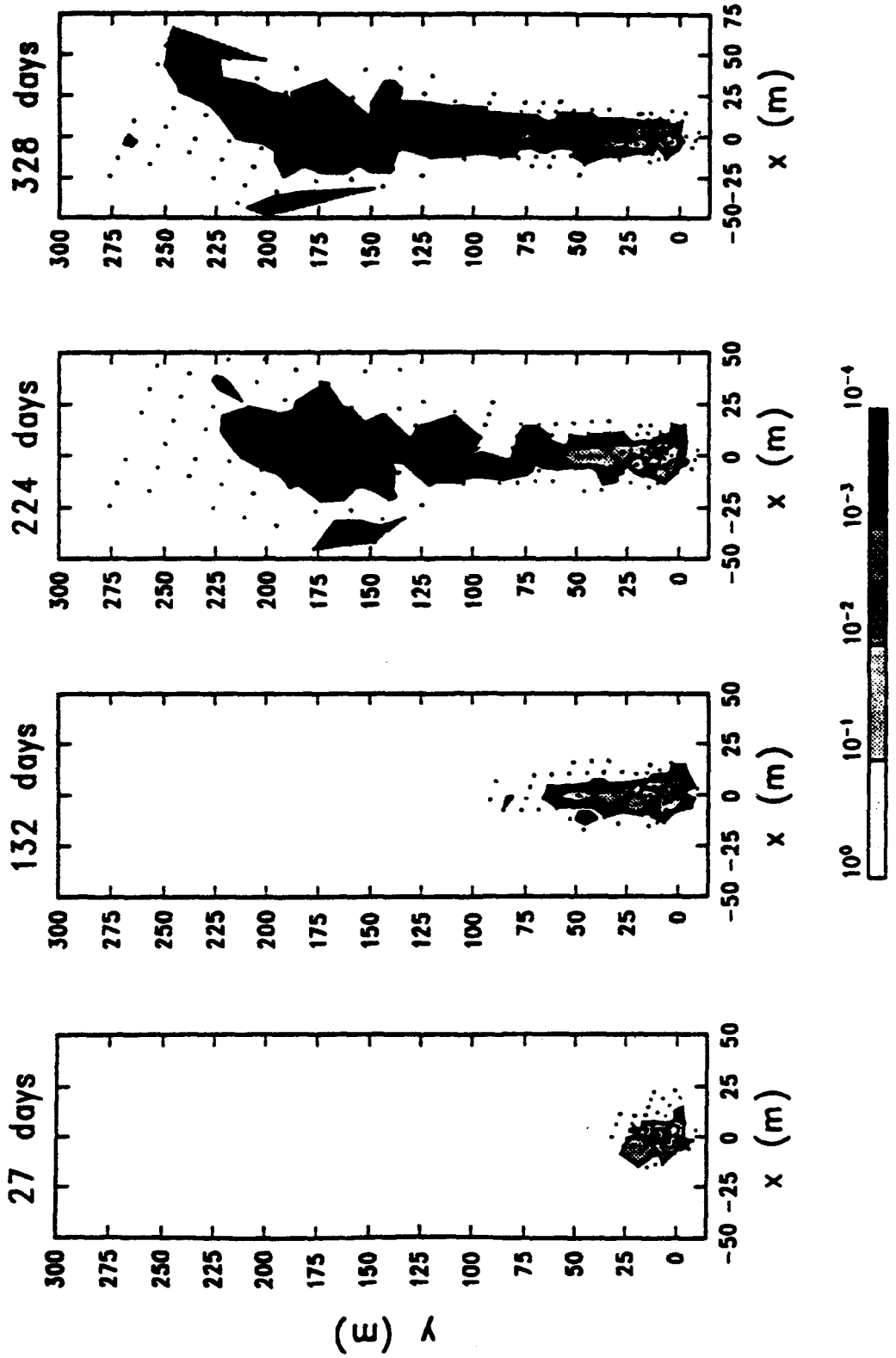

Figure 8. Horizontal Sections Through Tritium Plume at Elevation 59.5 m at 27, 132, 224, and 328 Days.

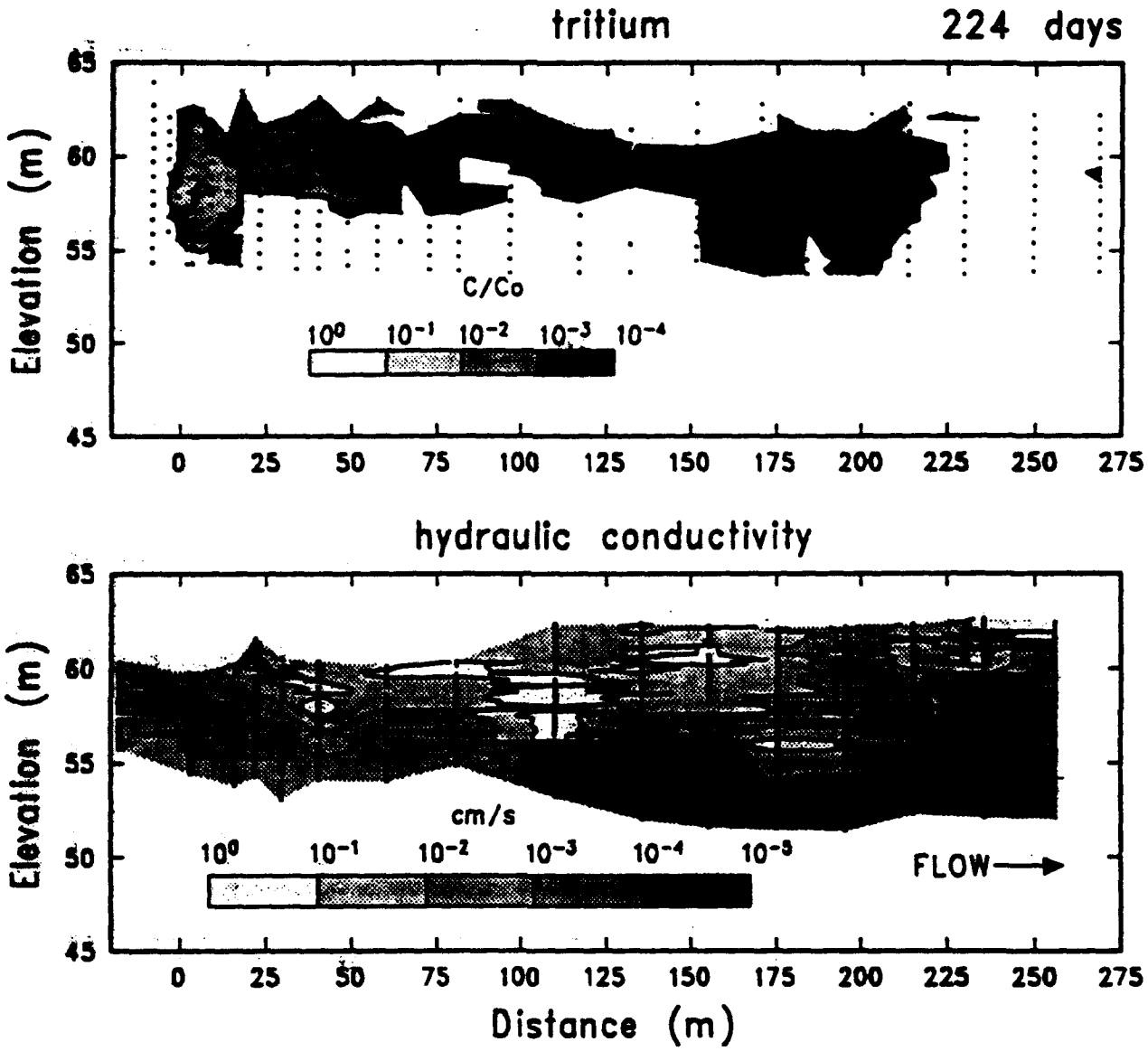

Figure 9. Comparison of Tritium and Hydraulic Conductivity Profiles in the Longitudinal Direction.

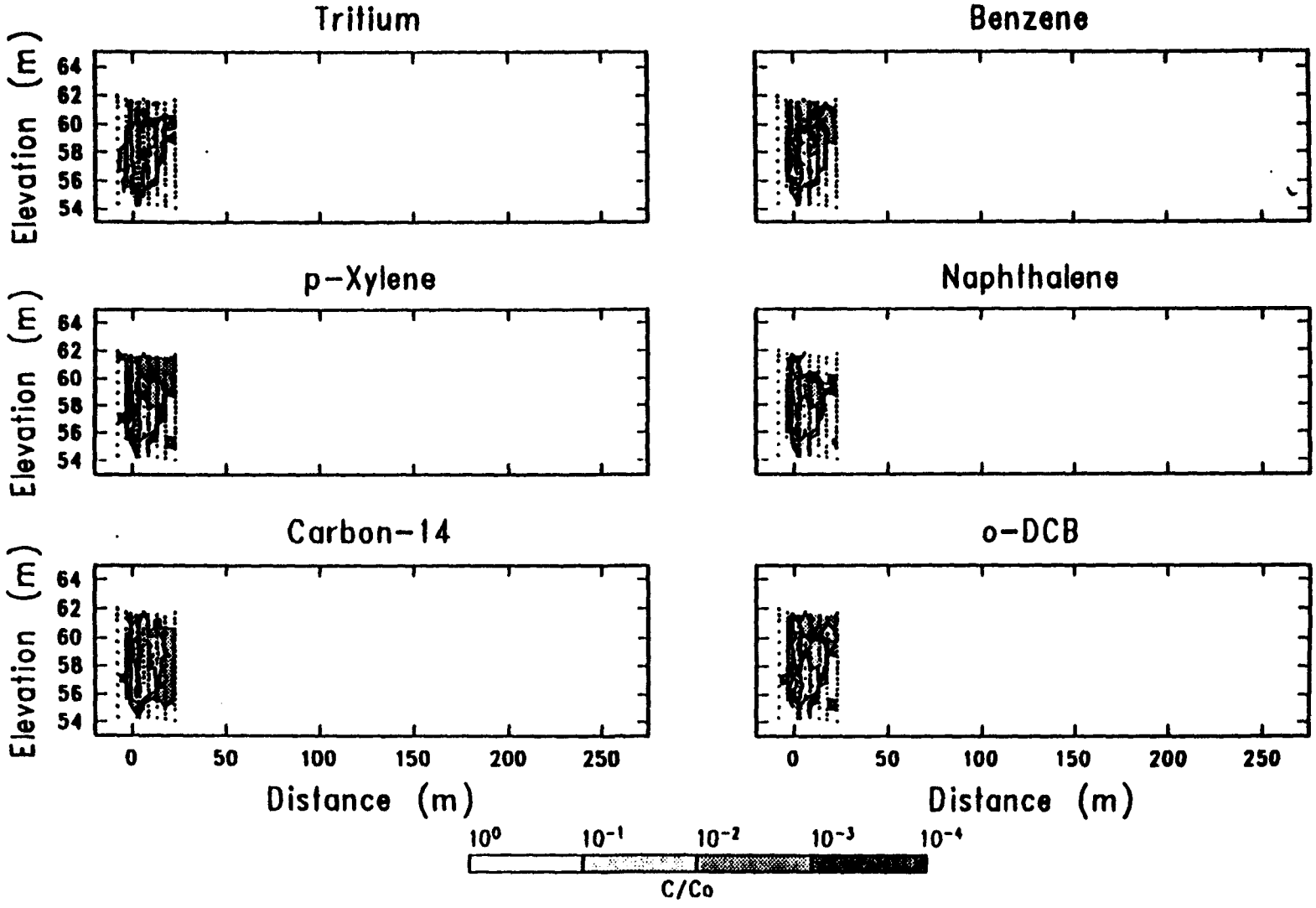

Figure 10. Longitudinal Profiles of Relative Concentration for All Solutes at 27 Days.

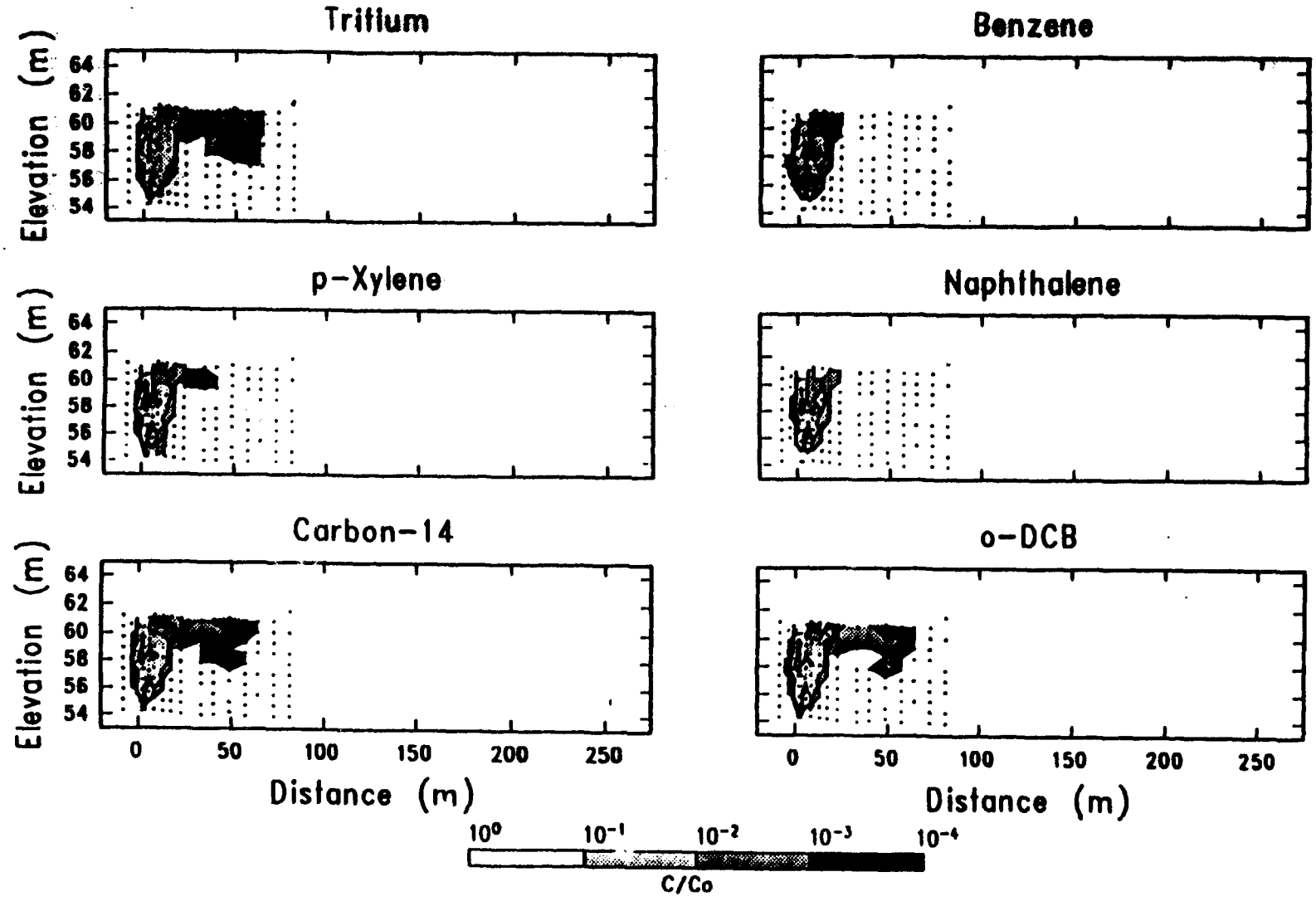

Figure 11. Longitudinal Profiles of Relative Concentration for All Solutes at 132 Days.

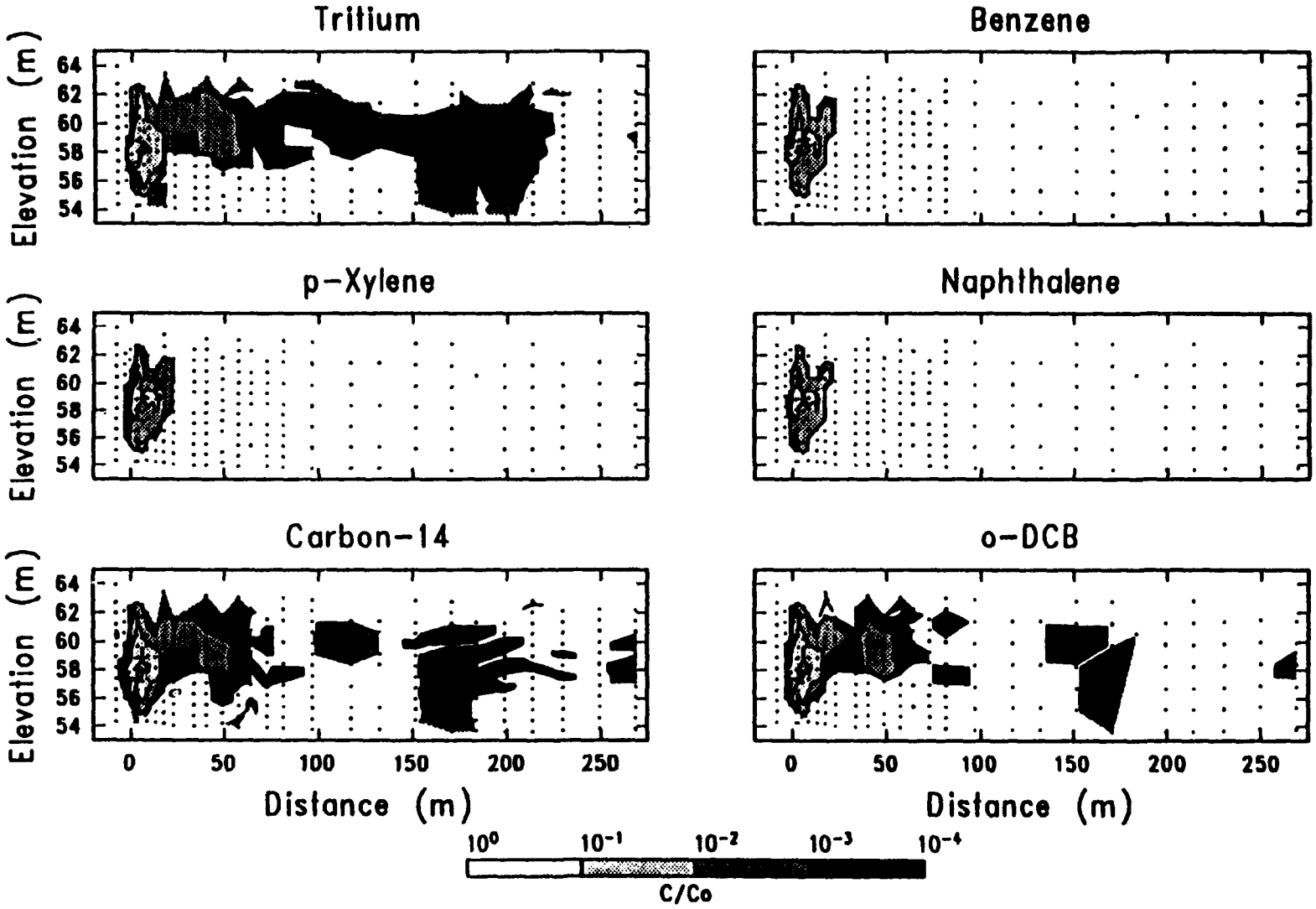

Figure 12. Longitudinal Profiles of Relative Concentration for All Solutes at 224 Days.

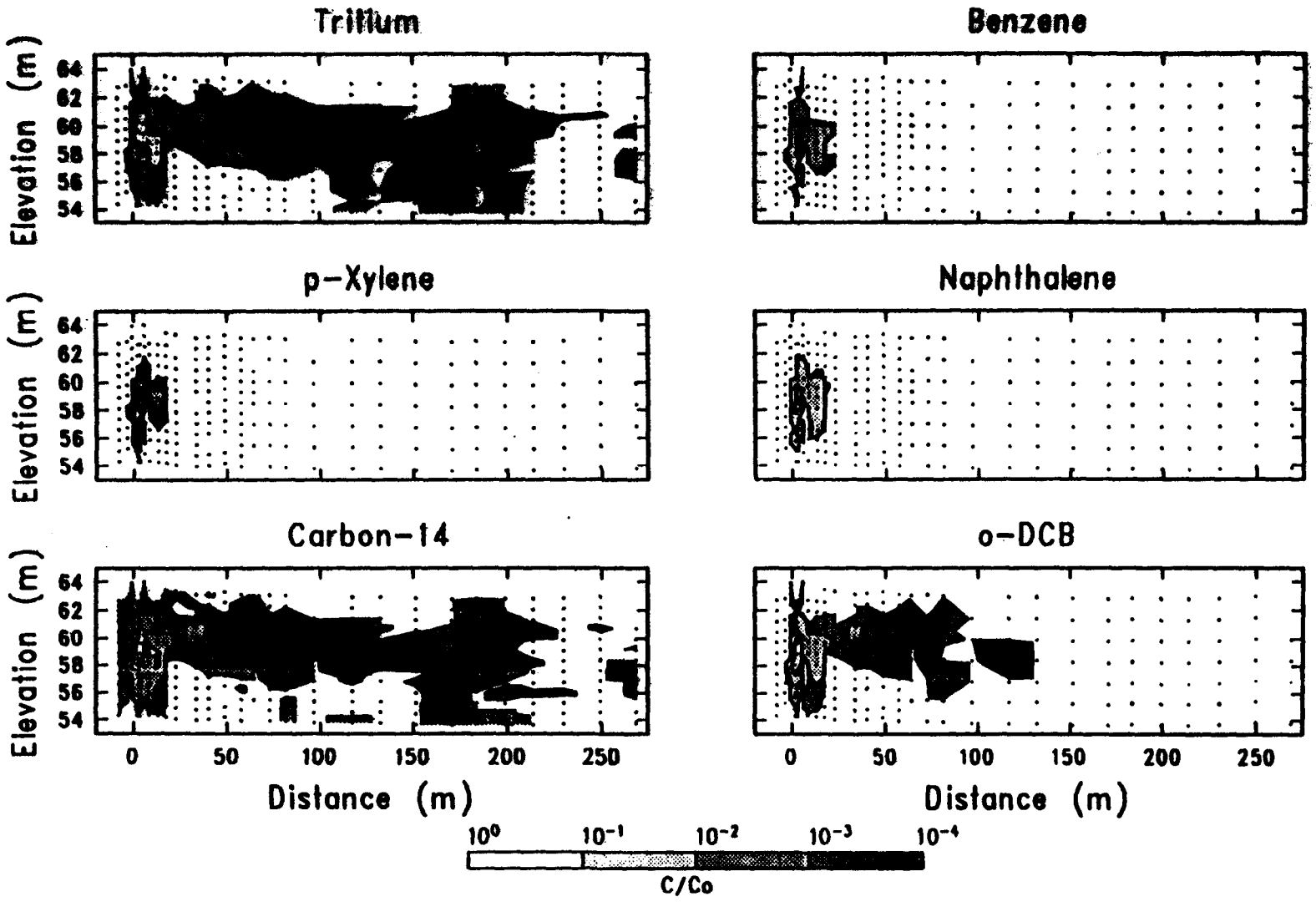

Figure 13. Longitudinal Profiles of Relative Concentration for All Solutes at 328 Days.

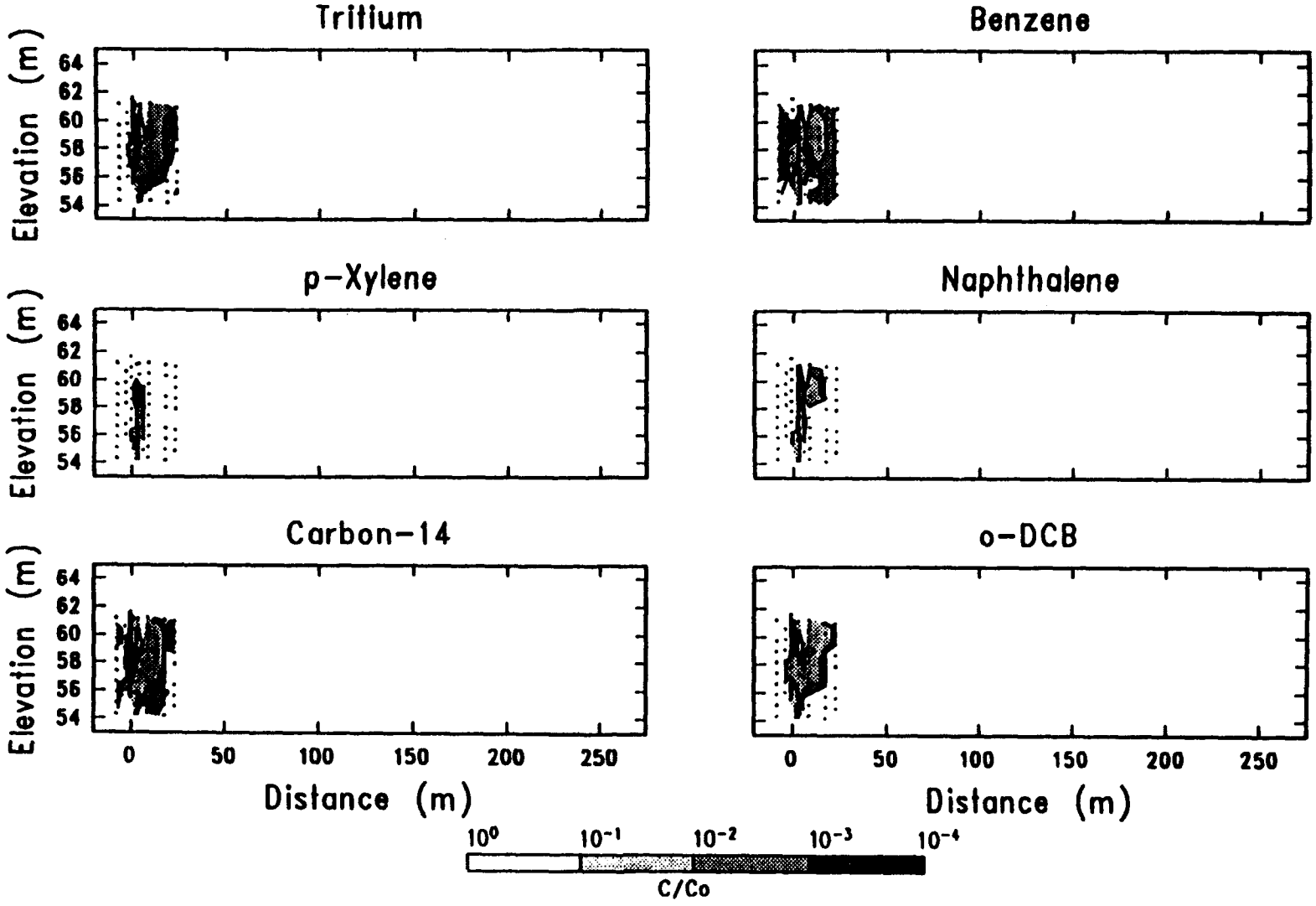

Figure 14. Longitudinal Profiles of Relative Concentration for All Solutes at 440 Days.

benzene and naphthalene suggests that they were either transformed or removed from solution during the experiment. The transport behavior of o-DCB was similar to that of tritium for the first 132 days of the field study. Major differences between the o-DCB and tritium plumes were first evident at 224 days. At this point, the o-DCB plume showed less overall displacement and spatial continuity than the tritium plume.

The use of a radiolabeled compound was critical towards establishing the degradation of these test chemicals. During the study, distinct differences were evident between the p-xylene and ^{14}C plumes, even though the ^{14}C was chemically associated with the injected p-xylene. The ^{14}C plume shape and size were similar to that of the tritium plume throughout the study. In contrast, p-xylene exhibited limited displacement (less than 50 meters in the down-gradient direction), and diminished plume volume and mass after 132 days. Again, transformation of the p-xylene can be inferred from these results.

DISSOLVED OXYGEN

Field dissolved oxygen (DO) data and coordinate locations of the points sampled during the experiment are given in Appendix A. Temporal average DO concentrations in the region near the injection wells for each well sample point were above 3.8 mg/L, and the minimum individual value was 2.6 mg/L. There was no significant difference between dissolved oxygen concentrations both near and far from the injection wells, or between measurements taken before and after injection. This result was anticipated, because aromatic hydrocarbon concentrations in the aquifer after the injection were too low to significantly deplete dissolved oxygen in the aquifer.

Figure 15 shows the vertically averaged dissolved oxygen data for wells along the longitudinal axis of the tracer plume at six times during the experiment. The data indicate considerable temporal and spatial variability in DO. Mean values ranged from 4.3 to 6.0 mg/L during the study period, and varied spatially by up to 3 mg/L over this transect for individual sampling dates. The DO near the injection site is consistently lower than the mean DO for the transect. This trend is evident in measurements made both before and after the injection, and may reflect the relatively slow rate of groundwater movement in this region.

Dissolved oxygen measurements made during the field study did not reveal conclusive evidence of the biological uptake of oxygen within the organic solute plumes. DO time-series data from MLS points within the more concentrated region of the plumes appear to indicate slight DO reductions of about 1 mg/L. These reductions correlate with the breakthrough of the organic solutes, but no relationship can be proven due to excessive noise in the DO data. Regions of greater DO uptake may have existed near the injection wells in the first few days, but there are no early data to test this possibility. The lack of significant DO uptake may also be explained by enhanced mixing of DO-rich groundwater, produced by the extreme heterogeneity of the aquifer. The importance of DO transfer by dispersive mixing during biotransformation of organic contaminants has been demonstrated in the numerical experiments of MacQuarrie and Sudicky (1990).

There is no evidence that anaerobic conditions occurred at any time in this experiment. The geochemical data presented earlier indicate that the nitrate and sulfate concentrations in the ambient groundwater are insufficient to support anaerobic degradation of aromatic hydrocarbons in the plume. Groundwater Eh and DO measurements indicate that, throughout the experiment, the aquifer environment was too oxidizing for anaerobic degradation.

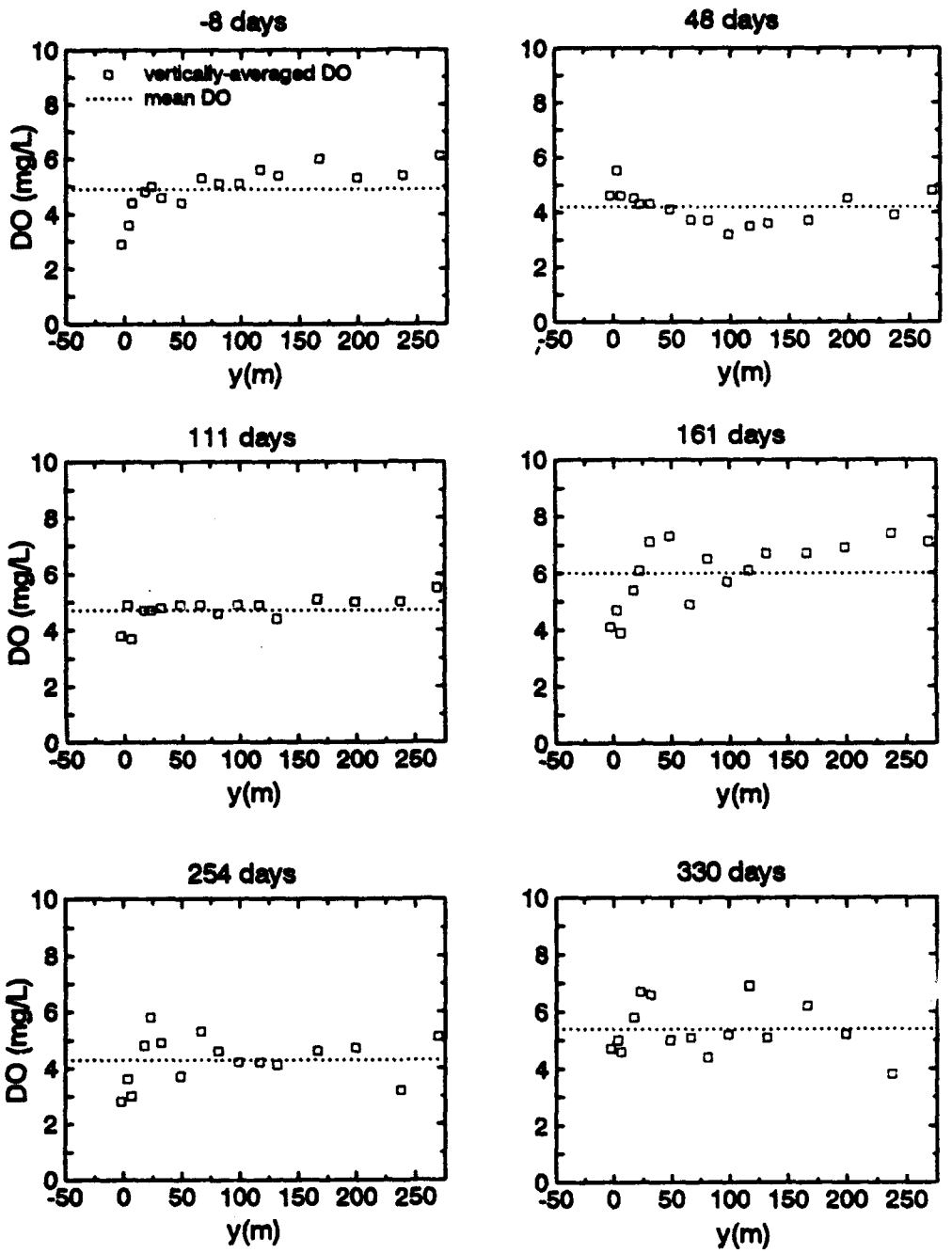

Figure 15. Vertically Averaged Dissolved Oxygen Concentrations at Monitoring Points Located Along the Longitudinal Axis of Solute Plumes.

As a check on the reasonableness of the field DO observations, the biological oxygen demand (BOD) associated with the observed aromatic hydrocarbon mass losses during the study was estimated. The reaction stoichiometry given in Equations (1) to (4) was assumed for these calculations.

benzene: $2C_6H_6 + 15O_2 \rightarrow 12CO_2 + 6H_2O$ (1)

p-xylene: $2C_8H_{10} + 21O_2 \rightarrow 16CO_2 + 10H_2O$ (2)

naphthalene: $C_{10}H_8 + 12O_2 \rightarrow 10CO_2 + 4H_2O$ (3)

o-DCB: $C_6H_4Cl_2 + 6.5O_2 \rightarrow 6CO_2 + 2H^+ + 2Cl^- + H_2O$ (4)

Estimates of total BOD for each snapshot are presented in Table 5. To obtain BOD data in concentration units for comparison with field DO measurements, it was necessary to first estimate the volume of oxygenated groundwater that had mixed with the organic tracers at each sampling date, then use this volume to convert oxygen mass to oxygen concentration. For example, initial mixing at 27 days was calculated by dividing the tritium plume volume of approximately 6 x 10^5 liters, by the injection solution volume of 9700 liters, to obtain a dilution factor of about 60.

TABLE 5. ESTIMATED BOD REQUIRED TO DEGRADE ORGANIC COMPOUNDS

Elapsed Time (days)	BOD (mg/L)	^{3}H Plume Estimated Mixing Vol. (L)
27	0.92	0.5923 E+6
132	1.35	0.1328 E+7
224	0.17	0.1581 E+8
328	0.14	0.2410 E+8

The volume of groundwater associated with the tritium plume for each snapshot date was assumed to be approximately equal to the total volume of groundwater coming in contact with the organic solutes for purposes of the calculation. Results indicate that the volume-averaged BOD required to transform all of the organic compounds at the observed disappearance rates is on the order of 1 mg/L or less. These estimates of low BOD may explain the nondetectability of DO uptake from the field measurements.

HYDROLOGICAL MEASUREMENTS

The maximum seasonal fluctuation in the water table during the study period was approximately 3 meters, as shown in Figure 16. This change resulted in about a 30 percent variation in the saturated thickness of the aquifer. Mathematical models of solute transport must therefore include a time-varying water table, since it is generally accepted that the variation should be less than 10 percent for application of the assumption of a time-invariant water table. Figure 16 also presents temporal variations in the magnitude of the horizontal hydraulic gradient, $|J_h|$, the direction of the horizontal gradient, Θ_h, and the magnitude of the vertical hydraulic gradient, $|J_z|$. $|J_h|$ was estimated by fitting a plane to the piezometric head measurements, and averaged 0.0017, with seasonal periodicity corresponding to water table fluctuations. The mean and standard deviation of Θ_h were -4 degrees (counterclockwise from the y-axis) and 28 degrees, respectively. The general direction of the hydraulic gradient is consistent with the observed direction of the tritium plume migration, as shown in Figure 8. The relatively large transverse dispersion of the tritium plume indicated on this figure may have been partially due to temporal variations in the horizontal direction of the hydraulic gradient. The vertical hydraulic gradients are equal to or greater than the horizontal gradients at several locations, and are generally correlated with water table fluctuations.

The temporal changes in the vertical hydraulic gradients estimated for three nested piezometers, were found to be dependent on their location at the field site. Typically, piezometers located upgradient of the injection point exhibited downward (positive) vertical gradients. The magnitude of the gradient in these piezometers occasionally exceeded 10 percent. Vertical gradients indicated for piezometers positioned downgradient of the injection point generally exhibited a lower magnitude and mixed directional components. The measured vertical gradients during the experiment were generally consistent with observations of the upward movement of the tritium plume near the injection wells, extensive vertical mixing farther downgradient, and upward motion of the plume near the downgradient boundary of the well field. These vertical gradients are thus in agreement with the tritium mass transport shown in Figure 7.

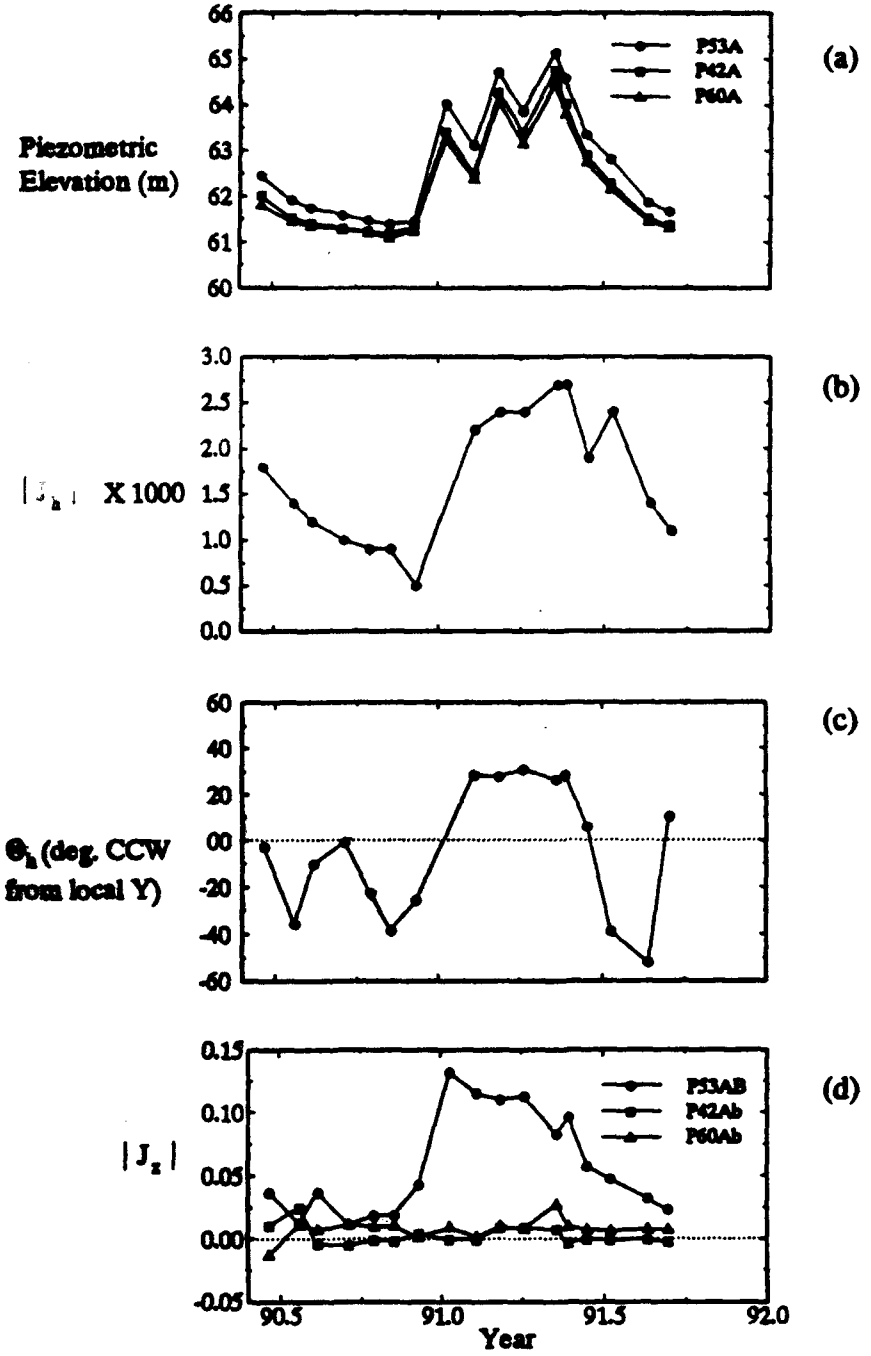

Figure 16. Temporal Variations of (a) Potentiometric Surface Elevation, (b) Magnitude of the Horizontal Hydraulic Gradient ($|J_h|$), (c) Direction of the Horizontal Gradient (Θ_h), and (d) Magnitude of the Vertical Hydraulic Gradient ($|J_z|$).

SECTION V
SPATIAL MOMENTS OF SOLUTE PLUMES

The spatial moments of the solute concentration measurements provide a means of characterizing and comparing the tritium and organic solute plumes. Important parameters determined by spatial moments analysis include the total solute mass (total activity of tritium and ^{14}C) in solution, the mean plume velocity, and the spatial covariance. Because the plumes had strongly non-Gaussian shapes, moments calculations of the skewness and kurtosis of the tracer concentration distributions at each sample time were done to further define the shape of each plume.

SPATIAL MOMENTS ESTIMATION

The formulation of the spatial moments estimators used in this study is essentially the same as that employed by Adams and Gelhar (1992) in their analysis of the MADE-1 bromide tracer experiment. Similar methods were also adopted in interpreting other recent field tracer experiments conducted at Borden (Freyberg, 1986) and Cape Cod (Garabedian *et al.*, 1991). In all cases, the method developed by Aris (1956) was used to relate the spatial moments of the tracer concentration data to the large-scale plume features. The general three-dimensional spatial moments are defined by:

$$M_{ijk} = \int \int \int ncx^i y^j z^k dxdydz, \qquad (x, y, z \rightarrow -\infty \text{ to } +\infty) \tag{5}$$

where $c = c(x,y,z,t)$ is the tracer concentration measurement, n is porosity (assumed constant and equal to 0.35 in our analysis), and i, j, and k are integers ranging from zero to infinity. The total mass associated with the tracer plume is given by the zeroth moment about the origin ($x = 0$, $y = 0$, $z = 0$) is given by:

$$M_{000} = \int \int \int ncdxdydz, \qquad (x, y, z \rightarrow -\infty \text{ to } +\infty) \tag{6}$$

The first moment about the origin provides the plume's center of mass coordinates,

$$x_c = M_{100}/M_{000}; \quad y_c = M_{010}/M_{000}; \quad z_c = M_{001}/M_{000} \tag{7}$$

The mean plume velocity vector is computed from the rate of translation of the plume's center of mass (centroid) as shown below,

$$V_x = dx_c/dt; \quad V_y = dy_c/dt; \quad V_z = dz_c/dt \tag{8}$$

and the magnitude of the mean velocity is given by:

$$V = (V_x^2 + V_y^2 + V_z^2)^{0.5} \tag{9}$$

The second moment about the center of mass coordinates of the plume yields the following symmetric spatial covariance tensor:

$$\sigma = \begin{bmatrix} \sigma_{xx} & \sigma_{xy} & \sigma_{xz} \\ \sigma_{yx} & \sigma_{yy} & \sigma_{yz} \\ \sigma_{zx} & \sigma_{zy} & \sigma_{zz} \end{bmatrix} \tag{10}$$

where,

$$\sigma^2_{xx} = M_{200}/M_{000} - x_c^2$$

$$\sigma^2_{yy} = M_{020}/M_{000} - y_c^2$$

$$\sigma^2_{zz} = M_{002}/M_{000} - z_c^2$$

$$\sigma^2_{xy} = \sigma^2_{yx} = M_{110}/M_{000} - x_c y_c$$

$$\sigma^2_{xz} = \sigma^2_{zx} = M_{101}/M_{000} - x_c z_c$$

$$\sigma^2_{yz} = \sigma^2_{zy} = M_{011}/M_{000} - y_c z_c$$

The principal second moments (σ^2_{11}, σ^2_{22}, and σ^2_{33}) are defined by the eigenvalues of Equation (10). The skewness and kurtosis estimators given in CRC (1959, p. 391) were adopted for the present analysis. Only the longitudinal skewness and kurtosis were estimated. The measure of longitudinal skewness, g_1, is given by:

$$g_1 = (M_{030}/M_{000} - 3M_{010}M_{020}/M_{000}^2 + 2M_{010}^3/M_{000}^3)/2\sigma^3_{yy} \tag{11}$$

where the numerator in Equation (11) represents the longitudinal third central moment, and y coincides with the longitudinal axis of the plume. Longitudinal kurtosis, g_2, is defined by:

$$g_2 = (M_{040}/M_{000} - 4M_{010}M_{030}/M_{000}^2 + 6M_{010}^2M_{020}/M_{000}^3 - 3M_{010}^4/M_{000}^4)/2\sigma^4_{yy} - 1.5 \tag{12}$$

where the numerator of the first term on the right-hand side of Equation (12) is the longitudinal fourth central moment of the concentration distribution. Moments of order higher than four could be calculated, but were not needed to adequately describe the plume behavior.

Numerical implementation of the moments calculation was necessarily three dimensional. The domain of integration was discretized into volumetric subdomains associated with the individual sampling points. A primary triangular grid was constructed in the horizontal plane using the MLS as grid points. The horizontal region of each subdomain was defined by constructing a secondary mesh with vertices at the centroids of triangles and at midpoints of their sides, as shown on Figure 17. The shaded region of the figure corresponds to the surface area, A_p, of the subdomain associated with sampling point p, and

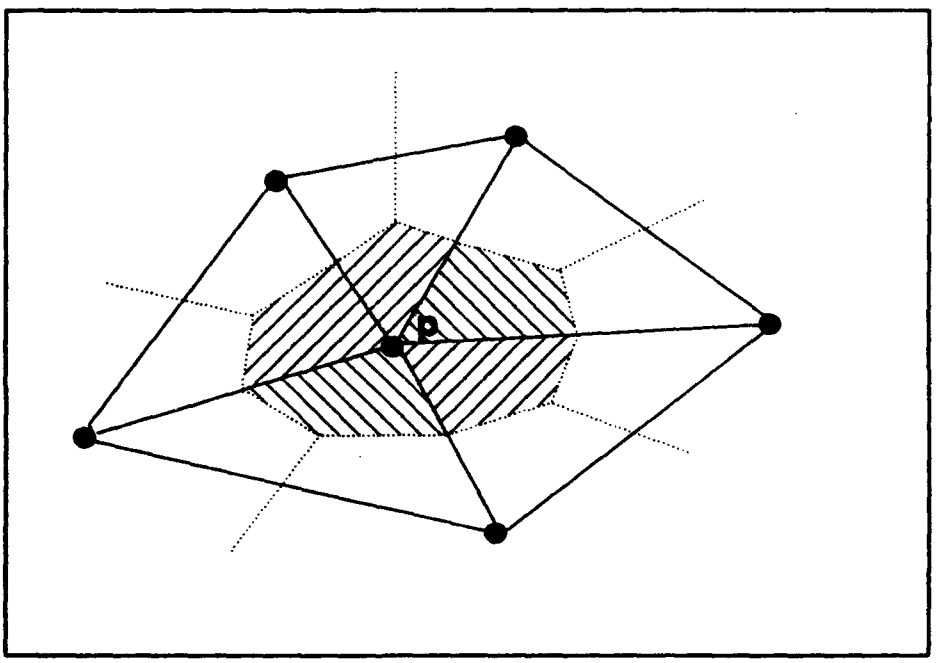

Figure 17. Solute Mass Integration Subdomain Associated With an MLS Point, p.

is equal to the sum of one-third of the areas of all primary grid triangles sharing a vertex at the point p.

The vertical dimension of the subdomain, z_p, was computed as the sum of one-half the distances between the sampling points directly above and below p. For the uppermost and lowermost sampling points on each MLS, the vertical dimension of the subdomain was set equal to one-half the distance between p and the next vertically-adjacent point, plus 0.19 meters (i.e., one-half the normal sample point spacing). The pore fluid within each subdomain was assumed to have uniform concentration equal to the measured tracer concentration at p. The mass of tracer associated with the sample point p is defined by:

$$m_p = nC_p z_p A_p \tag{13}$$

The discrete form of Equation (5) is,

$$M_{ijk} = \sum_{p=1}^{n} m_p x_p^i y_p^j z_p^k \tag{14}$$

where n is the total number of sampling points and x_p, y_p, and z_p are the coordinates of point p. The accuracy of the above mass integration scheme was evaluated through numerical experiments in which calculations were compared with analytical solution results for a test plume case. Details of methods and results of this evaluation are presented in Appendix B.

DATA PREPARATION FOR MOMENTS ANALYSIS

In the few instances where the MLS network did not adequately bound the plume laterally, adjacent imaginary MLS points having zero concentration were added at 6 meters (the typical intrarow MLS spacing) outside the boundary MLS location of concern. This permitted limited horizontal extrapolation of plume measurements outside the sampled MLS array. Vertical extrapolation of the plume was also performed in cases where the upper or lower point on an MLS showed above background (or above detection) concentrations. This extrapolation was based on imaginary zero concentration points added at 0.38 meters (one typical vertical sample point spacing) above or below the non-zero concentration boundary.

Measured tritium and ^{14}C counts were corrected for background activity. Estimated mean background activities of 2.0 and 2.8 pCi/mL were subtracted from the tritium and ^{14}C measurements, respectively. The tritium data were corrected for radiological decay, but the ^{14}C data were not because of the long half life of ^{14}C. The total decay during the 440 day field study was about 6.7 percent for tritium and less than 0.0002 percent for ^{14}C.

Two corrections were applied to the organics and ^{14}C data, referred to as Correction I and Correction II. Correction I was applied to data suspected to be affected by cross-contamination during sampling. Sample data exhibiting relative concentrations of ^{14}C or an organic compound greater than the relative concentration for tritium were considered suspect. In general, ^{14}C and organic compound relative concentrations in a sample should be less than or equal to the corresponding relative concentration for tritium, due to their susceptibility to attenuating processes such as sorption, volatilization, and biotransformation. Suspect ^{14}C or organic concentration measurements were adjusted such that their relative concentrations were

equal to that of the corresponding tritium measurement using the following equation:

$$C^*_i(org) = C_o(org)C_i(^3H)/C_o(^3H) \quad (15)$$

In this equation, $C^*_i(org)$ is the corrected organic or ^{14}C concentration for sample *i*, $C_o(org)$ is the initial injected concentration of the ^{14}C or organic compound, $C_i(^3H)$ is the tritium concentration of sample *i*, and $C_o(^3H)$ is the initial injected tritium concentration. Evidence of cross-contamination was limited almost entirely to data from the first snapshot .

Correction II was applied to samples with the background tritium activity level, but having detectable amounts of one or more of the organic compounds. For these samples, the suspect organic solute concentrations were set to zero. This procedure eliminated spurious analytical results in the low-concentration range, which could influence the higher moments estimates.

The sensitivity of the solute mass balance estimates to these corrections is illustrated on Figure 18. It is clear that, except for the first snapshot, mass estimates for the four organic solutes are insensitive to the data correction method. However, this is not the case for ^{14}C. After 132 days, the mass estimates of ^{14}C were highly sensitive to application of these data corrections, due to the presence of ^{14}C at near-background concentrations in most samples. On the basis of these results, Correction I was applied to the organics and ^{14}C data for the first snapshot. Corrections I and II were both applied to data from the later snapshots.

SOLUTE MASS (ACTIVITY) AT SAMPLING TIMES

Relative mass (activity) balances for each solute are given in Tables 6-11, along with summaries of the higher moments estimates. Figure 19 presents the relative mass balance trends during the experiment. No relative activity or higher moment estimates are given for tritium or ^{14}C for the snapshot at 440 days. As noted earlier, sampling at 440 days was limited to the near-field region, and thus did not completely encompass the radiological tracer plumes and may have only partially bounded the o-DCB plume.

The activity balance for tritium shows an overestimate at 27 days, followed by approximately 100 percent recovery for the two succeeding snapshots, and 77 percent recovery for the final snapshot at 328 days. The initial overestimation of tritium activity is attributed to the same sampling artifacts that produced the excess bromide recovery during the early stages of MADE-1. That is, preferential sampling by the MLS from relatively permeable aquifer zones in which solute concentrations are locally high may lead to mass overestimation because the mass integration scheme assumes local uniformity of tracer concentration (Boggs and Adams, 1992). In addition, suspected vertical hydraulic interconnection among sampling points associated with certain MLS located close to the injection site may result in over-prediction of tracer mass (Boggs *et al.*, 1988). The 23 percent tritium deficit at 328 days was due, at least in part, to apparent frontal truncation of the plume which had then passed the outermost boundary of the well field.

Aside from the frontal truncation, lateral bounding of the remainder of the tritium plume appears to have been reasonably complete. As evidence, the addition of the imaginary zero-concentration MLS adjacent to boundary MLS exhibiting above-background tritium levels produced an increase in relative activity of 2 percent or less for each snapshot. Some degree of vertical truncation of the plume was indicated by the occurrence of above-background tritium

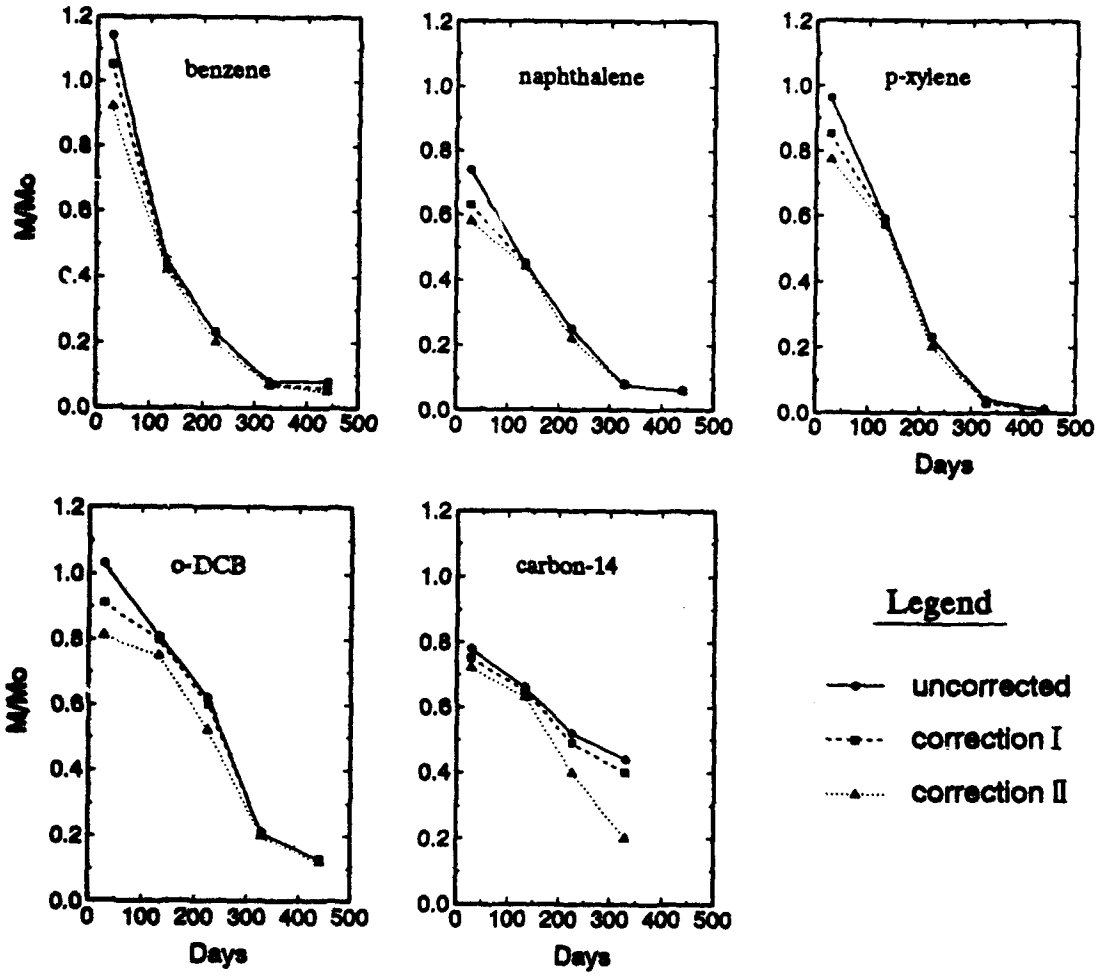

Figure 18. Sensitivity of Organic Solute Mass Estimates to Data Preparation Method.

TABLE 6. TRITIUM PLUME CHARACTERISTICS

	Time (days)				
	27	**132**	**224**	**328**	**440†**
M/M_o	1.52	1.05	0.98	0.77	--
x_c (m)	0.0	-0.9	0.2	2.1	--
yc (m)	3.9	8.1	46.5	76.8	--
zc (m)	58.22	58.68	58.80	58.48	--
Hor. Displ. (m)	3.9	8.2	46.5	76.8	--
Ver. Displ. (m)	0.42	0.88	1.00	0.68	--
σ_{11}^2 (m^2)	10.3	94.4	4,380	6,560	--
σ_{22}^2 (m^2)	8.6	7.9	52.5	107.	--
σ_{33}^2 (m^2)	2.0	1.3	2.5	2.9	--
g_1	0.72	1.5	0.74	0.32	--
g_2	1.5	6.3	0.34	-0.58	--
θ_h (deg. CCW from y-axis)	11.1	0.2	2.3	3.3	--
θ_v (deg. CCW from y-axis)	-1.1	3.1	1.7	2.0	--

† moments not estimated for spatially limited sampling at 440 days

TABLE 7. BENZENE PLUME CHARACTERISTICS

	Time (days)				
	27	**132**	**224**	**328**	**440**
M/M_o	0.92	0.43	0.23	0.07	0.06
x_c (m)	-0.2	-1.1	-0.8	-1.0	-1.1
y_c (m)	3.8	6.3	12.4	7.7	7.9
z_c (m)	58.13	58.68	59.24	58.90	58.67
Hor. Displ. (m)	3.8	6.4	12.4	7.7	7.9
Ver. Displ. (m)	0.33	0.88	1.44	1.10	0.87
σ_{11}^2 (m^2)	9.2	38.4	826	24.7	21.4
σ_{22}^2 (m^2)	7.9	6.9	6.1	8.4	10.7
σ_{33}^2 (m^2)	1.9	1.1	1.2	1.2	1.3
g_1	0.67	2.6	2.2	0.61	0.08
g_2	1.4	25.8	8.9	1.6	-0.13
θ_h (deg. CCW from y-axis)	39.0	0.4	3.6	1.6	14.1
θ_v (deg. CCW from y-axis)	3.8	6.7	-3.7	1.7	-4.4

TABLE 8. NAPHTHALENE PLUME CHARACTERISTICS

	Time (days)				
	27	**132**	**224**	**328**	**440**
M/M_o	0.58	0.45	0.25	0.08	0.06
x_c (m)	-0.3	-1.2	-1.4	-1.0	-1.8
y_c (m)	3.5	5.8	6.6	7.2	7.3
z_c (m)	58.05	58.54	59.03	58.71	58.62
Hor. Displ. (m)	3.5	5.9	6.8	7.2	7.6
Ver. Displ. (m)	0.25	0.74	1.23	0.91	0.82
σ_{11}^2 (m^2)	8.5	19.2	14.7	16.2	12.8
σ_{22}^2 (m^2)	7.3	6.7	6.1	4.8	4.7
σ_{33}^2 (m^2)	1.6	1.4	1.3	1.0	1.3
g_1	0.77	0.52	0.44	0.17	0.15
g_2	1.7	0.24	0.29	-0.43	-0.41
θ_h (deg. CCW from y-axis)	84.5	-9.8	-5.5	0.5	5.5
θ_v (deg. CCW from y-axis)	-0.8	-2.0	-1.4	1.1	-16.5

TABLE 9. p-XYLENE PLUME CHARACTERISTICS

	Time (days)				
	27	**132**	**224**	**328**	**440**
M/M_o	0.77	0.58	0.23	0.03	0.01
x_c (m)	-0.2	-1.0	-1.2	-1.1	-1.3
y_c (m)	3.6	6.1	6.4	10.5	6.4
z_c (m)	58.04	58.60	58.93	58.66	57.93
Hor. Displ. (m)	3.7	6.1	6.5	10.5	6.6
Ver. Displ. (m)	0.24	0.80	1.13	0.86	0.13
σ_{11}^2 (m^2)	9.1	22.8	16.3	213.	11.8
σ_{22}^2 (m^2)	7.2	5.8	6.4	4.6	4.0
σ_{33}^2 (m^2)	1.9	1.1	1.3	1.0	1.3
g_1	0.82	0.79	0.81	1.7	-0.12
g_2	1.9	3.1	3.3	5.2	-0.72
θ_h (deg. CCW from y-axis)	13.2	-11.3	5.0	3.4	28.0
θ_v (deg. CCW from y-axis)	5.3	-1.8	6.6	1.9	2.2

TABLE 10. o-DCB PLUME CHARACTERISTICS

	Time (days)				
	27	**132**	**224**	**328**	**440**
M/M_o	0.81	0.80	0.60	0.21	0.13
x_c (m)	0.0	-1.0	0.0	-0.2	-1.5
y_c (m)	3.9	7.4	34.7	22.1	8.1
z_c (m)	58.09	58.57	58.93	58.90	58.68
Hor. Displ. (m)	3.9	7.5	34.7	22.1	8.2
Ver. Displ. (m)	0.29	0.77	1.13	1.10	0.88
σ_{11}^2 (m^2)	11.3	64.4	3540	1180	21.9
σ_{22}^2 (m^2)	7.9	7.8	25.2	22.4	7.1
σ_{33}^2 (m^2)	2.1	1.4	2.0	1.6	1.8
g_1	0.82	1.7	1.0	1.6	0.12
g_2	1.6	8.3	1.2	6.5	-0.22
θ_h (deg. CCW from y-axis)	4.9	0.5	2.5	5.5	7.5
θ_v (deg. CCW from y-axis)	-1.6	5.5	2.4	0.7	-5.4

TABLE 11. CARBON-14 PLUME CHARACTERISTICS

	Time (days)				
	27	132	224	328	440†
M/M_o	0.72	0.65	0.49	0.40	--
x_c (m)	-0.2	-1.0	-0.4	1.5	--
y_c (m)	4.1	6.7	30.	68.5	--
z_c (m)	58.22	58.60	58.79	58.47	--
Hor. Displ. (m)	4.1	6.8	30.0	68.6	--
Ver. Displ. (m)	0.42	0.80	0.99	0.67	--
σ_{11}^2 (m^2)	11.4	39.8	2930	6490	--
σ_{22}^2 (m^2)	8.6	7.5	34.7	97.6	--
σ_{33}^2 (m^2)	1.9	1.4	2.3	2.7	--
g_1	0.71	1.4	1.2	0.42	--
g_2	1.3	6.2	2.3	-0.46	--
θ_h (deg. CCW from y-axis)	9.1	1.3	1.8	2.9	--
θ_v (deg. CCW from y-axis)	-0.8	6.3	0.8	2.1	--

† moments not estimated for spatially limited sampling at 440 days

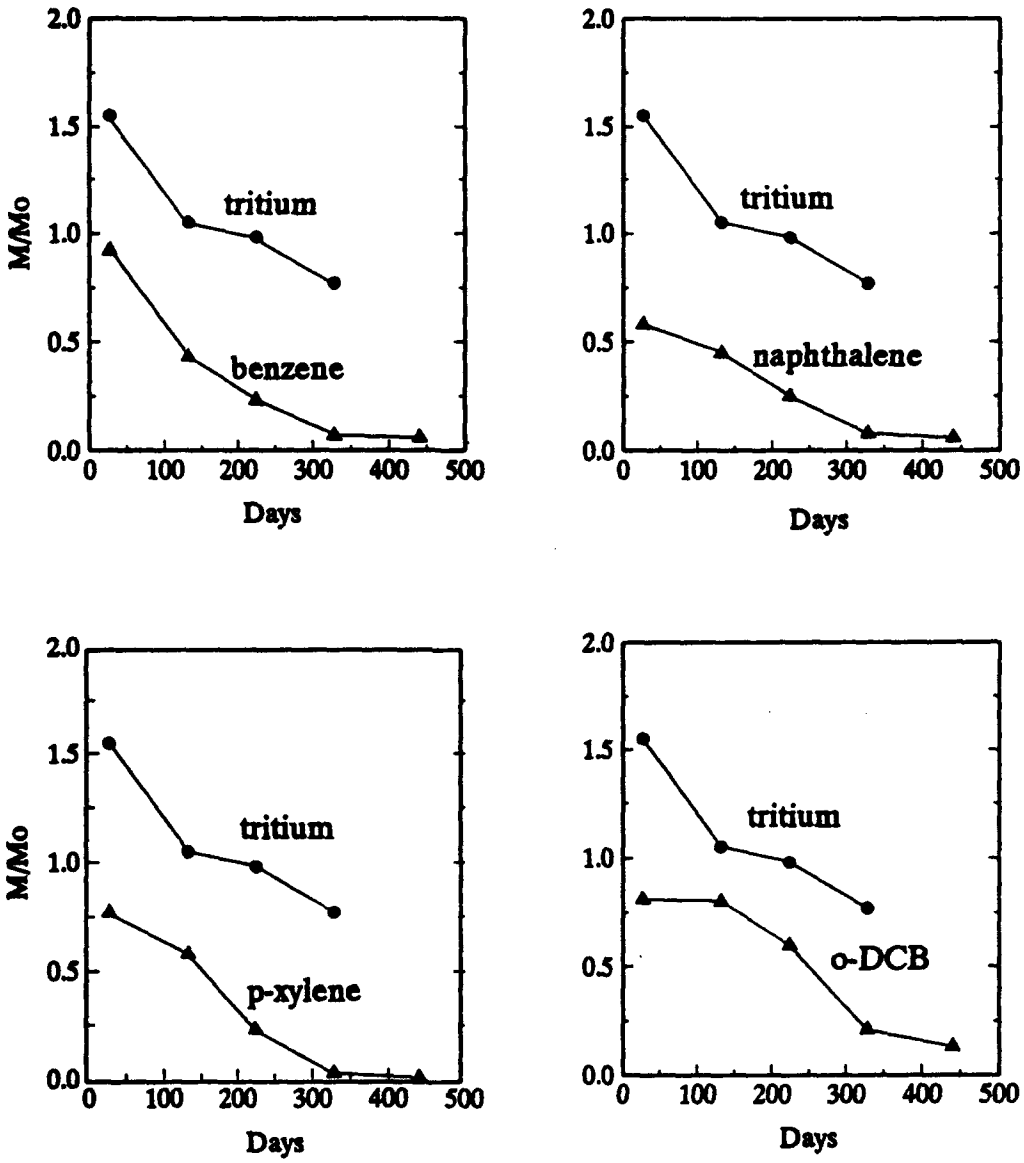

Figure 19. Benzene, Naphthalene, p-Xylene, and o-DCB Relative Mass Balances.

measurements at the uppermost and lowermost sampling points of certain MLS. The precise magnitude of the mass (activity) recovery error involved in the vertical truncation is unknown. However, sensitivity analyses in which fictitious zero-concentration points were added at a distance of 1.14 meters (three sample point spacings) instead of the normal 0.38 meters, indicate mass recovery increases ranging from 7 percent of injected mass for snapshot 1 to 2 percent for snapshot 4. These results make it unlikely that the magnitude of the error associated with the mass recovery estimates is greater than about 10 percent of the injected mass. This conclusion is consistent with that drawn by Adams and Gelhar (1992) regarding vertical truncation errors associated with the MADE-1 bromide experiment.

The organic solutes exhibit decreasing mass recoveries throughout the field experiment. Benzene shows an abrupt decline in mass recovery between 27 and 132 days, followed by a decreasing rate of mass decline during the remainder of the study. Except for a more gradual initial mass decrease, the mass balance trends for naphthalene and p-xylene are similar to that of benzene. The relative mass of o-DCB is essentially stable during the first 132 days after which an increasing rate of mass loss is observed. The apparent order of organics removal was, from greatest to least, benzene followed by p-xylene, naphthalene, and o-DCB. After 440 days, the relative mass recoveries for benzene, naphthalene, p-xylene, and o-DCB were 6, 6, 1, and 13 percent, respectively. The final mass estimate for o-DCB probably represents a lower limit, since some degree of truncation of the o-DCB plume was evident in the sample measurements.

The disparity between the mass balances for p-xylene and ^{14}C is noteworthy. The relative masses of p-xylene and ^{14}C were quite similar at 27 days (i.e., 77 and 72 percent, respectively). The initial similarity is expected since ^{14}C was chemically associated with p-xylene at the beginning of the experiment. However, the relative mass curves for the two compounds subsequently diverge indicating transformation of the p-xylene. After 328 days, the relative mass recovered for ^{14}C is 40 percent, while that of p-xylene is only 3 percent.

CENTER OF MASS AND VELOCITY

Figure 20 shows the mean horizontal trajectories of the solute plumes as indicated by the normal projections of the first moments of the solute plumes on a horizontal plane. During the experiment, the tritium plume followed an approximately linear trajectory, which was nearly parallel to the positive y-axis of the site coordinate system. This overall direction of movement is consistent with the horizontal hydraulic gradient shown earlier in Figure 3. ^{14}C exhibited a trajectory similar to that of tritium, but with a slightly lower overall displacement. The horizontal trajectories of the other solutes were similar to that of tritium during the first 132 days of the study, but deviated markedly thereafter. All of the organic compounds had smaller mean displacements than did tritium, and an apparent "retreat" of all organic plumes except naphthalene is indicated during the latter stages of the experiment. This retreat is a manifestation of organic solute degradation.

Figure 21 shows the mean horizontal displacement of the solute plumes during the study period. The mean velocity indicated for tritium during the first 132 days is 23 m/yr, while the mean velocity during the remainder of the study is 128 m/yr. The increase in the mean velocity is consistent with the increasing mean hydraulic conductivity along the plume travel path, and reflects the increasing fraction of tritium entering the relatively high-velocity groundwater present in the far-field. Naphthalene displacement increased monotonically over time, but at an apparent rate of only 6.8 m/yr. The mean horizontal displacements of the benzene, p-xylene,

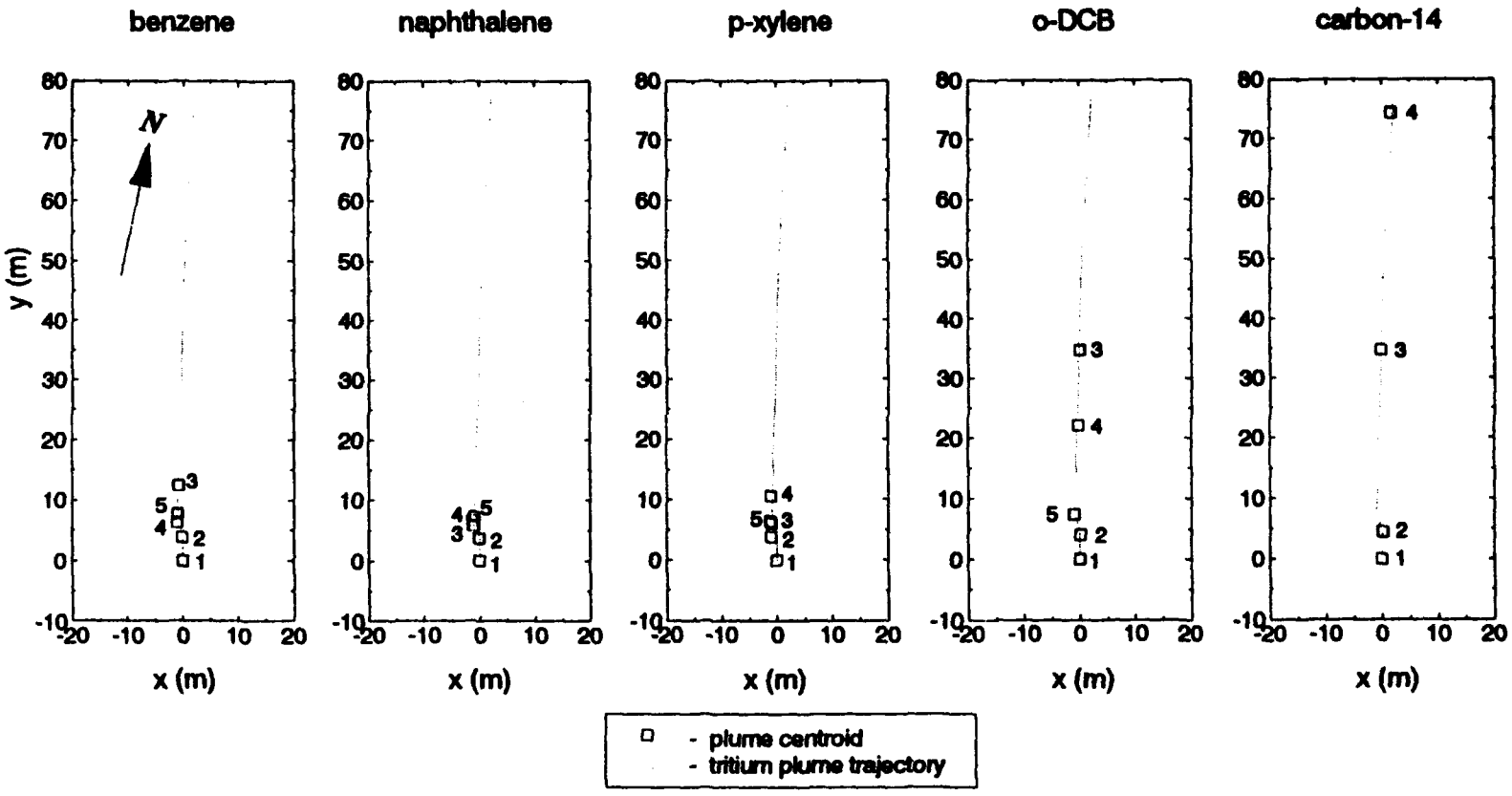

Figure 20. Solute Plume Trajectories Shown as Normal Projections of Center of Mass Locations

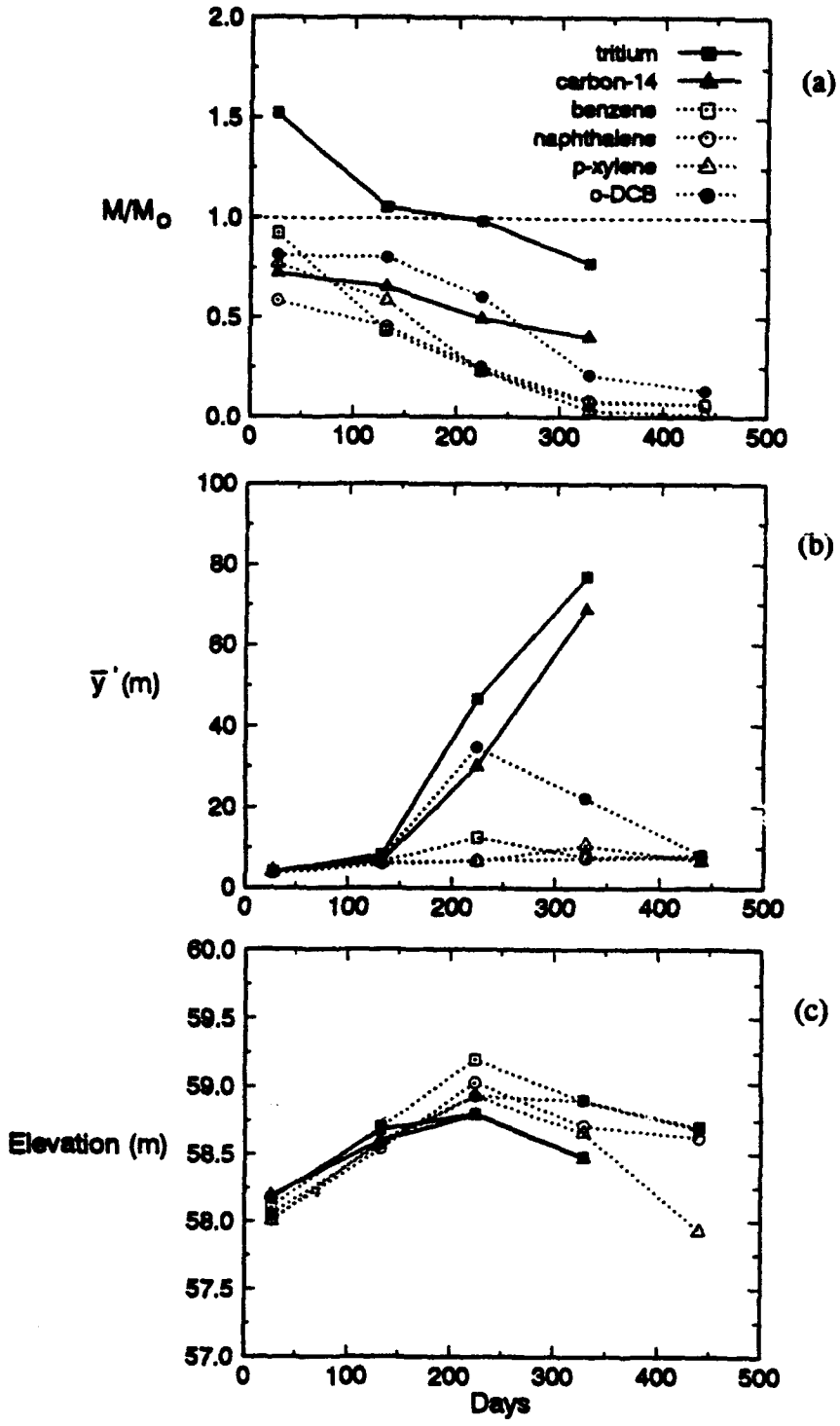

Figure 21. Temporal Variation in (a) Relative Mass Balance, (b) Mean Horizontal Displacement and (c) Mean Vertical Displacement, for Each Solute.

and o-DCB plumes decreased during the latter stages of the study. The displacement of ^{14}C was slightly less than that of tritium, but much greater than that of p-xylene.

To better quantify the average horizontal groundwater velocity of the near-field, where the majority of tritium tracer resided during the experiment, a separate set of first moments was estimated using only the tritium measurements for MLS located within approximately 25 meters of the injection point. These results are presented on Figure 22. The mean velocity indicated from the tritium displacement between 27 days and 440 days is approximately 5 m/yr (0.014 m/d). The vertical positions of the tracer plume centroids during the experiment are shown on Figure 21. All plumes exhibited upward movement during the first 224 days, followed by downward or near-stable vertical displacement. The initial upward displacement reflects the upward vertical hydraulic gradients present in the near-field. The relatively low centroid elevations indicated for tritium and ^{14}C after 224 days are attributed to the presence of a substantial fraction of these solutes in the far-field, where hydraulic gradients were downward to near neutral. No evidence of vertical movement resulting from density differences between the injection solution and ambient groundwater is apparent in these results. A density-induced hydraulic gradient of 0.00015 cm/s in the downward direction is estimated for the tracer injection solution. The density gradient is small, compared to the mean upward vertical gradient of 0.04 cm/s measured near the injection site.

SPATIAL VARIANCE, SKEWNESS, AND KURTOSIS

Figure 23 shows the principal components of the spatial variance of the tritium plume as a function of mean horizontal displacement. The longitudinal variance trend is approximately linear after the first 10 meters of displacement. The slight reduction in the rate of increase indicated between displacements of 46.5 and 76.8 meters is attributed to frontal plume truncation. The horizontal and vertical transverse variances both exhibit slight decreases in magnitude between 3.9 and 8.2 meters, followed by gradual nonlinear increases out to a displacement of 76.8 meters.

Temporal trends in the longitudinal variance, skewness, and kurtosis for all solutes are compared on Figure 24. The higher moments are useful to the extent that they further emphasize some of the similarities and differences in the ensemble characteristics of the solute plumes. Similar trends for the higher moments are observed for ^{14}C and tritium. Both exhibit nonlinear increases in longitudinal variance, and both show increasing skewness and kurtosis up to 132 days, followed by a gradual decrease to near zero at 440 days. The four organic solutes exhibit widely varying higher moment trends apparently due to differential transformation and sorption effects. The higher moments associated with the o-DCB plume are similar to those for tritium up to 224 days, but they then deviate subsequently from tritium due to the diminishing longitudinal extent of the o-DCB plume. The higher moments for benzene, naphthalene, and p-xylene are similar to those of tritium only for the snapshot at 27 days, after which they are quite dissimilar from tritium and from each other.

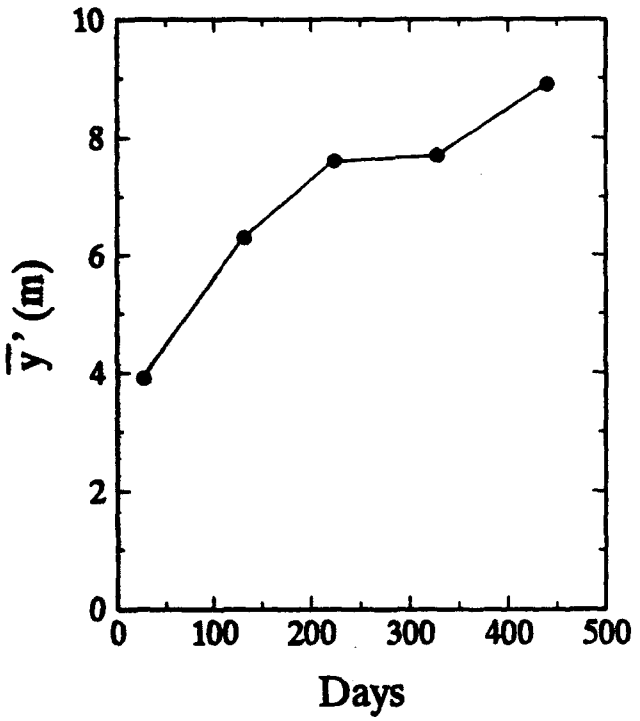

Figure 22. Temporal Variation of Mean Horizontal Displacement of the Tritium Plume Based on Spatial Moments Analysis of Near-Field Data.

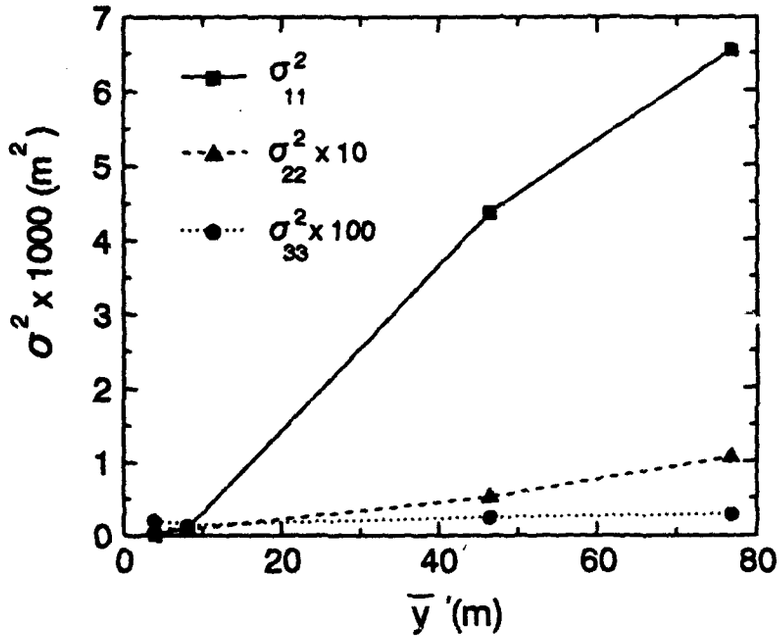

Figure 23. Variance of Tritium Data in Three Principal Directions Versus Mean Horizontal Displacement.

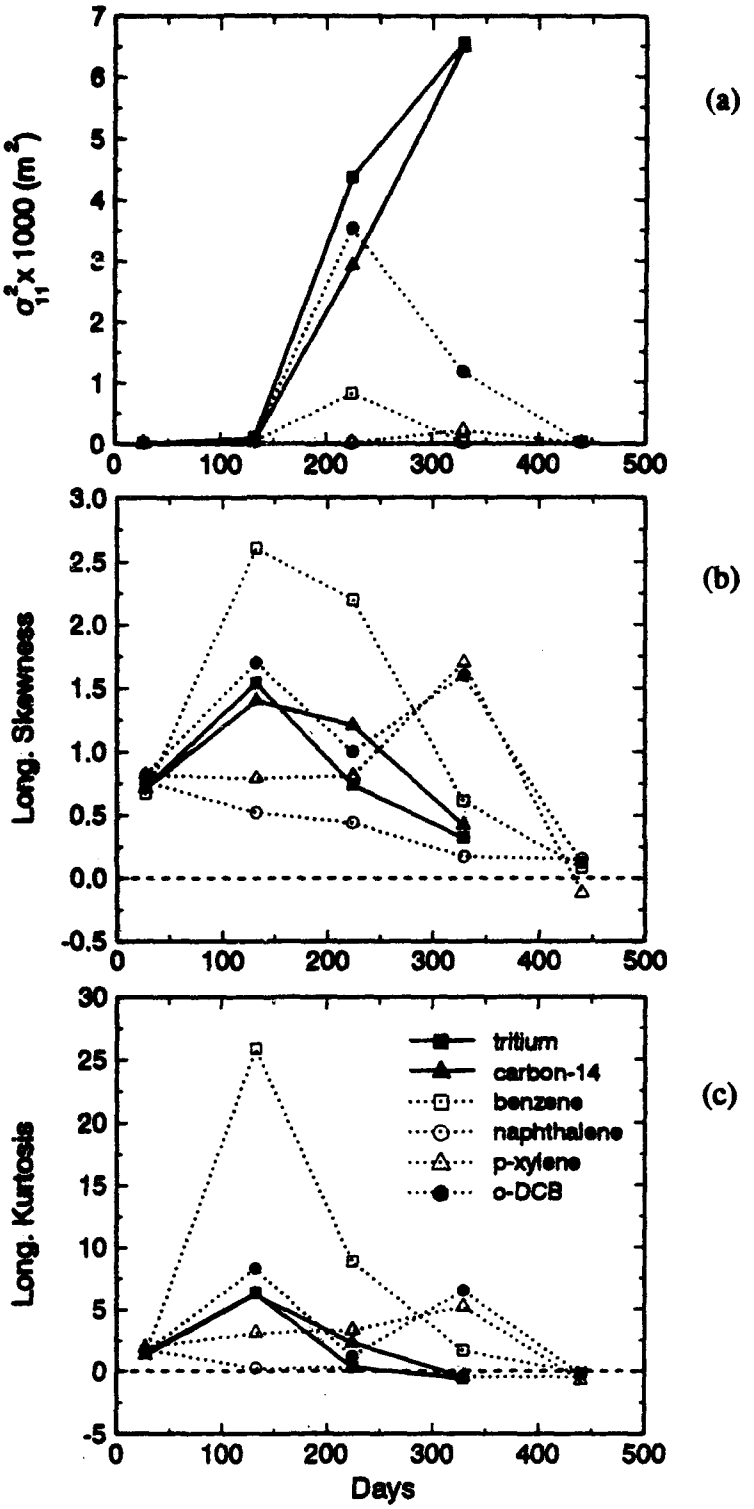

Figure 24. Temporal Trends in (a) Longitudinal Spatial Variance, (b) Skewness and (c) Kurtosis, for Each Solute.

SECTION VI
HYDROCARBON DEGRADATION RATES

Two separate sets of laboratory studies were performed prior to the field experiment in order to predict the degree of degradation of the organic compounds that might occur in the field. It was understood from the inception of these studies that laboratory measured degradation rates would probably be different than field degradation rates, and that laboratory results could identify, but not quantify the role of degradation in the field experiment. Procedures and results of the laboratory studies are given below.

MIXED BATCH REACTOR STUDIES OF DEGRADATION

Mixed batch reactor transformation studies were conducted with Columbus aquifer material to (1) determine the potential for degradation of the three aromatic hydrocarbon compounds selected for the field experiment (i.e., benzene, naphthalene, and p-xylene), and (2) to qualitatively compare the degradability of the more biologically resistant o-DCB with that of the aromatic hydrocarbons. These studies were qualitative in nature, and were not intended to provide quantitative biotransformation data for comparison with the field experiment.

Approximately 20,000 kg of aquifer material was excavated from the saturated zone of the Columbus aquifer to facilitate these, and other laboratory tests. The excavation location was just outside of the well field on the southwest corner of the test site. A subsample of this material was wet sieved on-site with groundwater using a 2 mm sieve and transferred to a cooler. To minimize biological contamination, sieves and coolers were cleaned with ethanol and air-dried prior to use. The samples were then saturated with groundwater, packed in ice, and transported to the AL/EQC Laboratories at Tyndall AFB where they were stored at 5°C. Approximately 40 liters of groundwater was also collected for use in these studies.

Saturated aqueous solutions of benzene, p-xylene, and naphthalene in Milli-Q water were prepared in sterilized saturator flasks as described by Burris and MacIntyre (1985). Aliquots of these saturated solutions were diluted with site groundwater to produce hydrocarbon concentrations of approximately 10 mg/L. These solutions were added to sterilized, 10 mL vials containing approximately 10 grams of aquifer material. Active vials were then sealed with Teflon®-backed septums and aluminum crimp seals. Poisoned vials were spiked with sodium azide to bring the azide concentration to 0.02 percent to inhibit degradation, and they were also sealed. Finally, control samples containing azide and hydrocarbons, but no aquifer material, were placed in vials and sealed. Each of the three different treatments was repeated in triplicate. The sealed bottles were placed on a rotator spinning at 30 revolutions per minute. The rotator was located inside an incubator held at 25°C. Triplicate samples of each treatment were removed from the rotator at weekly intervals. Sample bottles were centrifuged at 2,000 rpm and 3.0 mL of aqueous hydrocarbon solution was removed and added to a 4.0 mL vial. One-half mL of pentane, containing toluene as an internal standard, was then added to the vial and the hydrocarbons were extracted from the aqueous phase.

Separation and analysis of the extracted hydrocarbons was carried out on a Hewlett-Packard Model 85 gas chromatograph (GC) equipped with a 30-meter capillary column coated with methyl silicone. The GC was temperature programmed for an initial 2-minute hold at 40°C, followed by a steady increase to 150°C at 15°C/min, which was held for 6 minutes. Flame ionization detection was used to quantify the separated hydrocarbons. Relative response factors of the hydrocarbons were determined so that final concentrations could be calculated from the peak areas of the separate samples and the toluene internal standard.

Results from this set of experiments (designated as Study 1) showed that the hydrocarbons disappeared in the active vials (Figure 25), but remained relatively constant in the vials containing sodium azide inhibitor. Control solutions showed a slow loss over the experimental period. These losses may be attributed to sorption and/or vaporization, but are small, compared to the rapid loss of hydrocarbons in the active vials.

Due to the complete disappearance of hydrocarbons in Study 1, a second set of experiments was conducted. Study 2 was a complete replication of Study 1, except that o-DCB was added to the suite of compounds. This chemical is a common industrial solvent found at numerous groundwater contamination sites, and was purposely selected for its greater resistance to degradation.

Results from Study 2 (Figure 26) are similar to those of Study 1 except that the o-DCB showed a greater resistance to degradation than the other test compounds, as was anticipated. There were measurable quantities of o-DCB left in the active vials after 15 days. Based on the results from these preliminary experiments, it was decided to include o-DCB in the suite of compounds to be used in the field test, to provide an organic compound with a potentially lower degradation rate.

The results of these experiments were useful in designing the field experiment, and indicated that degradation of the selected aromatic hydrocarbons in the aquifer might be quite rapid. The investigators proceeded with the field experiment under the assumption that degradation of these solutes would occur in the aquifer, but at a considerably slower rate than in the laboratory. Fortunately, this assumption proved to be a correct one.

DEGRADATION OF ORGANICS FROM MOMENTS ANALYSIS

As described in Section 4, dissolved oxygen samples were taken 8 days before and 48, 111, 161, 264 and 330 days after the test injection. These samples were taken at three discrete levels from a set of 16 multilevel sampler wells located along the plume axis, including wells at 2.3 meters upgradient and 3.6 meters down gradient of the injection wells. The results show that the organic solutes degraded under aerobic conditions in the aquifer. This outcome was anticipated because the initial organic solute concentrations in the aquifer after mixing were estimated to be too low to significantly deplete the existing level of dissolved oxygen near the injection wells. These DO concentrations were high enough so that degradation rates of the organic compounds were probably not oxygen-limited. In support of this assumption, Hänel (1988) notes that the dissolved oxygen content in a normally operating activated sludge plant is 1-2 mg/L, which is adequate to support aerobic biodegradation processes.

Figure 2 shows the K_h distribution over a vertical section oriented along the test plume axis, and indicates large-scale heterogeneity and structures that Rehfeldt *et al.* (1992)

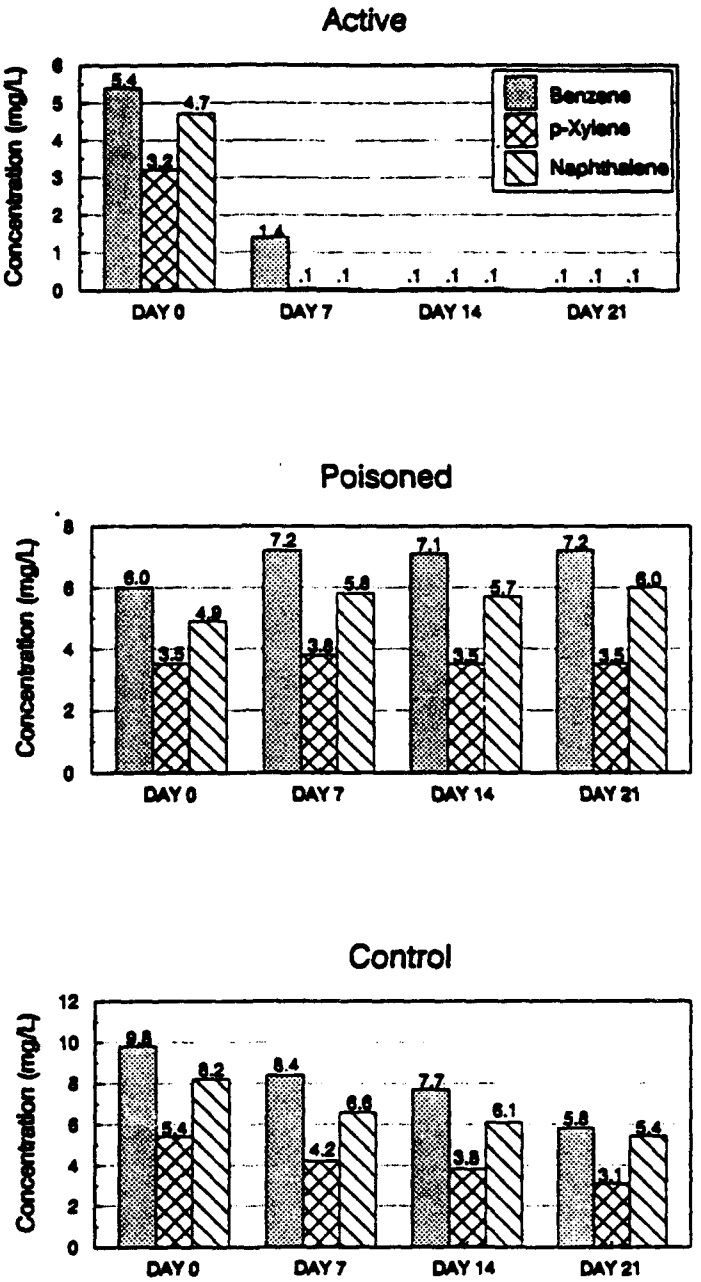

Figure 25. Batch Reactor Results from Study 1.

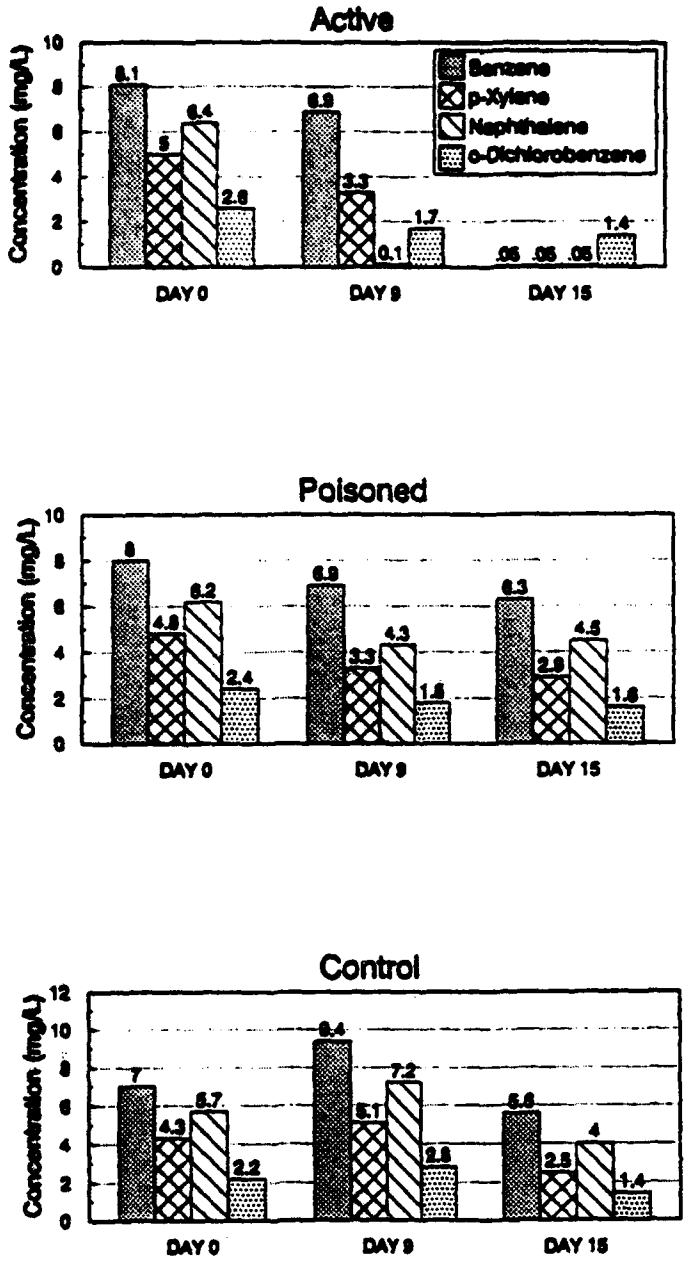

Figure 26. Batch Reactor Results from Study 2.

refer to as channels. Close to the injection wells K_h is relatively low, with values near 10^{-3} cm/s in a region extending from the phreatic surface to the lower confining layer, and to approximately 40 meters down-gradient from the injection location. From 40 meters out to 200 meters, K_h in the upper 3 meters of the aquifer is about 10^{-1} cm/s, while K_h in the deeper portion of the aquifer remains low. Thus, a near surface channel crosses the intermediate and far fields.

Most of the injected solute mass remained in the low K_h region (near the injection wells) throughout the course of the experiment. This situation allowed degradation rate constants to be determined separately from data for the entire plume, and from data for only the near field. Solute reactions included tritiated water (Tr) decay, with a k_d of 1.548×10^{-4} $days^{-1}$, and degradation of organic compounds with rate constants k_b, k_x, k_n and k_c for benzene, p-xylene, naphthalene and o-dichlorobenzene, respectively. Degradation rate constants based on data from the whole field were calculated for each snapshot using the zeroth moments of the plumes of tritiated water and of the organic solutes. For each organic solute, initial mass and mass remaining for each snapshot sampling time given in Tables 7-10 were used in a nonlinear least-squares regression to fit a first-order exponential function, thus assuming a first-order degradation process. Degradation rate constants from these regressions are given in Table 12. Maximum degradation rates for all solutes occurred between 224 and 328 days after injection, as can be seen from Figure 27, and these rates are included as k_{max} in Table 12.

TABLE 12. DEGRADATION RATE CONSTANTS FOR ORGANIC COMPOUNDS USING WHOLE-FIELD DATA

	k ($days^{-1}$)	k_{max} ($days^{-1}$)
benzene	0.0070	0.011
p-xylene	0.0107	0.020
naphthalene	0.0064	0.011
o-dichlorobenzene	0.0046	0.010

The observed mass loss is presumed to be due to microbial catabolism (biodegradation), but is referred to simply as degradation since biodegradation is indicated, but not proven by this experiment. Proof of biodegradation in the Columbus aquifer would require field application of molecular biology techniques similar to those described by Fleming *et al.*, (1993).

Spatial distributions of solutes are apparently related to the K_h distribution, as indicated by Figure 28(a), which shows the distribution of relative tritium concentrations at 224 days after injection. High ^3H_2O concentrations remained near the injection wells, with lower concentrations in the upper portion of the aquifer from about 30-250 meters downgradient. There was little ^3H_2O in the lower portion of the aquifer between 30 and 175

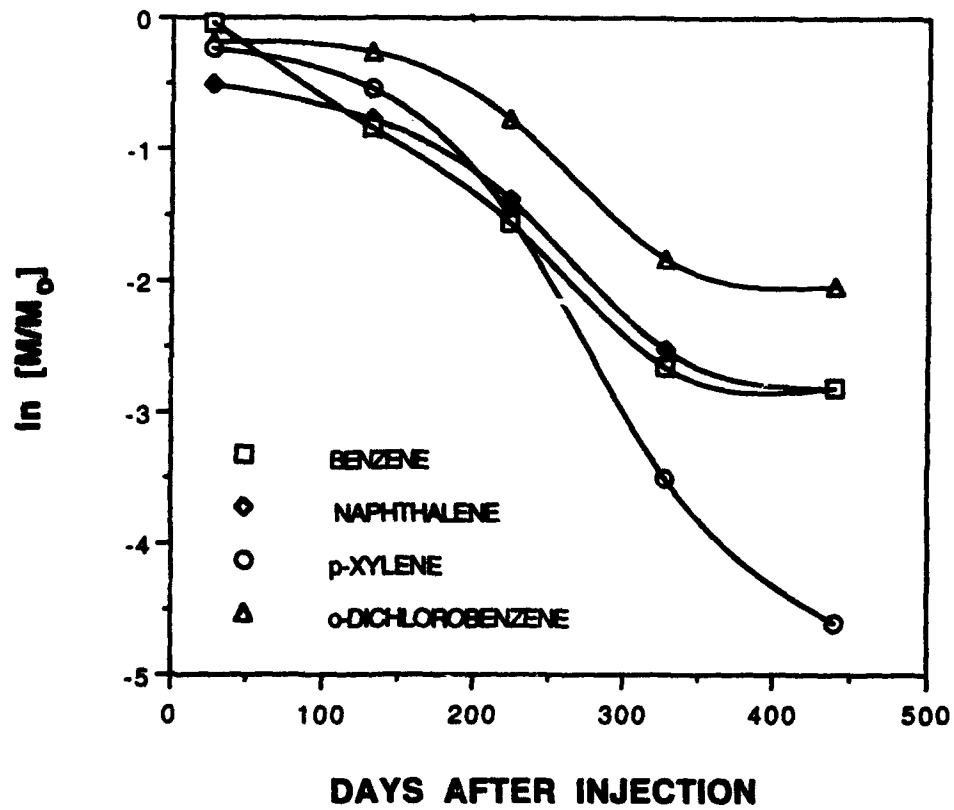

Figure 27. Plot of Organic Compound Masses Versus Time, Based on Data from the Whole Field.

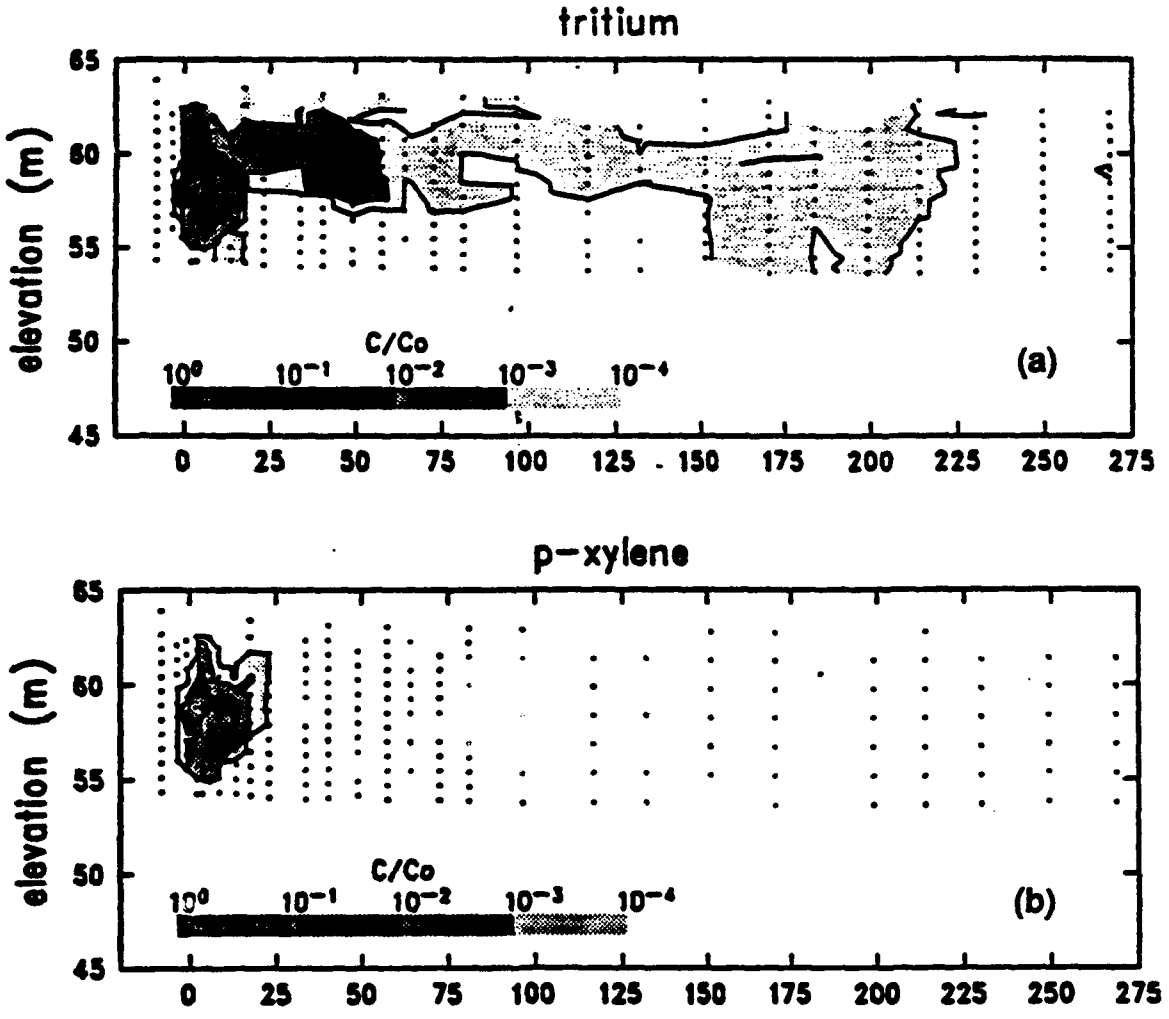

Figure 28. Distribution of (a) Relative Tritium Concentration and (b) Relative p-Xylene Concentration Over a Vertical Section Along the Plume Centerline at 224 Days.

meters downgradient. This distribution suggests that most of the tritium was transported from the low K_h zone near the injection wells to the far field through an upper channel whose size, location, and K_h govern the solute loss rate from the near field region.

The organic solutes were slightly retained, and thus more confined to the near field than was the unretained tritium. Accordingly, most degradation of the organic solutes occurred in the near field zone. This zone is approximately delineated by the p-xylene distribution at 224 days after injection, shown in Figure 28(b). Most of the p-xylene remained within 20 meters of the injection wells, and the other organic solutes were similarly distributed. They were primarily confined to the near field zone because they degraded rapidly relative to their transport from the near field. As a result, separate degradation rates could be calculated using only the near field data, treating the near field region zone as mixed reactor zone with a slow leak to the far field. A schematic diagram of the transport and degradation processes occurring in the near field region is shown in Figure 29. Separate degradation rates calculated from the reactor model were useful because the solute concentrations were much higher in the near field and less subject to analytical uncertainty.

Solute mass transport from the near field to the far field is assumed to be a first-order process with the same constant, k_t, for all solutes. Degradation and loss to the far field occurred simultaneously in the near field. The rate equations are:

$$-d[Tr]/dt = k_d[Tr] + k_t[Tr] \quad (16)$$

$$-d[B]/dt = k_b[B] + k_t[B] \quad (17)$$

$$-d[X]/dt = k_x[X] + k_t[X] \quad (18)$$

$$-d[N]/dt = k_n[N] + k_t[N] \quad (19)$$

$$-d[C]/dt = k_c[C] + k_t[C] \quad (20)$$

The initial conditions for these equations are: $t_0 = 0$; $[Tr]_0 = 0.539$ Ci; $[B]_0 = 660$ g; $[X]_0 = 402$ g; $[N]_0 = 70$ g; $[C]_0 = 318$ g.

Integration of rate Equations (16) to (20) with these conditions gives solute masses in the near field as a function of time. The transport rate constant, k_t, is calculated from the integrated form of Equation (16), using the known k_d of tritium. Degradation constants for the organic solutes are then determined by substitution of k_t, and solving the integrated forms of Equations (17) to (20) for k_b, k_x, k_n, and k_c, respectively.

Sorption of organic solutes was not included in rate calculations using the near field data. Aromatic solutes were weakly sorbed on Columbus aquifer material (Lion *et al.*, 1990; MacIntyre *et al.*, 1991). Using subsamples of a 20,000 kg composite sample of Columbus aquifer material, batch sorption coefficients measured for naphthalene, o-DCB, p-xylene and benzene were 0.085, 0.065, 0.048 and 0.059 L/Kg, respectively. Retardation effects on organic solute distributions in the near field were not detected due to the predominant influence of degradation. Sorption-desorption processes at aquifer material surfaces are assumed to be fast relative to the chemical degradation processes considered here, as indicated by Spiro (1989), and to be rate-limited by physical transport of organic solute

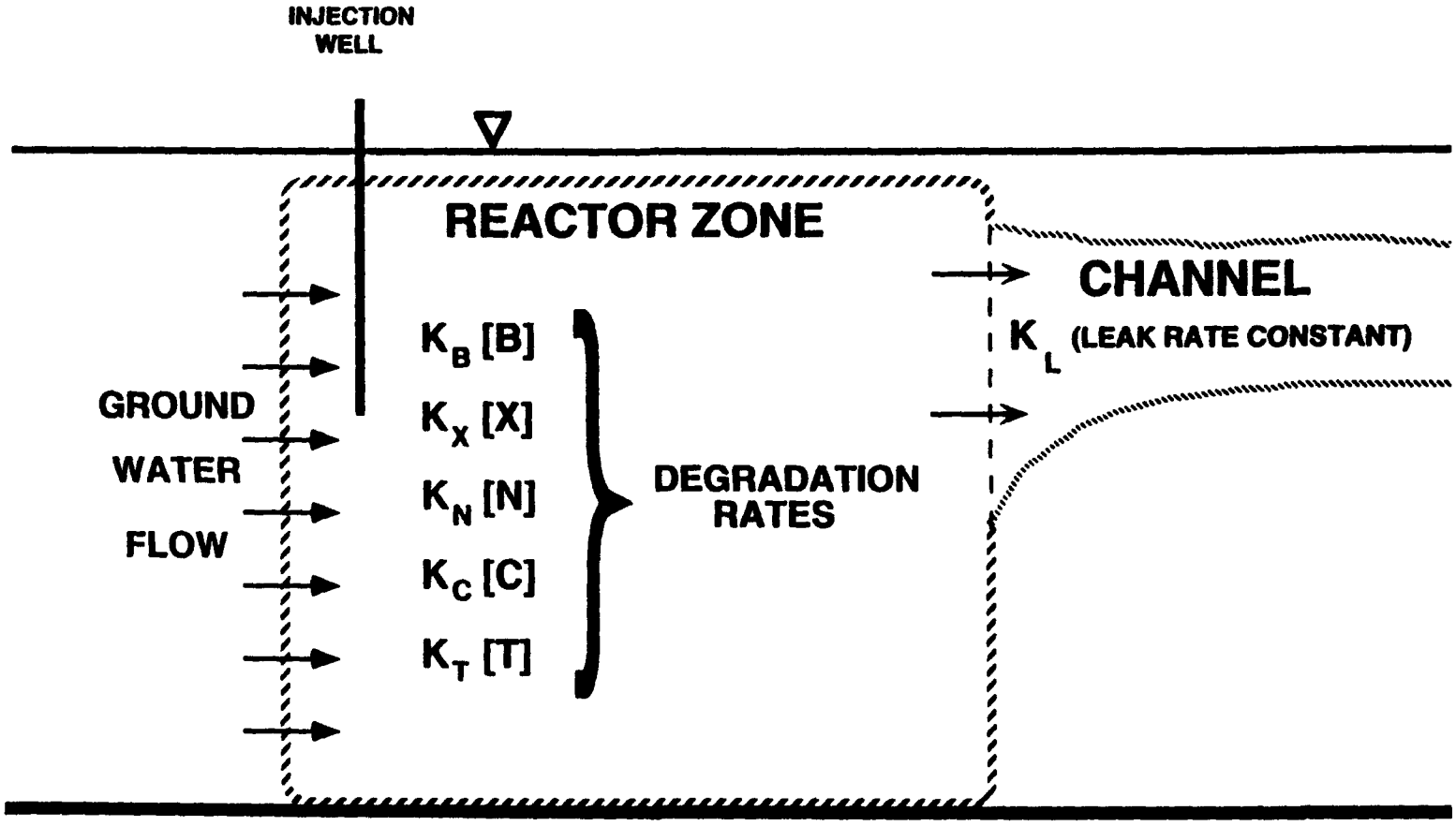

Figure 29. Schematic Diagram of Transport and Degradation Processes in the Near-Field Region.

molecules to and from the solid-solution interface. As was noted by Robinson *et al.* (1990) for toluene degradation on surface soils, the aromatic compounds may be microbially degraded from solution, sorbent surfaces, or both. This question is not resolved, but sorption processes probably did not limit microbial degradation of organic solutes due to the small sorption coefficients measured in this experiment.

Loss of organic solutes by transport from the near to the far field, was assumed to be proportional to the loss of tritium. The near field is defined as the portion of the plume volume within 10 meters downgradient from the injection wells. The amount of tritium in the near field at a given time, was calculated by the spatial integration method described above. The level of ^3H_2O, corrected for decay, decreased exponentially with time, as shown in Figure 30. This plot indicates that solute leakage from the reactor was apparently first order, with leakage rate constant, $k_l = 5.45 \times 10^{-4}$ days^{-1}. A mass balance for tritium over the entire plume showed that the injected tritium mass was accounted for at the times given in Figures 27 and 31. This result implies that the tritium mass loss in the near field was indeed due to leakage.

Degradation rates of organic solutes in the near field are shown in Figure 31. The curves shown in Figures 27 and 31 suggest that degradation in the Columbus aquifer may be first order, with an initial lag period. The departure of the curves in Figures 27 and 31 from linearity is attributed to microbial adaptation, cell growth and substrate limitation. Spain (1990) has described lag period dependence on microbial growth and adaptation to the substrate. The observed lag period is followed by degradation at a maximum rate, which is characteristic of the microbial metabolism. Simkins and Alexander (1984) have indicated that degradation in a laboratory microcosm can be expected to follow Monod kinetics for a microbial population not limited by nutrients and with a sufficient substrate concentration. However, first-order kinetics are often observed at low substrate concentrations. Because organic solute concentrations in the experiment were quite low, this conclusion is consistent with experimental results. Larson (1979) notes that the rate of decrease in concentration as a function of substrate concentration can often be expressed as a first-order equation, and that first-order kinetics are generally expected for biodegradation at low organic substrate concentrations.

Towards the end of this field study the solute degradation rate decreases, and this change is concurrent with reduced substrate concentrations due to both dilution and degradation. Rubin *et al.* (1982) have demonstrated in laboratory experiments that microbial degradation rates of aromatic compounds can be reduced at low substrate concentrations. Similar substrate limitations are thus a possible explanation for the rate decreases shown in Figures 27 and 31.

Table 13 shows degradation rate constants calculated from the near field data. Initial mass and mass remaining for each sampling time were used in a nonlinear least squares regression to fit a first-order exponential function to the data to determine the first-order rate constant, k (days^{-1}), for each compound. The maximum rate constants, k_{max}, were calculated from the maximum slopes of the curves shown in Figure 31. Rate constants corrected for organic solute leakage from the near field, $k_{max}(c)$, were obtained by subtracting the leak rate constant k_l from k_{max} values. The relative values of the degradation rates given in Tables 12 and 13 appear reasonable, with o-DCB being the most slowly degraded test chemical. These findings are in agreement with Callahan *et al.* (1979).

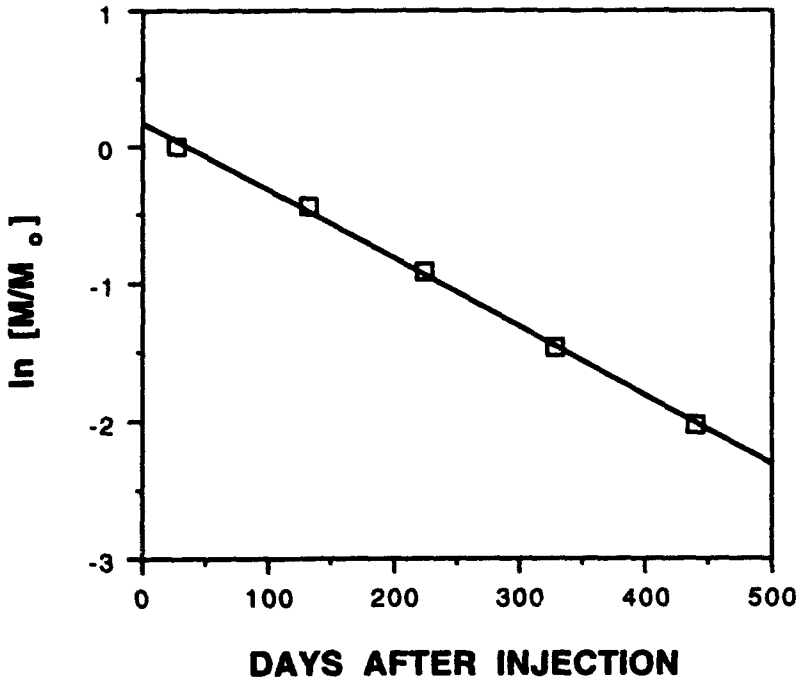

Figure 30. Plot of the Relative Tritium Concentration in the Near-Field Region.

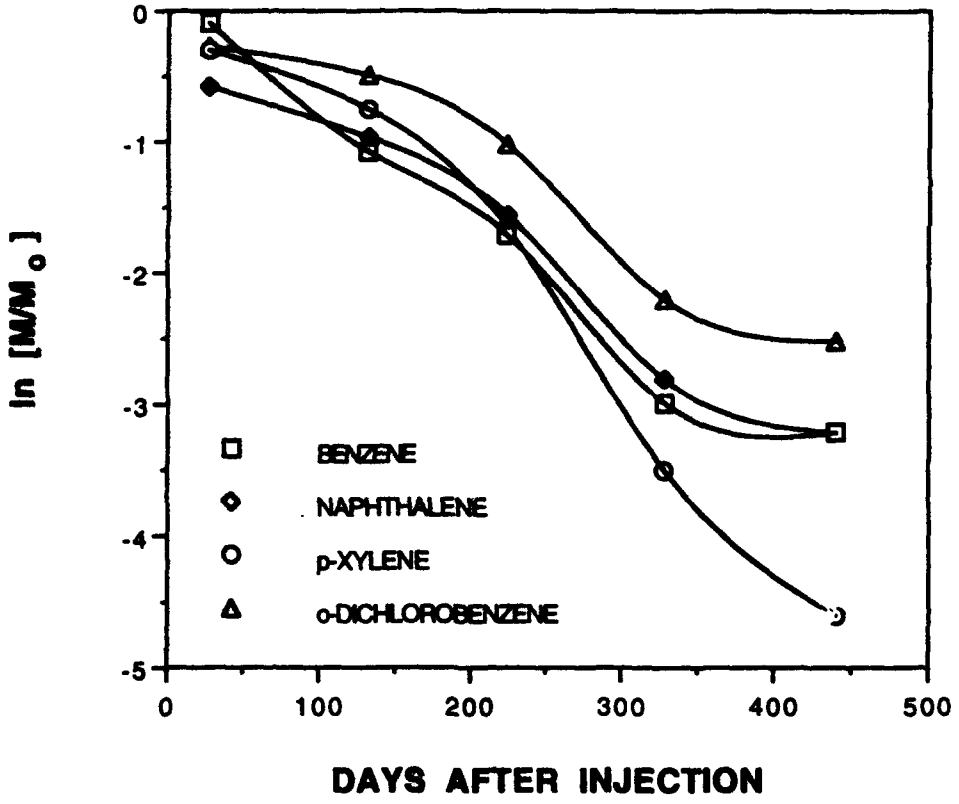

Figure 31. Plot of the Organic Compound Masses, Based on Near-Field Data.

TABLE 13. DEGRADATION RATE CONSTANTS FOR ORGANIC COMPOUNDS IN THE NEAR FIELD

	k ($days^{-1}$)	k_{max} ($days^{-1}$)	$k_{max}(c)$ ($days^{-1}$)
benzene	0.0079	0.0120	0.0066
p-xylene	0.0106	0.0196	0.0141
naphthalene	0.0072	0.0118	0.0063
o-dichlorobenzene	0.0060	0.0114	0.0059

Rate constants were based on the analysis of stable compounds by gas chromatography. Ring labeled ^{14}C p-xylene was used to show that it was degraded rather than lost in the aquifer. ^{14}C p-xylene was oxidized to ^{14}C labeled intermediates and carbon dioxide, which exists as $H_2{}^{14}CO_3$ and $H^{14}CO_3^-$ at the existing groundwater pH of approximately 5. The special sampling and analysis procedure described in MacIntyre *et al.* (1993) permitted measurement of ^{14}C p-xylene degradation products. ^{14}C in the carbonate precipitate was divided by ^{14}C in the basic sample (supernatant plus precipitate) to obtain the fraction of p-xylene converted to CO_2. The amount of ^{14}C in the water after extraction, was divided by ^{14}C in the unextracted water sample to obtain the fraction of p-xylene converted to polar intermediates and CO_2.

Applicability of the leaking reactor model is site specific, and its success with the MADE-2 test data is a fortuitous circumstance, dependent on the arbitrarily selected positions of the injection wells in the Columbus aquifer. It is encouraging that the reactor and whole field methods of calculating biodegradation rates gave similar results. This fact provides more confidence in the descriptive model and in the utility of these rates for predictive purposes, including the design of further experiments at the site.

Degradation of the organic solutes was confirmed by a special sampling of wells in high and low solute concentration regions of the plume at 421 days after injection. Selection of the wells was based on known concentration data from the previous snapshot sampling. Each water sample was subsampled and processed in the field. A 10 mL subsample was placed in a glass ampoule, made basic with 1 mL of 3N NaOH and 1 mL of 3N $Ca(NO_3)_2$ and immediately flame-sealed. A separate 2 mL subsample was mixed with scintillation cocktail and counted. A final 20 mL subsample was extracted with 2 mL of unlabeled p-xylene. One mL of the resulting xylene layer was transferred to scintillation cocktail and counted to determine the amount of undegraded ^{14}C p-xylene which remained in the organic layer. Two mL of the extracted water was transferred to scintillation cocktail and counted. After they were returned to the laboratory, the ampoules were centrifuged to separate a precipitate containing $Ca^{14}CO_3$, and then they were broken open. The precipitate and 2 ml of the supernatant water were placed in separate scintillation vials with cocktail, and counted.

Conversion results for p-xylene in well samples from high concentration regions of the plume are given in Table 14 using carbonate precipitation, and in Table 15 based on extraction with p-xylene. In Table 14, $^{14}CO_2$ DPM is calculated by correcting the precipitate counts for background and for ^{14}C carry over from the solution. Percent conversion is calculated from the $^{14}CO_2$ DPM / Total ^{14}C DPM quotient.

TABLE 14. p-XYLENE CONVERSION TO CO_2 DETERMINED BY THE PRECIPITATION OF CARBONATE FROM WATER SAMPLES TAKEN AT DAY 421

Well	Port	Precipitate DPM ^3H	Precipitate DPM ^{14}C	Solution DPM/ml ^3H	Solution DPM/ml ^{14}C	$^{14}CO_2$ DPM	Total ^{14}C DPM	% Conversion
D18	11	4532	700	2715	28	66	94	71
D18	13	4827	932	5149	82	82	164	50
D21	13	2544	742	2448	16	71	87	82
D6	12	2479	928	3420	38	85	123	70
D6	14	6033	1760	6952	87	164	250	65
M30	19	3017	841	2036	13	81	94	87
M35	11	1389	411	1646	15	37	52	71
M35	13	1210	354	698	10	33	42	78
M36	13	1081	366	933	6	34	40	86
M40	11	515	413	537	16	38	53	71
M41	13	3570	1642	3236	46	158	204	77
M41	15	4697	1145	3363	29	110	139	79
M41	17	1941	403	1268	11	37	48	77
M43	13	5371	1095	4470	41	104	145	72
M43	15	2079	420	1591	10	39	49	80
M45	13	2648	708	1646	13	68	80	84
M50	11	2163	445	1688	14	41	55	75
M50	13	2201	438	1989	23	40	63	63

Conversion percentages given in Table 15 are based on the assumption that ^{14}C p-xylene partitions almost completely into the xylene phase and $^{14}CO_2$ partitions almost completely into the water phase. This assumption is supported empirically by the agreement between p-xylene conversion pecentages determined by the p-xylene extraction and the carbonate precipitation methods. However, the behavior of the CO_2 and xylene buffered water system cannot be predicted from existing theory, and the literature does not contain experimental measurements on this system. One of the authors intends to make and publish these measurements in the near future, as the system contains some chemical curiosities. For example, CO_2 is many times more soluble in pure p-xylene than in pure water, but field measurements here indicated that most of the CO_2 produced by p-xylene degradation went into the water phase.

Since this matter was deemed worthy of further investigation, a series of extraction tests was done in the laboratory to determine the partititioning of $H^{14}CO_3^-$ between water and p-xylene in a volume ratio of 10:1 at water pH values of 4.8 and 7.0. It is apparent from the results given in Table 16, for five replicate extractions at each pH, that most of the $^{14}CO_2$ partititioned into the water phase, even at a pH of 4.8. The $^{14}CO_2$ behavior in these extraction tests was similar to that measured by the p-xylene extraction method used in the field, thus confirming the effectiveness of the field procedure.

TABLE 15. p-XYLENE CONVERSION TO CO_2 DETERMINED BY XYLENE EXTRACTION OF WATER SAMPLES TAKEN AT DAY 421

Well	Port	Phase	^3H/mL	^{14}C/mL	% Conversion
D18	11	Aqueous	2978	76	
D18	11	Organic	1	8	84
D18	11	Water	3221	91	
D18	13	Aqueous	5682	154	
D18	13	Organic	0	38	77
D18	13	Water	5936	199	
D21	13	Aqueous	2640	90	
D21	13	Organic	1	7	94
D21	13	Water	2657	96	
D6	12	Aqueous	3583	117	
D6	12	Organic	1	15	86
D6	12	Water	3781	136	
D6	14	Aqueous	7793	244	
D6	14	Organic	2	31	87
D6	14	Water	8162	281	
M3	19	Aqueous	2304	80	
M3	19	Organic	1	11	84
M3	19	Water	2266	95	
M35	11	Aqueous	1611	65	
M35	11	Organic	5	13	85
M35	11	Water	1618	77	
M35	13	Aqueous	648	37	
M35	13	Organic	1	6	79
M35	13	Water	651	46	
M36	13	Aqueous	988	41	
M36	13	Organic	1	6	152
M36	13	Water	972	27	

(Continued)

TABLE 15. p-XYLENE CONVERSION TO CO_2 DETERMINED BY XYLENE EXTRACTION OF WATER SAMPLES TAKEN AT DAY 421

Well	Port	Phase	^3H/mL	^{14}C/mL	% Conversion
M40	11	Aqueous	296	42	
M40	11	Organic	0	12	71
M40	11	Water	308	59	
M41	13	Aqueous	3907	182	
M41	13	Organic	1	40	83
M41	13	Water	3893	220	
M41	15	Aqueous	4187	128	
M41	15	Organic	1	15	93
M41	15	Water	4209	137	
M41	17	Aqueous	1460	44	
M41	17	Organic	2	5	91
M41	17	Water	1424	49	
M43	13	Aqueous	5216	125	
M43	13	Organic	2	27	77
M43	13	Water	5244	162	
M43	15	Aqueous	1724	43	
M43	15	Organic	1	5	87
M43	15	Water	1720	50	
M45	13	Aqueous	1796	64	
M45	13	Organic	0	11	82
M45	13	Water	1762	77	
M50	11	Aqueous	1961	55	
M50	11	Organic	5	7	87
M50	11	Water	1976	63	
M50	13	Aqueous	2218	60	
M50	13	Organic	1	12	77
M50	13	Water	2196	78	

TABLE 16. LABORATORY TEST OF $^{14}CO_2$ PARTITIONING BETWEEN WATER AND p-XYLENE

pH = 4.8

SAMPLE	DPM/mL	DPM/mL (corrected)	DPM (total)
Aqueous Phase	1226	1191	23820
Organic Phase	1904	1869	3737

Fraction of $^{14}CO_2$ in the organic phase = 0.157

pH = 7

SAMPLE	DPM/mL	DPM/mL (corrected)	DPM (total)
Aqueous Phase	1607	1572	31446
Organic Phase	168	133	266

Fraction of $^{14}CO_2$ in the organic phase = 0.008

The ^{14}C p-xylene conversion values compare well with mass losses calculated from the moments analysis of the p-xylene remaining in the plume. Mass loss at day 421 was obtained by interpolation between the mass losses at 328 and 440 days. It is assumed that all of the organics injected, because of their structural similarity, were degraded and not lost to other processes.

Conversion values in Table 17 imply that most of the p-xylene went to energy production and was neither incorporated into new biomass, nor lost to sorption or volatilization. Conversions were calculated separately for high (> 1ppm) and low (< 1ppm) solute concentration regions of the plume. The difference in degradation between these two regions of the aquifer were not found to be significant. Some of this difference may have been due to analytical errors (e.g. loss of $Ca^{14}CO_3$ during precipitate transfer prior to counting, or CO_2 dissolution in xylene). The similarity of these results imply nonlocalized, concentration independent degradation. Toxic effects and nutrient or oxygen limitations on the microbiota are not indicated.

TABLE 17. DEGRADATION OF ^{14}C p-XYLENE MEASURED IN WATER SAMPLES TAKEN AT 421 DAYS AFTER INJECTION, EXPRESSED AS A WEIGHT PERCENT

	Converted to CO_2 (precipitation method)	Converted to CO_2 (extraction method)	Mass Loss From moments analysis
[X] > 1ppm (n=8)	72.7 (± 11.5)	85.1 (± 6.3)	98
[X] < 1ppm (n=10)	75.7 (± 6.9)	82.6 (± 6.1)	98

These radiochemical results for ^{14}C p-xylene degradation to $^{14}CO_2$ provided quantitative support for a qualitative observation made in Section 5 regarding the spatial distributions of p-xylene and of ^{14}C in the snapshot samples. The results indicated that the bulk of the p-xylene remained in the near field throughout the study, while ^{14}C concentrations increased significantly in the far field, and even appeared to be transported along with the tritium in the far field. These distributions can only be explained by the degradation of p-xylene. The ^{14}C p-xylene had to have been converted to $^{14}CO_2$ in the near field through chemical and/or biological processes, and was then transported to the far field with the tritium tracer. The stability, or conservative nature, of $^{14}CO_2$ in the Columbus aquifer was mainly due to the acidic groundwater conditions, which prevented the formation of carbonate minerals. Equilibrium thermodynamic model calculations showed that the groundwater is highly undersaturated with respect to calcite. The absence of carbonate minerals inferred from these calculations was confirmed by the similarity of total carbon and organic carbon contents (at the 0.005 percent level) determined using a Leco Corp. (St Joseph, MI) Model WR112 carbon analyzer. Investigators considering use of the above radiochemical method should first determine whether the chemistry of the aquifer of concern will permit its use effectively. Conditions which would promote the precipitation of carbonate minerals in the saturated zone of an aquifer would preclude the use of the above ^{14}C method for measuring the degradation of organic compounds.

TIME-SERIES DATA ANALYSIS

Concentration time-series data for several sampling points in the near field were used to estimate the sorption of organic compounds during the field study, and to provide independent computations of the organic degradation rates for comparison with those derived from the spatial moments analysis. Retardation factors and degradation rates were estimated by fitting the time-series data to an analytical solution of the one-dimensional convection-dispersion equation containing linear equilibrium sorption and first-order decay terms.

Normalized solute breakthrough curves (BTCs) for three sampling points in the near field are shown on Figure 32. These data were typical for the site in the following respects. First, none of the BTCs showed complete passage of the tritium pulse. The slow transport of the tracer from the low hydraulic conductivity zone in the near field precluded complete monitoring of tracer breakthrough. Second, the normalized tritium concentrations for each sampling point were consistently the highest of all the solutes, as was expected. However, a

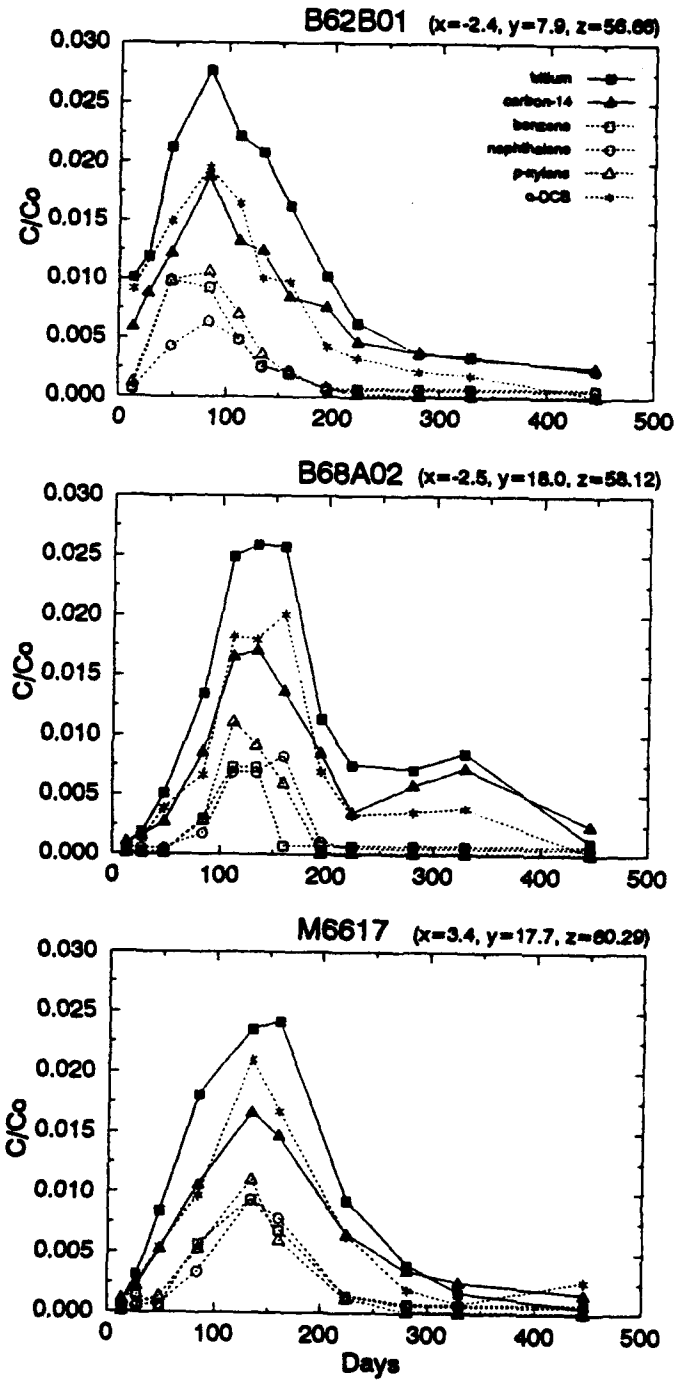

Figure 32. Solute Breakthrough Curves at Selected Points (x, y, z coordinates are in meters)

visual inspection of the breakthrough responses indicates that the area under the tritium BTC was consistently larger than those of all of the other solutes. One would expect, based on chromatographic theory, that the areas under all tracer BTCs would be approximately equal, assuming (1) complete or nearly-complete breakthrough of all solutes, (2) the absence of processes which remove tracer from solution (e.g., irreversible adsorption or biotransformation), and (3) steady-flow conditions. For the organic compounds and ^{14}C, areas under the normalized BTCs are smaller for benzene, naphthalene, and p-xylene than for o-DCB and ^{14}C. These results are generally consistent with the spatial moments results, which indicated the lowest mass recoveries from the most biodegradable organics (i.e., benzene, naphthalene, and p-xylene) with consistently higher recoveries for o-DCB.

DEGRADATION RATES AND RETARDATION FACTORS

Due to the geohydrologic conditions in the Columbus aquifer, retardartion factors for the organic solutes cannot be reliably estimated from a conventional comparison of corresponding first temporal moments for the organic solutes and for tritium. Inspection of the point time-series data indicates that the mean arrival times of the organic compounds are less than the corresponding mean arrival times of tritium in most cases, leading to obviously erroneous retardation factors of less than one. The source of this apparent error is that conventional mean arrival time analysis does not account for the degradation of organic compounds, as found during this field study, and thus cannot yield meaningful retardation factors. An alternative procedure was used to calculate retardation factors for the organic solutes that included solute degradation. In this procedure, the time-series concentration data for tritium and organic solutes were fitted to an analytical solution of the one-dimensional convection-dispersion equation which included both linear equilibrium sorption and first-order decay terms.

One-dimensional steady transport of a pulse release of solute undergoing linear equilibrium adsorption and first-order decay is described by:

$$\frac{\partial c_r}{\partial t} = D\frac{\partial^2 c_r}{\partial x^2} - V\frac{\partial c_r}{\partial x} + \frac{\rho_b}{\eta}\frac{\partial s}{\partial t} - \mu c_r \qquad (21)$$

In the case modeling this field experiment, the source boundary condition is,

$$\left(c_r - \frac{D}{V}\frac{\partial c_r}{\partial x}\right)_{x=0} = \begin{pmatrix} c_0, & 0 < t \le t_0 \\ 0, & t > t_0 \end{pmatrix} \qquad (22)$$

where c_r is the volume-averaged resident concentration of the solute in the liquid phase, s is the sorbed concentration per unit mass of the solid phase, x is distance, D is a dispersion coefficient reflecting the combined effects of diffusion and hydrodynamic dispersion, V is the average pore-water velocity, ρ_b is the bulk mass density, η is the porosity, and μ is the first-order decay rate constant.

A nonlinear least-squares inversion code developed by Parker and van Genuchten (1984) was used to estimate the solute transport parameters associated with Equations (21) and (22), from the time-series concentration data for discrete sampling points located in the

near field. In general, the procedure consisted of fitting the tritium breakthrough response for a specific sample point to obtain estimates for the physical transport parameters V and D. In estimating R and μ for each organic compound from their breakthrough curves, these V and D values were used as constants, and a fitting procedure was applied to obtain values for R and μ. Time-series data for 11 BarCad® samplers and 6 MLS points were selected for analysis. Only data for sampling points exhibiting complete (or nearly complete) single-peak breakthrough responses were analyzed. Breakthrough responses exhibiting multiple peaks were common among the sampling points evaluated, but were excluded from the analysis because they did not satisfy the assumptions inherent in Equation 21.

Physical transport parameter estimates for the 17 discrete sampling points are presented in Table 18. In addition, statistical summaries of the retardation factors and rate constants for the organic compounds are given in Tables 19 and 20. The mean retardation factors for benzene, naphthalene, p-xylene, and o-DCB are 1.20, 1.45, 1.16, and 1.33, respectively. The mean first-order rate constants describing degradation of benzene, naphthalene, p-xylene, and o-DCB are 0.010, 0.013, 0.016, and 0.005 d^{-1}, respectively.

Note that the estimates of D presented in Table 18 for the tritium data may not be reliable. Several features of this natural gradient experiment (e.g., extreme aquifer heterogeneity, three-dimensional non-steady flow, and a finite-volume tracer solution source) violate the simplistic physical transport assumptions embodied in Equation (21). The reported estimates of V and D represent a set of effective parameters which together produce a physical transport response that approximates the tritium breakthrough data. Our primary interest here is in the difference between the tritium and organic solute breakthrough responses caused by sorption and degradation, and not estimation of dispersion coefficients.

Transformation rates for the organic compounds were independently estimated from the solute mass balances (with results given in Table 12) and from the time-series data. A first-order rate process was assumed to approximate the overall degradation process in both analyses. A comparison of the estimated rate constants obtained by the two methods is given in Table 21, and indicates little difference between the methods for benzene, p-xylene, and o-DCB.

The disappearance and transformation of the organic solutes during this experiment demonstrated that natural degradation processes were able to effectively reduce these levels of dissolved organic contaminants in a reasonable time frame. This result suggests that, for similar organic compounds, it might be best to restrict aquifer remediation activities to the contaminant source region. Possible techniques could include pumping to remove NAPLs (non-aqueous phase liquids), or excavation of contaminated aquifer material. The source would then be reduced, but probably would not be eliminated entirely by this treatment. In an aquifer with approximately steady flow, and the correct physical, chemical and biological conditions, the plume of organic solutes from the reduced source could attain a steady-state limit. In such an aquifer, the spatial boundary of this plume would be determined primarily by the hydrology and geochemistry of the site, solute sorption, biodegradation by indigenous microbes, redox capacity, and oxygen and nutrient supply.

This observation represents the most important result of the field study, and could have important implications for the restoration of aquifers contaminated by organic chemicals. Active remediation would not be needed in situations where natural degradation rates were sufficient to reduce contaminant concentrations to safe levels before they were transported to regions presenting risks to human health or the environment. Remediation by

TABLE 18. VELOCITY AND DISPERSION COEFFICIENT ESTIMATES FROM TRITIUM TIME-SERIES DATA

Sample Point	x(m)	y(m)	z(m)	Velocity, V (m/d)	Dispersion Coefficient, D (m^2/d)	r^2
B61B02	-4.0	8.7	60.03	0.0433	0.0075	0.80
B62A02	-0.7	7.2	59.71	0.0227	0.0230	0.98
B62B01	-2.4	7.9	56.66	0.0687	0.2303	0.87
B63A02	2.6	6.1	57.02	0.0412	0.1728	0.95
B63B01	1.1	6.8	55.46	0.1531	0.8392	0.96
B64A01	5.5	5.0	55.08	0.1098	0.3497	0.96
B64A02	5.5	5.0	59.66	0.0601	0.0497	0.90
B68A02	-2.5	18.0	58.12	0.1187	0.2438	0.90
B68B02	0.1	17.0	59.98	0.0859	0.0769	0.79
B69A02	2.1	16.3	58.53	0.0533	0.0823	0.98
B70B02	5.3	15.4	60.01	0.0668	0.0330	0.94
M06515	-0.5	19.1	59.85	0.0591	0.5109	0.87
M06517	-0.5	19.1	60.61	0.1020	0.1551	0.94
M06615	3.4	17.7	59.53	0.0094	0.2893	0.98
M06617	3.4	17.7	60.29	0.1221	0.2400	0 94
M06619	3.4	17.7	61.05	0.1039	0.1614	0.98
M06719	7.1	16.4	61.04	0.1265	0.4454	0.92
			n	17	17	
			mean	0.0792	0.2300	
			std. dev.	0.0389	0.2082	
			95% CI	0.0200	0.1071	

TABLE 19. RETARDATION FACTOR ESTIMATES FROM HYDROCARBON TIME-SERIES DATA

Sample Point	Retardation Factor, R			
	Benzene	Naphthalene	p-Xylene	o-DCB
B61B02	1.00	1.00	1.02	1.08
B62A02	1.08	1.26	1.02	1.14
B62B01	1.15	1.61	1.20	1.14
B63A02	1.00	1.56	1.00	1.40
B63B01	1.71	2.00	1.46	1.54
B64A01	--	--	--	1.41
B64A02	1.00	1.11	1.00	1.09
B68A02	1.06	1.21	1.08	1.06
B68B02	1.24	1.41	1.14	1.18
B69A02	1.29	1.57	1.02	1.36
B70B02	--	--	--	1.23
M06515	--	--	--	1.47
M06517	--	--	--	1.12
M06615	1.32	2.00	1.28	1.77
M06617	1.14	1.23	1.13	1.08
M06619	1.36	--	1.69	1.65
M06719	--	--	1.00	1.84
n	12	11	13	17
mean	1.20	1.45	1.16	1.33
st. dev.	0.20	0.32	0.20	0.25
95% CI	0.13	0.21	0.12	0.13

TABLE 20. ESTIMATES OF FIRST-ORDER BIOTRANSFORMATION RATE CONSTANTS FROM TIME-SERIES DATA

Sample Point	First-Order Decay Rate Constant, μ (d^{-1})			
	Benzene	Naphthalene	p-Xylene	o-DCB
B61B02	0.0113	0.0120	0.0148	0.0035
B62A02	0.0024	0.0022	0.0029	0.0005
B62B01	0.0160	0.0214	0.0138	0.0046
B63A02	0.0144	0.0257	0.0211	0.0132
B63B01	0.0104	0.0163	0.0053	0.0027
B64A01	--	--	--	0.0118
B64A02	0.0150	0.0183	0.0151	0.0055
B68A02	0.0132	0.0107	0.0094	0.0027
B68B02	0.0051	0.0090	0.0118	0.0038
B69A02	0.0070	0.0083	0.0124	0.0045
B70B02	--	--	--	0.0049
M06515	--	--	--	0.0037
M06517	--	--	--	0.0056
M06615	0.0039	0.0058	0.0155	0.0022
M06617	0.0094	0.0095	0.0091	0.0028
M06619	0.0105	--	0.0164	0.0103
M06719	--	--	0.0547	0.0094
n	12	11	13	17
mean	0.0099	0.0127	0.0156	0.0054
st. dev.	0.0043	0.0067	0.0122	0.0035
95% CI	0.0027	0.0045	0.0074	0.0018

natural degradation processes is likely to be applicable to residual organic contaminants (i.e., NAPL organics immobilized by capillary forces that cannot be effectively removed from the aquifer by pumping). The monetary and environmental cost savings of allowing natural biological restoration of the residual contaminants are potentially enormous.

The degradation rates determined for the four aromatic compounds in the Columbus aquifer are now being used in the design and modeling stages of a new field test which will use an emplaced NAPL source. This test at the Columbus site will be a demonstration of the practicality of natural degradation (natural attenuation) as a remediation action for a steadily leaching source in an aquifer. Assuming that a steady-state contaminant concentration situation is attained in this test, natural degradation will be a verified groundwater contaminant treatment option. It is proposed that experiments similar to this one should be done at several other test sites in order to prove the general applicability of this method, and for determining accurate aerobic degradation rates for use in the development of more accurate fate and transport models. The test sites could then be used to conducted NAPL tests which might further support the natural attenuation treatment option, and might even suggest this technique as the action of first choice in certain groundwater contamination situations.

TABLE 21. SUMMARY OF FIRST-ORDER DEGRADATION RATE CONSTANTS AND HALF-LIVES OF AROMATIC COMPOUNDS

Tracer	Method	Rate Constant (d^{-1})	Half-Life (d)
benzene	SMA	0.007	87
	TA	0.010	69
naphthalene	SMA	0.006	99
	TA	0.013	53
p-xylene	SMA	0.011	63
	TA	0.016	43
o-DCB	SMA	0.005	116
	TA	0.005	139

SMA = spatial moments analysis
TA = time-series analysis

The rate constants estimated by the two methods for naphthalene are significantly different, i.e., rate estimates differ by a factor of about two. The explanation for the difference between the naphthalene rate constants is not evident. In general, results for both methods are consistent with the expected relative biodegradabilities of the four compounds. The lowest transformation rates are estimated for o-DCB, the least degradable organic, while

higher rates are indicated for benzene, p-xylene, and naphthalene, which have been shown in laboratory studies to be more susceptible to biodegradation (Tabak *et al.*, 1981).

COMPARISON OF SORPTION IN LABORATORY AND FIELD EXPERIMENTS

As shown in Table 22, the mean retardation factors estimated for these organic compounds from the time-series data for discrete sampling points, are remarkably consistent with the laboratory measured values reported by MacIntyre *et al.* (1993) using aquifer material samples from the Columbus site. Furthermore, the same relationship in the relative magnitudes of the retardation factors among the four organic compounds is indicated for both the field and laboratory results.

TABLE 22. COMPARISON OF AVERAGE RETARDATION FACTORS ESTIMATED FROM LABORATORY TESTS AND FIELD DATA

	Lab	Field
benzene	1.30	1.20
naphthalene	1.42	1.45
p-xylene	1.24	1.16
o-DCB	1.32	1.33

The mechanism responsible for the sorption of these compounds is unknown. The compounds range from slightly to moderately hydrophobic, as indicated by their octanol-water partitioning coefficients: benzene=135; naphthalene=2000; p-xylene=1410; o-DCB=2500 (Gherini *et al.*, 1989). For soils and aquifer materials with organic carbon contents of greater than 0.1 percent, the sorption mechanism for hydrophobic organics is assumed to involve the partitioning of the sorbate into organic matter that is bound to the mineral surfaces (Karickhoff *et al.*, 1979). However, the average organic carbon content of this aquifer is much less than 0.1 percent (MacIntyre *et al.*, 1991). As might be expected from such a low carbon content material, MacIntyre *et al.* (1991) found a low correlation (r^2=0.048) between the K_d for naphthalene and organic carbon content in their analysis of 50 aquifer samples collected from the test site. Although these investigators did not identify the naphthalene sorption mechanism, they did confirm through a series of batch sorption kinetic and equilibrium experiments that (1) the sorption process was rapid with equilibrium achieved within 24 hours, and (2) the naphthalene isotherm was linear in the range of 0-5 mg/L. These findings support our presumption of linear equilibrium sorption reactions in the parameter estimation analysis of the time-series data for the organic compounds.

The similarity between the field and laboratory retardation factors is encouraging. It suggests that small-scale laboratory tests can provide meaningful estimates of field average sorption properties when measurements are sufficient to capture the field variability. However, we qualify this by noting that transport scale of the time-series data was only on the order of 20 meters. This scale of observation is considerably smaller than the transport scales usually connected with groundwater contamination problems (i.e., tens to hundreds of meters).

SECTION VII
AQUIFER DISPERSIVITY

Dispersivity in the aquifer can be calculated from the first and second spatial moments of the tritium plume presented in Section 5. Because the mean velocity field at the Columbus site is nonuniform, dispersivity cannot be predicted directly from the rate of change of the second moments as has been done for other experiments at other, more homogeneous sites (e.g., Freyberg, 1986; Garabedian *et al.*, 1991) Adams and Gelhar (1992) developed a method to calculate dispersivity at the Columbus site, and applied it to the results of a bromide tracer field test. They derived general moments equations for two-dimensional advective-dispersive transport in a spatially nonuniform flow field, following an instantaneous discharge of mass. The two-dimensional velocity field is defined by,

$$V_L = V_0 (1 + \alpha y) \tag{23}$$

$$V_T = -V_0 \alpha x \tag{24}$$

where V_L is the longitudinal velocity, α is a constant, V_o is the initial longitudinal velocity, V_T is the transverse velocity, and y and x are spatial coordinates aligned with the longitudinal and transverse flow directions, respectively. Substitution of this function into the general moments equation (Equation 5-5 of Adams and Gelhar, 1992), and solution of the resulting ordinary differential equations corresponding to the first and second moments (Equations 5-8, 5-9, and 5-12 of Adams and Gelhar, 1992) yields analytical expressions for the mean displacement, $\tilde{y}'$

$$\tilde{y}'(t) = c_1 (\exp(c_2 t) - 1) \tag{25}$$

the longitudinal second moment, σ_{11}^2,

$$\sigma_{11}^2(t) = -2A_{11}c_1 e^{c_2 t} + \left(\sigma_{11}^2(0) + \frac{A_{11}V_o}{c_2} + A_{11}c_1\right) e^{2c_2 t} - \frac{A_{11}(V_o - c_1 c_2)}{c_2} \tag{26}$$

the horizontal transverse second moment, σ_{22}^2

$$\sigma_{22}^2(t) = \frac{2A_{22}c_1 e^{c_2 t}}{3} + \left(\sigma_{22}^2(0) - \frac{2A_{22}c_1}{3} - \frac{A_{22}(V_o - c_1 c_2)}{c_2}\right) e^{-2c_2 t} + \frac{A_{22}(V_o - c_1 c_2)}{c_2} \tag{27}$$

where $c_1 = (1 + \alpha A_{11})/\alpha$, $c_2 = \alpha v_o$, A_{11} is the longitudinal dispersivity, and A_{22} is the transverse dispersivity.

Results of this dispersion analysis are summarized in the four graphs shown on Figure 33. The predicted and observed tritium plume mean displacements over time are shown on Figure 33(a). The corresponding longitudinal and horizontal transverse second moments are

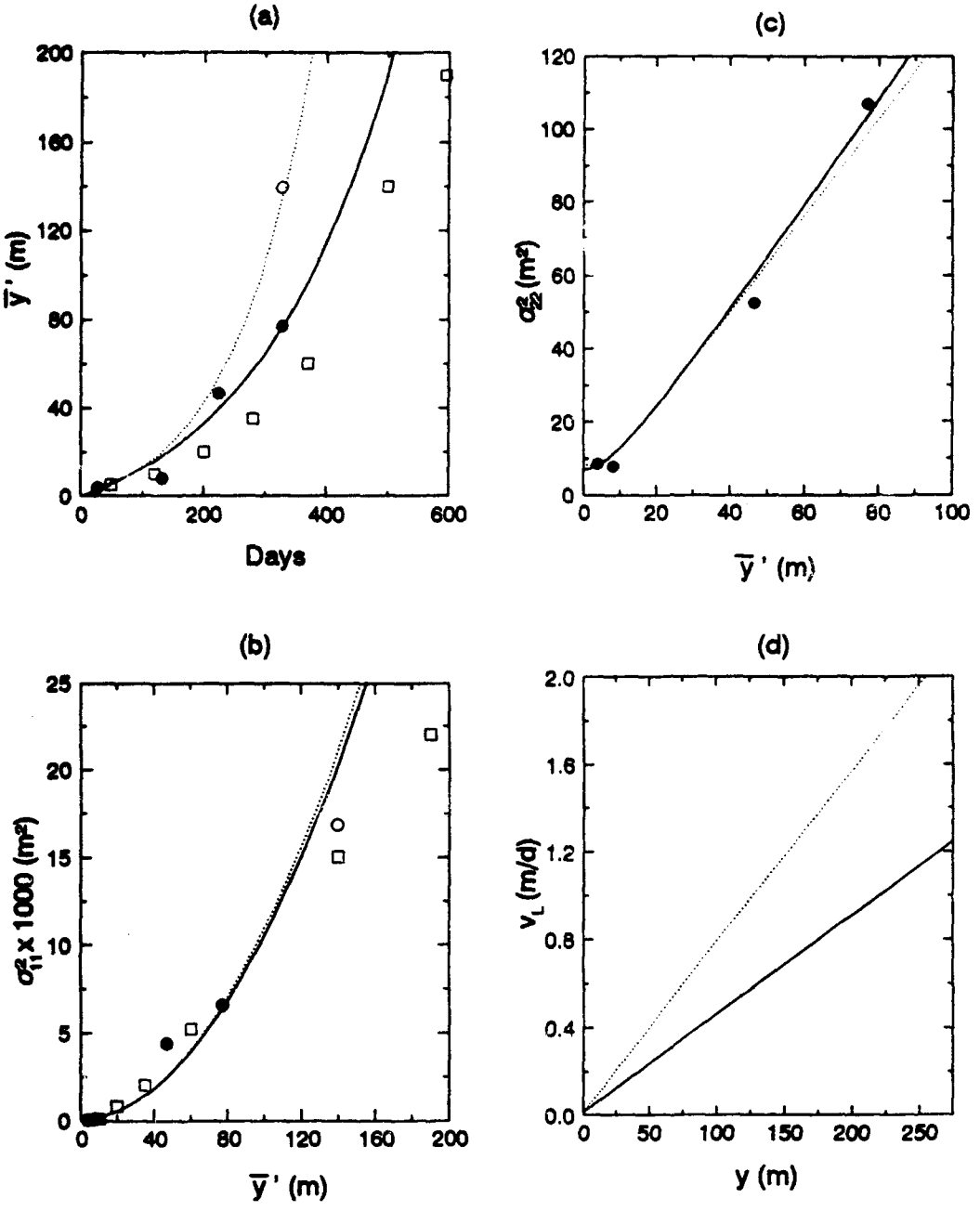

Figure 33. Comparison of (a) Mean Displacement, (b) Longitudinal Second Moment, and (c) Transverse Second Moment From Tritium Data and Nonuniform Flow Model. Open and Solid Circles Represent Tritium Data With and Without Extrapolation at 328 Days, Respectively. Open Square is Bromide Data From Adams and Gelhar (1992). Dotted and Solid Lines Denote Model Predicted Fits to Tritium Data With and Without Extrapolation. Diagram (d) Shows Mean Longitudinal Velocity as a Function of Displacement for Base and Extrapolated Cases.

plotted against mean displacement on Figures 33(b) and 33(c). The bromide plume displacement and moment results of Adams and Gelhar (1992) are also presented in these figures for comparison with the tritium plume behavior seen in this experiment. Figure 33(d) shows the velocity in the longitudinal direction as a function of displacement. Two different tritium moments are presented for the snapshot at 328 days; one for the moments estimated directly from the tritium measurements, and the other for moments estimated by extrapolation of the tritium plume front to account for it's truncation. The extrapolation assumed that the tritium activity deficit of approximately 23 percent observed at 328 days was entirely due to truncation. The missing tritium activity was assumed to be linearly distributed within a region equivalent to the advance of the tritium plume between 132 and 224 days.

The parameters assumed or estimated in fitting Equations (25), (26) and (27) to the tritium plume data are given in Table 23. Note that, for both the base case and the extrapolation case, V_o was assumed to be 0.014 m/d (5 m/yr) based on the estimated rate of movement of the plume in the near field (Section 5). Figure 33(a) indicates that the longitudinal first moments of the plume data are approximated reasonably well by Equation (25) for both cases. The linear velocity trends in the longitudinal direction are shown in Figure 33(b). The longitudinal velocity at a displacement of 100 meters is 0.46 m/d for the base case, and 0.79 m/d for the extrapolation case. Both estimates are below the seepage velocity of ≥ 1.1 m/d estimated from the advance of the tritium front between 132 and 224 days, and are therefore within the realm of possible mean velocities.

TABLE 23. FLOW AND DISPERSIVITY PARAMETER ESTIMATES FOR THE TRITIUM PLUME

Parameter	Base Case	Extrapolation Case
U_o (m/d)	0.0137	0.0137
α	0.328	0.569
A_{11} (m)	19.6	9.5
A_{22} (m)	2.2	--
$\sigma_{11}^2(0)$ (m^2)	7.0	7.0
$\sigma_{22}^2(0)$ (m^2)	7.0	7.0

The predicted trends in the longitudinal second moments are nearly coincident for the base case and the extrapolation case, and generally capture the overall trend indicated by the tritium data. Longitudinal dispersivities of 9.5 and 19.6 meters are estimated for the extrapolation and base cases, respectively. The insensitivity of the longitudinal second moments to the magnitude of dispersivity over the expected range of V_L and α reflects the dominant influence of advective transport in the evolution of the tritium plume. Because frontal truncation of the tritium plume was evident in the data, the extrapolation case longitudinal dispersivity estimate of approximately 10 meters is considered the more reliable of the two estimates.

A horizontal transverse dispersivity of 2.2 meters produced the best agreement with the observed transverse second moments. However, this value is probably overestimated because the transport model used in the analysis assumes a convergent flow field, when in fact the region of convergence is limited to the southern one-third to one-half of the sampling network (see Figure 3). Consequently, an unrealistically large transverse dispersivity is required in fitting Equation (27) to the observed transverse second moments, to compensate for the converging flow assumed to exist over the full length of the flow field.

The relative quality of dispersivity values obtained from the bromide tracer experiment (Adams and Gelhar, 1992) and from this tritium tracer experiment is not treated here. However, tritiated water is the better tracer, since solute chemical properties cannot affect calculated water transport properties. Also, the tritiated water snapshots included more of the field site than was the case in snapshots of the earlier bromide experiment.

SECTION VIII
CONCLUSIONS AND RECOMMENDATIONS

The disappearance and transformation of the organic solutes during this experiment demonstrated that natural degradation processes were able to effectively reduce these levels of dissolved organic contaminants in a reasonable time frame. This result suggests that, for similar organic compounds, it might be best to restrict aquifer remediation activities to the contaminant source region. By reducing this source, the resulting plume of organic solutes could possibly maintain a steady-state limit, given the correct physical, chemical and biological conditions. In such an aquifer, the spatial boundary of this plume would be determined primarily by the hydrology and geochemistry of the site, solute sorption, biodegradation by indigenous microbes, redox capacity, and oxygen and nutrient supply.

This observation represents the most important result of this field study, and could have important implications for the restoration of aquifers contaminated by organic chemicals. Active remediation would not be needed in situations where natural degradation rates were sufficient to reduce contaminant concentrations to safe levels before they were transported to regions where they might be dangerous to human health or the environment. Remediation by natural degradation processes is likely to be applicable to residual organic contaminants (i.e., NAPL organics immobilized by capillary forces that cannot be effectively removed from the aquifer by pumping). The monetary and environmental cost savings of allowing natural biological restoration of the residual contaminants are potentially enormous. After a review of the current scientific literature, it appears that this study is the first field experiment to prove conclusively that hydrocarbon solute losses were due to chemical degradation rather than physical losses, such as sorption and vaporization.

Further research is needed to build upon results of this study, to further support the observation of natural attenuation and to attempt to quantify the environmental requirements for this process. The degradation rates determined for the four aromatic compounds in the Columbus aquifer are now being used in the design and modeling stages of a new field test which will use an emplaced NAPL source. This test at the Columbus site will demonstrate the practicality of natural degradation (natural attenuation) as a remediation action for a steadily leaching source in an aquifer. This experiment more closely emulates the effects of a fuel spill. Assuming that a steady-state contaminant concentration situation is attained in this test, natural degradation will be a verified groundwater contaminant treatment option.

Experiments similar to this one should be done at several other test sites to prove the general applicability of this method, and to measure both aerobic and anaerobic degradation rates for use in the development of more accurate fate and transport models. The technique of using ^{14}C-labeled compounds is suggested for future field experiments, because it distinguishes solute degradation from solute losses by sorption and evaporation, and permits the demonstration of more accurate mass balances throughout the course of the investigation. If multiple test sites become available, they could then be used to conduct NAPL studies which might further support the natural attenuation treatment option, and might even suggest this technique as the action of first choice in certain groundwater contamination situations.

SECTION IX
REFERENCES

Adams, E.E. and L.W. Gelhar. "Field study of dispersion in a heterogeneous aquifer 2. Spatial moments analysis," *Water Resour. Res.*, 28(12), 3293-3291, 1992.

Aris, R. "On dispersion of a solute in a fluid flowing through a tube," *Proc. Royal Soc. London*, Ser. A, 235, 67-78, 1956.

Barker, J.F., G.G. Patrick and D. Major. "Natural attenuation of aromatic hydrocarbons in a shallow sand aquifer," *Ground Water Monitoring Review*, Winter, 1987.

Boggs, J.M., S.C. Young, H.F. Hemond, L. Richardson and M.E. Schaefer. "Evaluation of tracer sampling devices for macrodispersion experiment," EPRI Topical Report EA-5816, Electric Power Res. Inst., Palo Alto, CA, 1988.

Boggs, J.M., S.C. Young, D.J. Benton and Y.C. Chung. "Hydrogeologic characterization of the MADE site," EPRI Topical Report EN-6915, Electric Power Res. Inst., Palo Alto, CA, 1990.

Boggs, J.M., S.C. Young, L.M. Beard, L.W. Gelhar, K.R. Rehfeldt and E.E. Adams. "Field study of dispersion in a heterogeneous aquifer 1. Overview and site description," *Water Resources Research*, 28(12), 3281-3291, 1992.

Boggs, J.M. and E.E. Adams. "Field study of dispersion in a heterogeneous aquifer 4. Investigation of adsorption and sampling bias," *Water Resources Research*, 28(12), 3325-3336, 1992.

Burris, D.R. and W.G. MacIntyre. "Water solubility of binary hydrocarbon mixtures," *Environmental Toxicology and Chemistry*, 4, 371-377, 1985.

Callahan, M.A., M.W. Slimak, N.W. Gabel, I.P. May, J.R. Fowler, P. Jennings, R.L. Durfee, F.C. Whitmore, B. Maestri, W.R. Mabey, B.R. Holt and C. Gould. Water-Related Environmental Fate of 129 Priority Pollutants, Volume II. Report No. EPA-440/4-79-029b, U.S. Environmental Protection Agency, Washinton D.C., 1979.

CRC Standard Mathematical Tables, 12th ed., C.D. Hodgman, editor, Chemical Rubber Publishing Co., Cleveland, OH, 1959.

Fleming, J.T., J. Sanseverino and G.S. Sayler. "Quantitative relationship between naphthalene catabolic gene frequency and expression in predicting PAH degradation in soils at town gas manufacturing sites," *Environ. Sci. Technol.*, 27(6), 1068-1074, 1993.

Freyberg, D.L. "A natural gradient experiment on solute transport in a sand aquifer 2. Spatial moments and the advection and dispersion of nonreactive tracers," *Water Resources Research*, 22(13), 2031-2046, 1986.

Garabedian, S.P., D.R. LeBlanc, L.W. Gelhar and M.A. Celia. "Large-scale natural gradient tracer test in sand and gravel, Cape Cod, Massachusetts 2. Analysis of spatial moments for a nonreactive tracer," *Water Resources Research*, 27(5), 911-924, 1991.

Geraghty and Miller, Inc. Existing and proposed USEPA maximum contaminant levels in drinking water as of August 1991, compiled by R.A. Saar, Geraghty and Miller, Inc., Albuquerque, NM, August 1991.

Gherini, S.A., K.V. Summers, R.K. Munson and W.B. Mills. Chemical data for predicting the fate of organic compounds in water, Volume 2. Database, EPRI Report EA-5818, 1988.

Hänel, K., Biological Treatment of Sewage by the Activated Sludge Process, p. 299, John Wiley and Sons, New York, 1988.

Harvey, R.W., N.E. Kinner, D. MacDonald, D.W. Metge and A. Bunn. "Role of physical heterogeneity in the interpretation of small-scale laboratory and field observations of bacteria, microbial-sized microphere, and bromide transport through aquifer sediments," *Water Resources Research*, 29(8), 2713-2721, 1993.

Karickhoff, S.W., D.S. Brown and T.A. Scott. "Sorption of hydrophobic pollutants on natural sediments," *Water Resources Research*, 13(2), 241-248, 1979.

Larson, R.J. "Role of Biodegradation Kinetics in Predicting Environmental Fate," in Biotransformation and Fate of Chemicals in the Aquatic Environment, pp. 67-86, Ed. A.W. Maki *et al.*, American Society for Microbiology, Washington D.C., 1979.

Lion, L., T.B. Stauffer and W.G. MacIntyre. "Sorption of hydrophobic compounds on aquifer materials: Analysis, methods and the effect of organic carbon," *J. Contam. Hydrol.*, 5, 215-234, 1990.

MacIntyre, W.G., T.B. Stauffer and C.P. Antworth. "A comparison of sorption coefficients determined by batch, column, and box methods on low organic carbon aquifer material," *Ground Water*, 29(6), 1991.

MacIntyre, W.G., J.M. Boggs, C.P. Antworth and T.B. Stauffer. "Degradation kinetics of aromatic organic solutes introduced into a heterogeneous aquifer," *Water Resources Research, [in press]*, 1993.

MacQuarrie, K.T.B. and E.A. Sudicky. "Simulation of biodegradable organic contaminants in groundwater: 2. Plume behavior in uniform and random fields," *Water Resources Research*, 26(2), 223-239, 1990.

Madsen, E.L. "Determining *in situ* biodegradation, facts and challenges," *Environ. Sci. Technol.*, 25(10), 1663-1673, 1991.

Parker, J.C. and M.T. van Genuchten. "Determining transport parameters from laboratory and field tracer experiments," *Va. Agr. Exper. Station Bull.*, 84-3, 1984.

Rehfeldt, K.R., P. Hufschmied, L.W. Gelhar and M.E. Schaefer. Measuring hydraulic conductivity with the borehole flowmeter, EPRI Topical Report EN-6511, Electric Power Res. Inst., Palo Alto, CA, 1989a.

Rehfeldt, K.R., L.W. Gelhar, J.B. Southard and A.M. Dasinger. Estimates of macrodispersivity based on analyses of hydraulic conductivity variability at the MADE site, EPRI Topical Report EN-6405, Electric Power Res. Inst., Palo Alto, CA, 1989b.

Rehfeldt, K.R., J.M. Boggs and L.W. Gelhar. "Field study of dispersion in a heterogeneous aquifer 3. Geostatistical analysis of hydraulic conductivity," *Water Resources Research,*, 28(12), 3309-3324, 1992.

Robin, M.J.L., E.A. Sudicky, R.W. Gillham and R.G. Kachanoski. "Spatial variability of strontium distribution coefficients and their correlation with hydraulic conductivity in the Canadian Forces Base Borden aquifer," *Water Resour. Res.*, 27(10), 2619-2632, 1991.

Robinson, K.G., W.S. Farmer and J.T. Novak. "Availability of sorbed toluene in soils for biodegradation by acclimated bacteria," *Wat. Res.*, 24(3), 345-350, 1990.

Rubin, H.E., R.V. Subba-Rao and M. Alexander. "Rates of mineralization of trace concentrations of aromatic compounds in lake water and sewage samples," *Appl. Environ. Microbiol.*, 43(5), 1133-1138, 1982.

Simkins, S. and M. Alexander. "Models for mineralization kinetics with the variables of substrate concentration and population density," *Appl. Environ. Microbiol.*, 47(6), 1299-1306, 1984.

Spain, J.C. "Microbial adaptation in aquatic ecosystems," in Enhanced Biodegradation of Pesticides in the Environment, Eds. K.D. Racke and J.R. Coats, pp. 181-190, ACS Symposium Series 426, American Chemical Society, Washington DC, 1990.

Spiro, M. "Heterogeneous catalysis of solution reactions," in Comprehensive Chemical Kinetics, Vol. 28, Reactions at the Liquid-Solid Interface. Ed. R.G. Compton, pp. 69-159, Elsevier, 1989.

Sudicky, E.A. "A natural gradient experiment on solute transport in a sand aquifer: Spatial variability of hydraulic conductivity and its role in the dispersion process," *Water Resources Research*, 22(13), 2069-2082, 1986.

Sutton, P.A. and J.F. Barker. "Migration and attenuation of selected organics in a sandy aquifer - A Natural gradient experiment," *Groundwater*, 23(1), 1985.

Tabak, H.H., S.A. Quave, C.I. Mashni and E.F. Barth. "Biodegradability studies with organic priority pollutant compounds," *Water Pollution Control Fed. J.*, 53(10), 1503- 1518, 1981.

(Reverse of this page is blank)

SECTION X
APPENDIX A

DISSOLVED OXYGEN MEASUREMENTS

Dissolved oxygen (DO) data for six sampling dates are given in Tables A-1 through A-6. Each table provides the MLS or piezometer number, the measured dissolved oxygen concentration in mg/L, and the temperature in degrees centigrade for each water sample at the time DO was measured. The spatial coordinates of each DO monitoring well are presented in Table A-7.

TABLE A-1. LOCATIONS OF DISSOLVED OXYGEN MONITORING SITES

MLS	Port	X (m)	Y (m)	Z (m)	MLS	Port	X (m)	Y (m)	Z (m)
D006	6	-1.5	6.6	56.62	M172	1	3.1	98.6	53.85
D006	10	-1.5	6.6	57.63	M172	10	3.1	98.6	57.28
D006	20	-1.5	6.6	60.17	M172	20	3.1	98.6	61.09
D010	3	-2.8	-2.3	55.17	M181	1	-1.6	117.0	53.80
D010	10	-2.8	-2.3	57.83	M181	10	-1.6	117.0	57.23
D010	20	-2.8	-2.3	61.64	M181	20	-1.6	117.0	61.04
M041	1	-.2	3.6	54.27	M190	1	3.1	132.1	53.80
M041	10	-.2	3.6	57.70	M190	10	3.1	132.1	57.23
M041	20	-.2	3.6	61.51	M190	20	3.1	132.1	61.04
M066	1	3.4	17.7	54.19	M202	1	1.4	166.6	53.65
M066	10	3.4	17.7	57.62	M202	10	1.4	166.6	57.07
M066	20	3.4	17.7	61.43	M202	20	1.4	166.6	60.88
M075	1	2.9	23.0	54.07	M235	1	4.4	199.1	53.66
M075	10	2.9	23.0	57.50	M235	10	4.4	199.1	57.09
M075	20	2.9	23.0	61.31	M235	20	4.4	199.1	60.90
M089	1	-.1	31.8	54.02	M244	1	-10.1	237.8	53.63
M089	10	-.1	31.8	57.45	M244	10	-10.1	237.8	57.06
M089	20	-.1	31.8	61.26	M244	20	-10.1	237.8	60.87
M109	1	-.6	48.8	54.18	M255	1	-1.9	268.7	53.81
M109	10	-.6	48.8	57.61	M255	10	-1.9	268.7	57.24
M109	20	-.6	48.8	61.42	M255	20	-1.9	268.7	61.05
M138	1	-1.6	66.3	53.97	P42A	--	5.6	71.8	60.04
M138	10	-1.6	66.3	57.40	P61B	--	-47.8	264.1	56.32
M138	20	-1.6	66.3	61.21	P60A	--	26.3	226.3	60.80
M162	1	3.7	81.4	53.88	P59B	--	18.8	88.3	56.13
M162	10	3.7	81.4	57.31	P57A	--	29.3	127.2	60.70
M162	20	3.7	81.4	61.12	P55B	--	29.1	24.6	56.51

Table A-2. DISSOLVED OXYGEN AND TEMPERATURE DATA ON 6/18/90

MLS	Port	DO mg/L	Temp °C
D010	03	2.6	30.5
D010	10	3.2	31.0
D010	20	2.9	29.8
D006	06	4.8	31.0
D006	10	4.6	31.9
D006	20	3.7	30.8
M041	01	3.4	31.0
M041	10	3.8	33.5
M041	20	3.5	37.0
M066	01	4.9	33.5
M066	10	4.8	33.5
M066	20	4.6	34.0
M075	01	5.2	34.0
M075	10	4.9	34.5
M075	20	5.0	36.0
M089	01	4.8	35.0
M089	10	4.8	34.0
M089	20	4.3	32.2
M109	01	5.0	32.1
M109	10	4.6	31.0
M109	20	3.7	36.0
M138	01	6.0	31.5
M138	10	4.8	32.0
M138	20	5.1	33.5
M162	01	5.8	30.5
M162	10	5.0	30.3
M162	20	4.6	29.8
M172	01	5.6	28.5
M172	10	5.0	27.8
M172	20	4.8	27.0
M181	01	5.4	30.3
M181	10	5.7	28.2
M181	20	5.7	27.7
M190	01	6.3	28.0
M190	10	4.9	27.5
M190	20	5.0	27.3
M202	01	6.7	28.5
M202	10	6.2	27.7
M202	20	5.0	27.7
M235	01	5.1	31.5
M235	10	5.7	28.2
M235	20	5.1	29.5
M244	01	5.4	32.0
M244	10	5.0	31.3
M244	20	5.7	33.5
M255	01	7.1	29.0
M255	10	6.1	27.3
M255	20	5.0	27.5
Piezometers			
P42A	--	3.9	18.7
P61B	--	6.3	18.9
P60B	--	2.1	18.0
P59B	--	3.0	19.9
P57A	--	5.0	22.2
P55B	--	5.3	20.0

TABLE A-3. DISSOLVED OXYGEN AND TEMPERATURE DATA ON 8/13/90

MLS	Port	DO mg/L	Temp °C	MLS	Port	DO mg/L	Temp °C
D010	03	5.0	32.0	M162	01	4.0	27.0
D010	10	5.1	31.0	M162	10	4.2	27.0
D010	20	3.8	31.0	M162	20	3.0	27.0
D006	06	4.6	31.0	M172	01	3.6	27.0
D006	10	4.5	31.0	M172	10	3.4	27.0
D006	20	4.8	29.0	M172	20	2.6	26.0
M041	01	5.1	32.0	M181	01	4.0	26.0
M041	10	6.2	32.0	M181	10	3.2	26.0
M041	20	5.2	31.0	M181	20	3.2	25.0
M066	01	4.6	32.0	M190	01	3.8	27.0
M066	10	4.4	31.0	M190	10	3.6	27.0
M066	20	4.4	31.0	M190	20	3.4	26.5
M075	01	4.8	30.0	M202	01	5.0	27.0
M075	10	4.2	29.0	M202	10	4.0	26.0
M075	20	3.8	28.0	M202	20	2.0	25.0
M089	01	5.2	28.0	M235	01	5.0	25.0
M089	10	4.4	29.0	M235	10	4.6	25.0
M089	20	3.4	29.0	M235	20	4.0	25.0
M109	01	4.2	28.0	M244	01	4.0	26.0
M109	10	3.4	29.0	M244	10	3.8	25.0
M109	20	4.6	29.0	M244	20	3.8	26.0
M138	01	4.2	28.0	M255	01	5.4	29.0
M138	10	4.0	28.0	M255	10	5.2	31.0
M138	20	3.0	26.0	M255	20	4.4	27.0

TABLE A-4. DISSOLVED OXYGEN AND TEMPERATURE DATA ON 10/15/90

MLS	Port	DO mg/L	Temp °C
D010	03	4.0	31.0
D010	10	3.8	30.0
D010	15	3.6	31.0
D006	03	3.2	27.0
D006	10	3.8	28.0
D006	20	4.2	27.0
M041	01	5.0	30.0
M041	10	5.0	29.0
M041	15	4.8	30.0
M066	01	4.6	28.0
M066	10	4.8	31.0
M066	15	4.6	29.0
M075	01	4.8	29.0
M075	10	4.8	31.0
M075	16	4.6	28.0
M089	01	5.2	31.0
M089	10	4.8	30.0
M089	20	4.4	29.0
M109	01	5.2	31.0
M109	10	4.8	31.0
M109	17	4.6	30.0
M138	01	5.2	31.0
M138	10	5 0	31.0
M138	20	4.4	31.0
M162	01	4.8	31.0
M162	10	4.6	31.0
M162	20	4.4	31.0
M172	01	4.8	31.0
M172	10	5.0	31.0
M172	20	4.8	31.0
M181	01	4.8	31.0
M181	10	4.8	29.0
M181	20	5.0	29.0
M190	01	4.6	31.0
M190	10	4.4	31.0
M190	16	4.2	31.0
M202	01	5.4	29.0
M202	10	5.2	31.0
M202	20	4.8	30.0
M235	01	5.2	31.0
M235	10	4.8	29.0
M235	20	5.0	31.0
M244	01	5.2	31.0
M244	10	5.0	29.0
M244	20	4.8	30.0
M255	01	5.6	31.0
M255	10	5.4	29.0
M255	20	5.6	28.0
Piezometers			
P42A	--	4.4	20.8
P61B	--	3.7	19.6
P60A	--	4.6	20.7
P59B	--	2.6	27.2
P57A	--	4.6	22.2
P55B	--	5.9	18.5

TABLE A-5. DISSOLVED OXYGEN AND TEMPERATURE DATA ON 12/4/90

MLS	Port	DO mg/L	Temp °C
D010	03	4.0	11.5
D010	11	3.9	11.0
D010	15	4.3	10.5
D006	08	4.1	12.0
D006	10	4.1	10.0
D006	20	3.5	11.0
M041	01	4.6	10.0
M041	10	5.0	10.0
M041	19	4.5	12.0
M066	01	5.8	10.0
M066	10	6.0	11.0
M066	15	4.4	11.0
M075	01	6.4	12.0
M075	10	6.7	12.2
M075	19	5.2	12.5
M089	01	7.0	11.0
M089	10	7.2	12.0
M089	19	7.2	11.5
M109	01	7.5	13.5
M109	10	7.8	14.0
M109	19	6.5	13.8
M138	01	5.0	13.0
M138	10	4.4	13.8
M138	20	5.3	14.5
M162	01	7.2	13.0
M162	10	5.5	14.0
M162	20	6.8	13.5
M172	01	6.8	13.0
M172	10	5.2	14.0
M172	19	5.2	14.0
M181	01	5.5	13.2
M181	10	6.8	14.5
M181	20	6.0	14.8
M190	01	7.2	14.5
M190	10	6.6	14.0
M190	20	6.4	14.0
M202	01	7.2	16.5
M202	10	7.6	17.0
M202	20	5.2	17.5
M235	01	5.8	16.0
M235	10	7.6	16.2
M235	20	7.4	16.0
M244	01	9.0	17.0
M244	10	6.6	16.8
M244	20	6.6	16.8
M255	02	7.6	16.2
M255	10	7.7	15.0
M255	20	6.0	14.8
Piezometers			
P42A	--	3.5	19.1
P61B	--	6.2	17.6
P60A	--	4.3	18.0
P59B	--	3.2	18.2
P57A	--	4.6	17.9
P55B	--	4.6	18.4

TABLE A-6. DISSOLVED OXYGEN AND TEMPERATURE DATA ON 3/7/91

MLS	Port	DO mg/L	Temp °C
D010	03	2.8	13.4
D010	11	2.6	13.4
D010	20	3.1	13.4
D006	03	3.5	13.4
D006	10	2.9	13.5
D006	20	2.6	13.8
M041	01	3.6	13.1
M041	10	4.0	12.7
M041	20	3.2	13.5
M066	01	4.5	13.5
M066	10	4.6	13.1
M066	20	5.2	13.0
M075	01	5.2	13.6
M075	10	5.3	13.4
M075	20	7.0	13.5
M089	01	5.2	14.9
M089	10	5.1	15.0
M089	20	4.3	14.9
M109	01	4.2	14.9
M109	10	3.3	14.9
M109	20	3.5	14.7
M138	01	4.9	14.7
M138	10	3.1	14.6
M138	20	7.8	14.3
M162	01	5.0	14.9
M162	10	4.0	15.0
M162	20	4.9	14.7
M172	01	3.9	14.6
M172	10	5.0	15.0
M172	20	3.7	14.6
M181	01	3.3	16.3
M181	10	4.8	16.1
M181	20	4.6	15.6
M190	01	4.4	16.1
M190	10	3.3	16.0
M190	20	4.5	16.0
M202	01	5.6	16.0
M202	10	5.1	15.9
M202	20	3.0	15.7
M235	01	5.3	16.4
M235	10	5.1	16.1
M235	20	3.6	16.5
M244	01	2.9	17.1
M244	10	3.0	16.7
M244	20	3.6	16.5
M255	01	6.1	16.8
M255	10	5.7	16.5
M255	20	3.5	16.6
Piezometers			
P42A	--	7.4	16.4
P61B	--	7.1	17.7
P60A	--	5.0	16.4
P59B	--	4.8	17.3
P57A	--	8.5	16.2
P55B	--	6.9	17.6

TABLE A-7. DISSOLVED OXYGEN AND TEMPERATURE DATA ON 5/22/91

MLS	Port	DO mg/L	Temp °C
D010	03	3.8	20.8
D010	11	5.2	20.6
D010	20	5.0	21.0
D006	03	4.8	22.3
D006	10	4.7	21.7
D006	20	4.2	22.0
M041	01	5.0	21.7
M041	10	5.1	22.0
M041	20	5.0	21.6
M066	01	6.8	22.7
M066	10	5.2	22.3
M066	20	5.4	22.7
M075	01	7.2	22.7
M075	10	6.3	22.3
M075	20	6.6	22.5
M089	01	7.8	24.8
M089	10	6.4	23.7
M089	20	5.6	23.5
M109	01	5.4	23.2
M109	10	5.0	23.8
M109	20	4.5	23.8
M138	01	5.2	23.5
M138	10	4.0	23.2
M138	20	6.1	23.0
M162	01	4.7	23.3
M162	10	4.2	23.3
M162	20	4.2	23.0
M172	01	6.1	24.5
M172	10	5.8	24.5
M172	20	3.8	23.8
M181	01	7.0	26.5
M181	10	7.1	26.0
M181	20	6.5	26.4
M190	01	5.7	25.0
M190	10	4.5	24.7
M190	20	5.1	24.8
M202	03	6.2	24.0
M202	10	6.6	25.7
M202	20	5.8	25.5
M235	01	4.4	24.3
M235	10	5.6	23.6
M235	20	5.6	24.2
M244	01	4.0	24.0
M244	10	3.5	23.8
M244	20	4.0	24.8
M255	01	7.4	24.2
M255	10	7.0	24.0
M255	20	5.1	24.6
Piezometers			
P42A	--	9.2	17.5
P61B	--	7.2	18.4
P60A	--	6.7	18.3
P59B	--	4.3	18.4
P57A	--	8.3	18.3
P55B	--	6.5	18.5

SECTION XI
APPENDIX B

EVALUATION OF THE SPATIAL MOMENTS CODE

The accuracy of the code used to estimate the spatial moments of the solute plumes was evaluated through a set of numerical tests. In these tests, three-dimensional Gaussian solute plumes of known mass were analytically generated within the sampling network used in the natural-gradient experiment. Calculated solute concentrations were obtained for each sampling point in the network using Yeh's (1983) analytical solution to the advection-dispersion transport equation for an instantaneous finite-volume source. Spatial moments for the analytically generated plumes were then estimated by the moments code and compared with the known theoretical values. The level of agreement between the calculated and theoretical values is a measure of the effectiveness of the particular moments code that is used.

In these numerical tests, the strength and dimensions of the finite volume source were similar to those of the tritium solution injected during the natural-gradient study. The total injected activity was 0.6 Ci, and the volume of the source solution was 10 cubic meters. For an assumed aquifer porosity of 30 percent, this corresponded to a bulk aquifer source volume of 33.3 cubic meters. The source was centered at coordinates (0, 0, 58.5), and source dimensions of 4.08, 4.08, and 2 meters were assigned in the x, y, and z dimensions, respectively. A seepage velocity of 0.140 m/d in the y direction was assumed. Dispersivities of 0.30, 0.03, and 0.0003 meters were assumed in the longitudinal, lateral, and vertical directions. These dispersivities produced plumes that were roughly similar to the tritium plumes observed during MADE-2.

Solute concentration distributions were computed at sample points at elapsed times of 37, 71, 142, 214, 285, and 356 days. Longitudinal profiles of the solute concentration for the artificial snapshots are shown in Figure B-1. The overall dimensions of the artificial plumes are similar to those of the actual tracer plumes during the early stages of MADE-2. However, the magnitude and variability of concentration gradients observed in the field study are not represented in the analytically generated plumes.

The predicted relative activity recovery (M/M_o) and plume centroid coordinates (X_c, Y_c, and Z_c) are given in Table B-1. The activity recovery error oscillates somewhat varying from -3 percent of the injected activity at a displacement of 5 meters, to a maximum of +13 percent at 20 meters, and reaches a minimum of -1 percent at 50 meters. These results indicate acceptable accuracy of the zeroth moments for near-source conditions where large concentration gradients typically produce the greatest numerical error. The predicted first moments for the analytically generated plumes are also reasonably accurate. The estimated coordinates of the plume centroid are within 3 percent of the theoretical mean displacement for each case.

These numerical tests do not provide a rigorous mathematical verification of the moments code used. Nevertheless, the results indicate the code yields reasonably accurate lower (zeroth and first) moment estimates for Gaussian plumes defined by spatial measurements that correspond to the actual field sampling network.

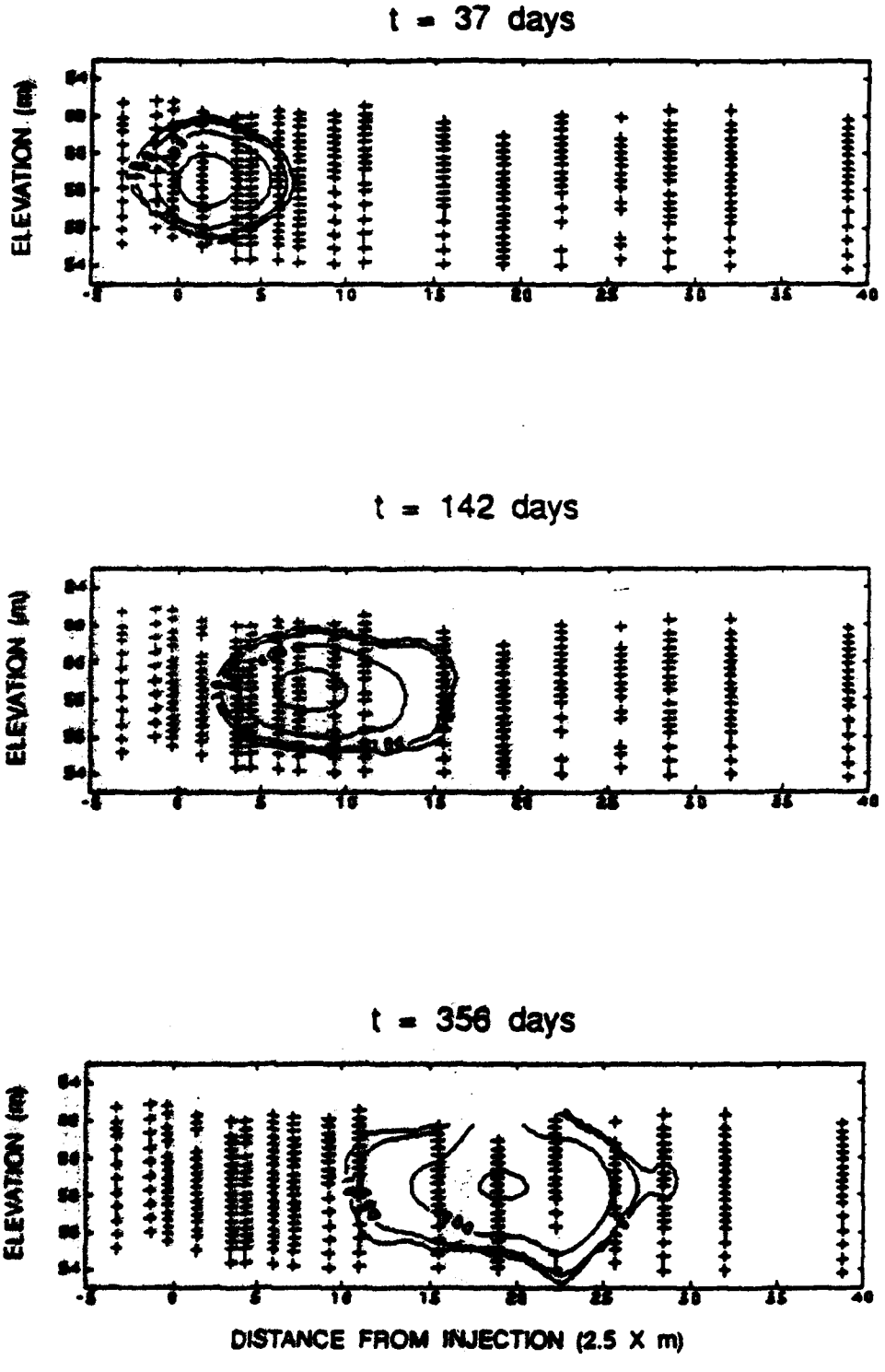

Figure B-1. Longitudinal Profiles of Analytically Generated Solute Plume.

TABLE B-1. COMPARISON OF THE THEORETICAL AND PREDICTED PLUME MASS AND CENTROID

Elapsed Time(days)	Plume Characteristic	Theoretical	Predicted	Difference
37	M/M_o	1.00	0.97	-0.03
	x_c(m)	0.00	-0.04	-0.04
	y_c(m)	5.00	5.15	0.15
	z_c(m)	58.50	58.80	0.30
71	M/M_o	1.00	1.11	0.11
	x_c(m)	0.00	0.10	0.10
	y_c(m)	10.00	10.13	0.13
	z_c(m)	58.50	58.50	0.00
142	M/M_o	1.00	1.13	0.13
	x_c(m)	0.00	-0.16	-0.16
	y_c(m)	20.00	19.89	-0.11
	z_c(m)	58.50	58.50	0.00
214	M/M_o	1.00	0.96	-0.04
	x_c(m)	0.00	0.17	0.17
	y_c(m)	30.00	29.64	-0.36
	z_c(m)	58.50	58.49	-0.01
285	M/M_o	1.00	0.98	-0.02
	x_c(m)	0.00	0.77	0.77
	y_c(m)	40.00	40.02	0.02
	z_c(m)	58.50	58.50	0.00
356	M/M_o	1.00	0.99	-0.01
	x_c(m)	0.00	-0.04	-0.04
	y_c(m)	50.00	50.08	0.08
	z_c(m)	58.50	58.50	0.00